Universidade de Lisboa
Instituto Superior de Agronomia

Separação preparativa e caracterização espectroscópica dos principais monómeros da suberina da cortiça

Tese apresentada para obtenção do grau de Doutor em Engenharia Florestal e dos Recursos Naturais

Sara Cristina Pereira Guedes Ribeiro dos Santos

Orientador: Professor Doutor José Afonso Rodrigues Graça

Júri

Presidente: Reitor da Universidade de Lisboa

Vogais: Doutora Helena Margarida Nunes Pereira
Professora Catedrática
Instituto Superior de Agronomia, Universidade de Lisboa

Doutor Armando Jorge Domingues Silvestre
Professor Associado
Universidade de Aveiro

Doutor António Jorge Velez Marques
Professor Coordenador
Instituto Superior de Engenharia de Lisboa do Instituto Politécnico de Lisboa

Doutor José Afonso Rodrigues Graça
Professor Auxiliar
Instituto Superior de Agronomia, Universidade de Lisboa

Doutora Maria Manuel Martinho Sequeira Barata Marques
Investigadora Auxiliar
Faculdade de Ciências e Tecnologia da Universidade Nova de Lisboa

Lisboa
2013

Universidade de Lisboa
Instituto Superior de Agronomia

Separação preparativa e caracterização espectroscópica dos principais monómeros da suberina da cortiça

Tese apresentada para obtenção do grau de Doutor em Engenharia Florestal e dos Recursos Naturais

Sara Cristina Pereira Guedes Ribeiro dos Santos

Orientador: Professor Doutor José Afonso Rodrigues Graça

Júri

Presidente: Reitor da Universidade de Lisboa

Vogais: Doutora Helena Margarida Nunes Pereira
Professora Catedrática
Instituto Superior de Agronomia, Universidade de Lisboa

Doutor Armando Jorge Domingues Silvestre
Professor Associado
Universidade de Aveiro

Doutor António Jorge Velez Marques
Professor Coordenador
Instituto Superior de Engenharia de Lisboa do Instituto Politécnico de Lisboa

Doutor José Afonso Rodrigues Graça
Professor Auxiliar
Instituto Superior de Agronomia, Universidade de Lisboa

Doutora Maria Manuel Martinho Sequeira Barata Marques
Investigadora Auxiliar
Faculdade de Ciências e Tecnologia da Universidade Nova de Lisboa

Lisboa
2013

O Capítulo 2 deste trabalho de doutoramento está incompleto por questões de confidencialidade

Contents

Chapter 3: Stereochemistry of monounsaturated cork suberin acids

Chapter 4: Stereochemistry of 9,10-epoxy and 9,10-diol cork suberin acids

Acknowledgments

This work would not exist without my Ph.D. advisor and mentor Professor José Graça. The common ground we have found on which we work enables the dream of great achievements! My deep gratitude goes to you.

I would also like to thank my colleagues and friends Ana Lourenço, Cristiana Alves, Isabel Baptista, Jorge Gominho, José Carlos, Teresa Quilhó and Vanessa Cabral for your constant help, support and encouragement.

A special thanks to André Santos, Irene Izquierdo and Vanessa Cabral for having the patience to read my work and for all your precious advices.

I am also grateful for the important help of Eurico Cabrita and Ângelo Figueiredo (Portuguese National NMR network, Universidade Nova de Lisboa), Pedro Aguiar (Universidade Nova de Lisboa), Luís Pimentel and Filomena Nobre (Organic Materials for Construction Testing Laboratory, LNEC), José Carlos Rodrigues (Flor, IICT) and Luís Santos (Materials Engineer Department, IST/TULisbon).

I dedicate this journey to my parents, my brothers André and Emanuel, my sisters Raquel and Irene, and to my best friend and companion, Ricardo! Thank you all for your patience and faith. I am eternally grateful.

This work was supported by the Portuguese Technology and Science Foundation Grant SFRH/BD/31033/2006 and Projects POCTI/AGR/46419/2002, PTDC/QUI/70589/2006 and PLANT-KBBE/AGR-GPL/0002/2009. It is also part of the activities of the Forest Research Center.

Abstract

Suberin is a vital biomacromolecule responsible for the protection of plants, and yet its molecular structure remains mostly unknown. Cork is the ideal material for suberin extraction because of its suberin content (≥40%) and availability in industrial quantities. Suberin is a polyester made of glycerol and long-chain a,ω-bifunctional fatty acids, mainly C_{18} ω-hydroxyacids and a,ω-diacids with mid-chain substituents, either an unsaturation, an epoxide or a *vic*-diol group.

The objective of this work was twofold: to develop techniques to isolate the main suberin acids from cork in preparative quantities and high purity (≥99.5%); and to develop spectroscopic techniques, namely NMR-based, to unambiguously assign the stereochemical configuration of the C_{18} suberin acids.

The multi-step process developed comprised suberin depolymerization and suberin acids separation in solvents of contrasting polarities and temperatures, followed by successive purification by normal-phase LC and reversed-phase HPLC.

The $C_{18:1}$ suberin acids were proved to be *cis*, through the analysis of their olefinic and allylic proton and carbon chemical shifts, and coupling constants extracted by spectra simulation. A NMR technique was developed using the chemical shifts of the benzylidene acetal derivatives of *vic*-diols, proving that the suberin acids C_{18} 9,10-epoxyacids were *cis*, and the C_{18} 9,10-diol acids were *threo*, in both cases present as racemic mixtures.

The stereochemistry of these acids will be determinant to understand the macromolecular structure of suberin, and the techniques developed for their preparative isolation can be the basis for their industrial commercialization.

Key-Words: suberin, cork, stereochemistry determination by NMR, *cis*/*trans* configuration analysis, *erythro*/*threo* configuration analysis

Resumo

A suberina é uma biomacromolécula vital na protecção das plantas, e contudo a sua estrutura molecular continua desconhecida. A cortiça é adequada para extrair suberina pelo seu teor elevado (≥40%) e disponibilidade em quantidades industriais. A suberina é um poliéster de glicerol e ácidos gordos a,ω-bifuncionais de cadeia longa, nomeadamente ω-hidroxiácidos e a,ω-diácidos em C_{18}, 9,10-substituídos por uma insaturação, grupo epóxido ou *vic*-diol.

Este trabalho teve 2 objectivos principais: desenvolver técnicas para isolar os ácidos suberínicos em quantidades preparativas e pureza elevada (≥99,5%); e desenvolver técnicas espectroscópicas, particularmente de RMN, para determinar a configuração estereoquímica dos ácidos suberínicos em C_{18}.

Foi desenvolvido um processo para isolar os ácidos suberínicos após despolimerização da suberina usando solventes de polaridade e temperatura contrastantes, seguido da sua purificação por dupla cromatografia líquida em fase normal (média pressão) e em fase reversa (HPLC).

Provou-se que os ácidos suberínicos $C_{18:1}$ são *cis*, pelos desvios químicos em RMN dos protões e carbonos olefínicos e alílicos, e extracção das constantes de acoplamento por simulação dos espectros. Foi desenvolvida uma técnica, baseada nos desvios químicos dos metinos dos derivados benzilideno-acetal dos *vic*-dióis, provando que os ácidos suberínicos C_{18} 9,10-epóxido são *cis* e que os ácidos C_{18} 9,10-diol são *threo*, sendo ambos misturas racémicas.

A estereoquímica dos ácidos suberínicos será determinante para a compreensão da estrutura macromolecular da suberina e as técnicas desenvolvidas para o seu isolamento preparativo poderão ser a base para a sua comercialização à escala industrial.

Palavras-chave: suberina, cortiça, determinação da estereoquímica por RMN, análise da configuração *cis*/*trans*, análise da configuração *eritro*/*treo*

Introduction

1. Context and importance of suberin

"Suberin" is the name used to describe a family of natural polymeric macromolecules that together with cutin confine and insulate plants from the environment. Suberin and cutin are the main constituents of specialized cell walls that are found in the frontier tissues of plants: cutin is deposited in the outer part of the epidermis, the cell layer that covers the leaves, fruits and stems; suberin is the structural component of suberized cell walls, which are found as "cork" in the outer bark of plants with secondary growth, as trees typically are [1] (Figure 1). Suberized cell walls also develop in other parts of plants, wherever protection and insulation are needed, namely as wound-response tissue, abscission tissue after the fall of leaves, or when water flow needs to be controlled, like in the root hypodermis. Suberin and cutin-rich cell walls act as the barrier "membrane" that protect plants against water-loss, heat and temperature variability, biotic pathogenic attacks, and allows controlled exchanges with the exterior [1]. They are the plants' "skin". The development of these biomacromolecules is believed to have been a key moment in the colonization of land by plant-precursor organisms about 450 million years ago [2]. In spite of their essential role in plants' life, suberin and cutin are still poorly known, both at molecular and macromolecular level. The difference between suberin and cutin is mostly histological (as described above), but some systematic differences might exist in their chemical structure and composition [3,4]. In this work our focus is suberin, although many of the aspects presented and discussed will also be valid to cutin.

In suberized cells suberin can represent up to 45% of the dry weight of the cell walls, making it its most important structural constituent. Using cork as example, suberized cell walls are composed of (average values) extractives (15.6%), suberin (38.6%, not considering glycerol), polyaromatics determined as lignin (21.7%) and polysaccharides (18.2%) [5]. Extractives, which can be removed by simple solvent extraction, are non-polymeric and non-structural compounds associated with the cell walls (Figure 1). In the case of cork, about a third of them are soluble in low-polarity organic solvents, and are col-

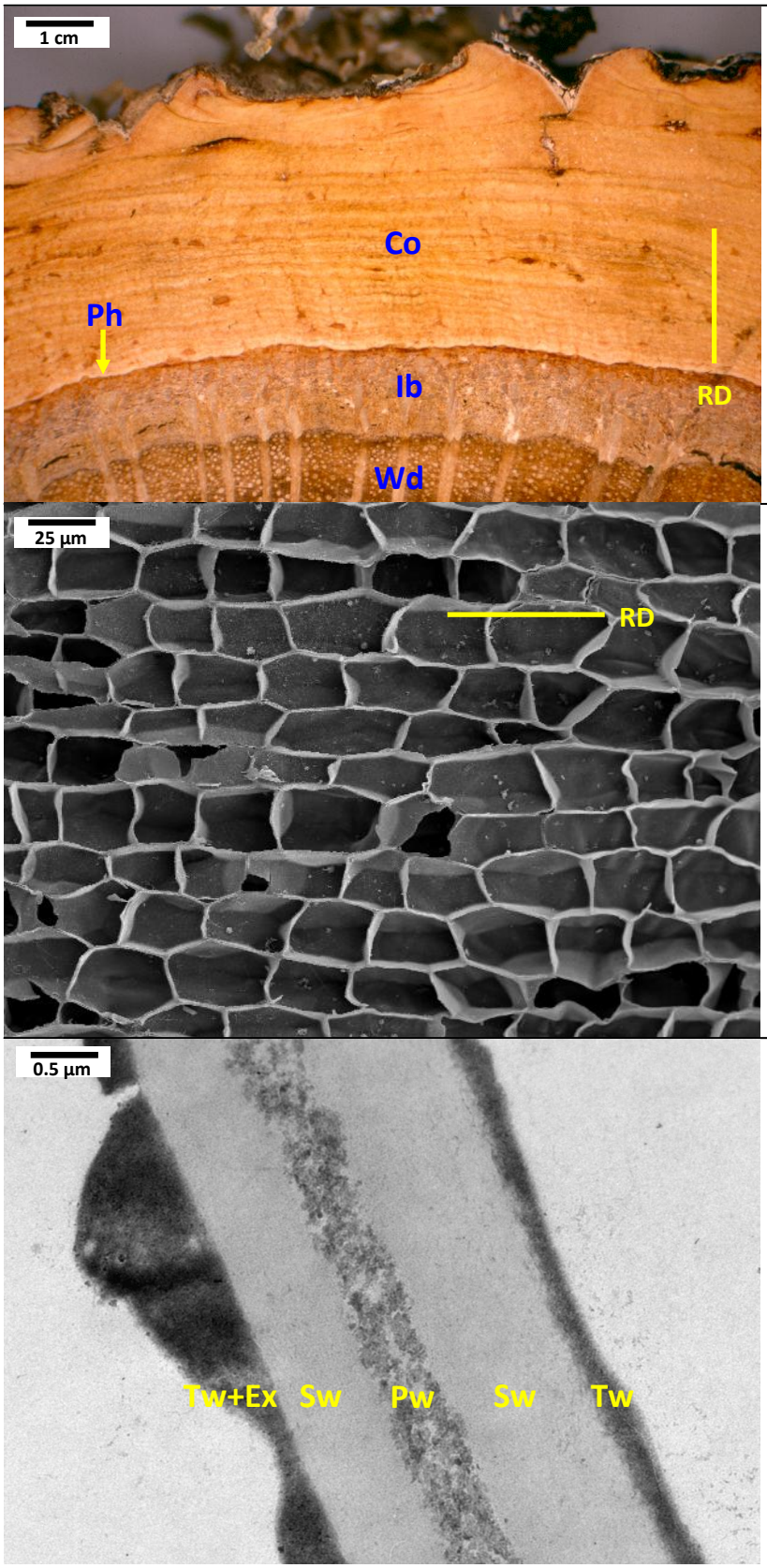

Cork

Outer part of a trunk of a cork-oak tree (transversal section):

Co – cork (outer bark)
Ph – phellogen (cork mother cells)
Ib – inner bark
Wd – wood

RD – radial direction

Cork cells

Transversal section of cork with the cork cells oriented in rows in the radial direction (**RD**)

Cork cell wall

Double cork cell wall:

Pw – double primary wall (polysaccharides + lignin)
Sw – secondary wall (suberin + aromatics)
Tw – tertiary wall (polysaccharides + lignin)
Ex – extractives (triterpenes + waxes)

[Photos by Sofia Cardoso & José Graça, ISA, UTL]

Figure 1. Overview of: cork as part of the tree trunk's tissues; cork cellular structure; and cork cell wall ultrastructure and topochemistry (the latter in part based in the interpretation of Sitte[6]

lectively known as "waxes". These waxes are rich in triterpenes, the more relevant being friedelin, a compound for which a number of processes have been developed to isolate it from cork. After extractives removal, suberin is depolymerized by an ester-breaking reaction and the recovered materials quantified as suberin. This "suberin" is mostly an aliphatic material whose structure is discussed below. The polyaromatics that remain in the residue after suberin removal are in part a true lignin [7,8], but the other part will be a non-lignin aromatic polymer, whose structure and composition are still not known. This latter non-lignin "polyaromatics" are probably associated with the aliphatic suberin in the suberin layer of cork cell walls (Figure 1), and some authors include them under the same designation "suberin" [4,9]. However in the present work "suberin" is defined exclusively as the aliphatic polyester domain.

Suberin is a lipid-like polyester, composed by glycerol and α,ω-bifunctional fatty acid "monomers", named "suberin acids", assembled together by ester bonds. The suberin acids, which typically account for about 85% of suberin, are mostly long-chain, C_{16} to C_{24}, ω-hydroxy fatty acids and α,ω-fatty diacids (Chapter 1). In spite of some relatively recent results that showed how glycerol and the suberin acids are sequentially linked (Chapter 1), practically nothing is known about how the polyester builds up as a macromolecule and is assembled in three dimensions. The two main families of α,ω-bifunctional suberin acids, ω-hydroxyacids and α,ω-diacids, are found in suberin with saturated chains, typically with the C_{16} and C_{22} chain lengths as the most abundant. However, in most suberins, the major group of suberin acids is the one with C_{18} chain length, substituted at mid-chain in carbons C-9 and C-10, in the form of a double bond, an epoxide ring or two vicinal hydroxyl groups (*vic*-diol) (Chapter 1). These C_{18} 9,10-substituted acids are typically dominant in the composition of suberins from different plant sources (Chapter 1).

The C_{18} mid-chain 9,10-substituted suberin acids can have different stereochemical configurations: each of them can exist in the form of two to four stereoisomers (Figure 2). In the case of the 9-unsaturated suberin acids, they

Possible stereoisomers of C_{18} 9-unsaturated suberin acids

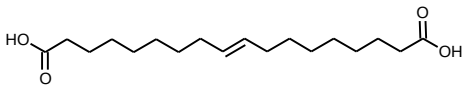

C_{18} *trans*-9-unsaturated a,ω-diacid

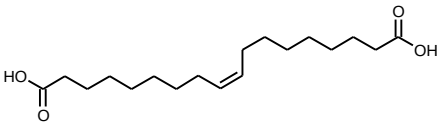

C_{18} *cis*-9-unsaturated a,ω-diacid

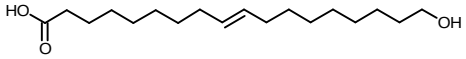

C_{18} *trans*-9-unsaturated ω-hydroxyacid

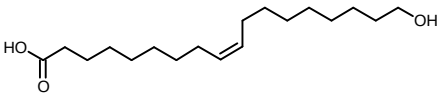

C_{18} *cis*-9-unsaturated ω-hydroxyacid

Possible stereoisomers of C_{18} 9,10-epoxy suberin acids

Absolute configuration	**Relative configuration**
 (*9R**,10*S**)-C_{18} 9,10-epoxy a,ω-diacid [*meso*]	C_{18} *cis*-9,10-epoxy a,ω-diacid
 (*9R*,10*R*)-C_{18} 9,10-epoxy a,ω-diacid	C_{18} *trans*-9,10-epoxy a,ω-diacid
 (*9S*,10*S*)-C_{18} 9,10-epoxy a,ω-diacid	
 (*9S*,10*R*)-C_{18} 9,10-epoxy ω-hydroxyacid	C_{18} *cis*-9,10-epoxy ω-hydroxyacid
 (*9R*,10*S*)-C_{18} 9,10-epoxy ω-hydroxyacid	
 (*9S*,10*S*)-C_{18} 9,10-epoxy ω-hydroxyacid	C_{18} *trans*-9,10-epoxy ω-hydroxyacid
 (*9R*,10*R*)-C_{18} 9,10-epoxy ω-hydroxyacid	

Possible stereoisomers of C_{18} 9,10-diol suberin acids

Absolute configuration	Relative configuration
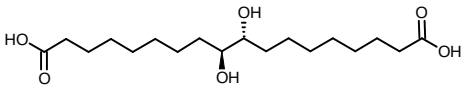 (*9R**,10*S**)-C_{18} 9,10-diol a,ω-diacid [*meso*]	*erythro*-C_{18} 9,10-diol a,ω-diacid
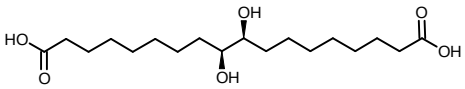 (*9S*,10*S*)-C_{18} 9,10- diol a,ω-diacid	*threo*-C_{18} 9,10-diol a,ω-diacid
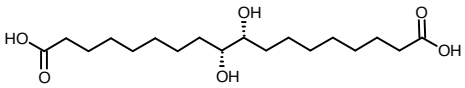 (*9R*,10*R*)-C_{18} 9,10-diol a,ω-diacid	
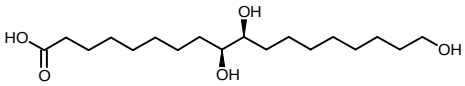 (*9S*,10*S*)-C_{18} 9,10-diol ω-hydroxyacid	*threo*-C_{18} 9,10-diol ω-hydroxyacid
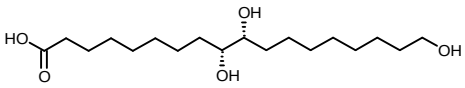 (*9R*,10*R*)-C_{18} 9,10-diol ω-hydroxyacid	
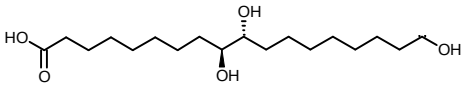 (*9S*,10*R*)-C_{18} 9,10-diol ω-hydroxyacid	*erythro*-C_{18} 9,10-diol ω-hydroxyacid
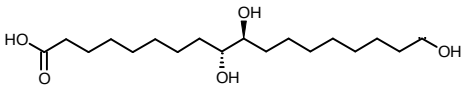 (*9R*,10*S*)-C_{18} 9,10-diol ω-hydroxyacid	

Figure 2. Possible stereoisomers of the main C_{18} cork suberin acids

can be either *cis* or *trans*; in the case of the 9,10-epoxy and 9,10-diol suberin acids, because of their two asymmetric carbons, C-9 and C-10, each one can exist in the form of four different stereoisomers. These four possible stereoisomers correspond to two pairs of enantiomers, each pair with a defined relative configuration (Figure 2). The C_{18} 9,10-epoxyacids can have either *cis* or *trans* relative configuration, each one with two possible absolute configurations. An exception is the C_{18} 9,10-epoxy a,ω-diacid in which the two possible enantiomers of the *cis* form are identical, due to the molecule

symmetry, making it a *meso* compound (Figure 2). The C_{18} 9,10-diol suberin acids can have either *erythro* or *threo* relative configuration, each of them with two possible absolute configurations. The two possible absolute configurations of the *erythro* enantiomeric pair of the C_{18} 9,10-diol α,ω-diacid are however identical molecules, again due to the molecule symmetry, making it also a *meso* compound (Figure 2, see also Figure 1 in Chapter 4). Which stereoisomers of the above discussed suberin acids, or mixtures of them, are actually present in suberin, is not known. The stereochemistry of these suberin acids was studied in a few pioneering works in the 50's and 60's of the last century, but their results were sometimes contradictory and the purity of the samples analyzed in some cases arguable, as those authors themselves mentioned. The determination of the stereochemistry of these suberin acids in cork is one of the main goals of this work (Chapters 3 and 4).

2. Context and importance of cork

Cork from the cork-oak tree is the most representative plant material rich in suberin in such a way that even the name "suberin" is derived from it ("suber" is the Latin word for "Cork-oak" tree). Cork, the outer bark of the cork-oak, is extracted from the trees in a renewable and sustainable manner. When the trees' trunk or branches have a perimeter at breast height of 70 cm (legal minimum) the cork can be removed for the first time; during the spring-summer months, when the cork mother cells (the "phellogen") are active, the cork is stripped away from the tree, after applying a few cuts both longitudinal and transversal, with an axe, through the cork tissue down to the phellogen cell layer. Every nine years (legal minimum) a new cork layer forms and can be harvested again. The cork of best industrial quality is the one from the third extraction on, which is named "amadia" in Portuguese. Cork-oak trees can remain active in cork production and exploitation for hundreds of years, typically around 200 years, to which correspond about 15 consecutive cork harvests [10].

The cork oak occupies about a quarter of the Portuguese forest area (730,000 ha) where it is the more represented species. Portugal produces 52% of the world cork, to which corresponds an average production of 157,000 ton/year [11]. Portugal is also leader in cork industrial transformation, with an exportation value in 2011 of about 800 Million Euro, accounting for 2% of all national exportations (in value) [12]. Due to its economic and social importance the cork oak-tree has been recently nominated as the Portuguese National tree.

Cork production and industry is however strongly dependent in one single product: the cork-stoppers. About 66% of the total Portuguese cork production is destined to the wine industry, namely as natural cork stoppers (43%) and other types of cork-based stoppers (23%) [11]. The exportation of natural cork stoppers represents by itself ca 50% of the value of all exported cork products [11]. Threats from the growing use of plastic and aluminium artificial stoppers, particularly in the more recent wine-producing countries, could put at risk the entire Portuguese cork sector. Therefore, it is urgent to find new, and preferably, complementary and value-added applications for cork. A convenient source for "new uses" for cork can be the actual residues of cork transformation, namely for "chemical uses": the Portuguese cork industry is estimated to produce each year between 17,000 and 45,000 tons of "cork powders" [13]. These cork powders are of heterogeneous origin, and result from different operations of grinding and polishing of several cork products. They can have different particle sizes, down from 0.5 mm to very fine powders with a few micrometers. Some of these cork powders are convenient for the extraction of "chemicals", namely from its most abundant and specific component, suberin [14]. To find a suitable way to extract the suberin acids from cork powders is the other main goal of the present work (Chapter 2).

3. Potential uses of suberin acids

The interest on suberin acids and recognition of their potential for industrial applications goes back to the pioneering works in the last century which showed that suberin was rich in long-chain bifunctional fatty acids. In 1950, one of the most relevant suberin researchers at that time, André Guillemonat, started a company in France to extract chemicals from suberin, named "Fransuber" which commercialized a mixture of suberin acids obtained from cork, named "subéroline" [15]. This researcher patented the method used for the extraction of these suberin acids in 1952 [16]. More recently intense efforts of research were made to find valuable uses for the cork industrial powders [17], including polymeric materials after chemical modification of suberin [18-21]. Suberin from the outer bark of *Betula* spp, was also considered as a source of one of the suberin acids, namely the 9,10-epoxy-18-hydroxyoctadecanoic acid (C_{18} 9,10-epoxy ω-hydroxyacid) [22-24]. Most of these approaches, however, targeted suberin as a whole to be used and processed as a mixture, or after relatively simple purification procedures. Here, the focus is on the potential uses of suberin acids as individual compounds of high purity.

Suberin acids have in the same molecule two structural characteristics that together, make them unique: they have a long-chain hydrocarbon backbone and they have functional reactive groups at both chain ends, either hydroxyl or carboxylic acid. This makes them different from the common fatty acids or alcohols, which have only one functional group, and therefore cannot grow by themselves macromolecules of high molecular mass. Some of the main suberin acids with C_{18} chain-length (discussed in this work) have, besides the two reactive groups at both chain ends, also reactive groups at mid-chain, making them "poly-functional" fatty acids and thus further extending their reactivity and properties. The suberin acids share the properties of the fatty acids and other lipids, like low-polarity, hydrophobicity or capability to self-assemble [25], added to the capacity of establishing covalent linkages, like ester, ether or amide, with at least two other molecules; the latter can be the suberin acids themselves or any other compounds which

can be linked to their functional groups, with the possibility of building polymeric structures.

In the last years, a lot of research has been made concerning possible applications of the long-chain a,ω-bifunctional fatty acids, structurally identical to the suberin monomers, both in academia as well as in private companies. This interest led to continued efforts to produce some of these compounds by biotechnological [26] or synthetic routes [27], and some of the techniques developed have been patented [27]. However, despite of all their promising performance, little has been assayed, mainly because these compounds are not commercially available.

The main potential uses for the suberin acid-like compounds are in the areas of cosmetics for skin care, dermatology, fragrances, medical applications and technical polymers. A few examples of applications already tested, on which some of them gave rise to commercial products, is here listed: a mixture of suberin acids (extracted from cork) esterified to polyols is already commercially available as a skin care ("anti-aging") active ingredient [28], and is already part of some cosmetics [29,30]; civetone and ambrettolide, two important natural "musk" aroma molecules were synthesized starting from suberin acids [31,32]; long-chain ω-hydroxyacids were shown to be effective against a relevant skin disease named atopic dermatitis [33], and some of them showed carcinostatic or anti-mutagenic activity [34]; interest also exist for suberin acids for the synthesis of polyamides [35], specialty elastomers or "biomimetic" membranes [36]. The rationale behind the present work is that the higher the purity of these compounds, the more specific and high-performing their applications will be, and of higher added-value the products they might originate will be.

4. Objectives of this work

This present work had two main objectives:

(1) to develop techniques to extract and isolate the main suberin acid monomers from cork and purify them to very high purity grades, in laboratory scale preparative quantities;

(2) to assign the stereochemical configuration of the C_{18} suberin acids with stereogenic centers derived from their mid-chain substituted groups, using NMR-based and other spectroscopic techniques, in the context of their full structural characterization.

These objectives are included and intend to contribute to wider projects aimed to i) increase the current knowledge on suberin and ii) to find eventual valuable uses for it.

The knowledge of the stereochemistry of the suberin acid monomers is essential for the understanding of the suberin macromolecular structure, namely to know how those monomers organize and pack themselves at three-dimensional level building up eventual ordered structures. The understanding of suberin macromolecular structure will allow a better comprehension of the properties and behavior of cork as a technological material, and to realize how the natural polymers that constitute plants frontier tissues isolate and protect them from the surrounding environment.

The development of techniques to isolate and purify the suberin acids in preparative quantities can also be the basis for the industrial scale-up of their extraction from cork. These suberin acids, due to their chemical and structural specificity, can be the basis for innovative applications, some of them already perspectivated in abundant literature. In that way, and because cork industry residues are a convenient source of suberin, this work expects to contribute in finding new valuable uses for cork.

5. Thesis structure

The present work was mostly developed during the last five years, from 2007 to 2012. The main results were published or are waiting for approval as three international peer-reviewed research papers and one European and International patent.

This manuscript is divided in five chapters. The first chapter, "What is known about suberin?" comprehends the state-of-the art of what was known regarding suberin composition and structure, proposes a model for the suberin macromolecular structure, and was the starting point for the development of the current work. It was published in *Macromolecular Bioscience* in 2007 under the title "Suberin: a biopolyester of plant´s skin" [37].

On chapter two "Extraction and purification of suberin acids from cork", the process that has been developed for the extraction and purification of suberin acids from cork is described. It was submitted for an European and International Patent.

Chapters three "Stereochemistry of monounsaturated cork suberin acids" and four "Stereochemistry of 9,10-epoxy and 9,10-diol cork suberin acids" describe the analysis of the stereochemistry of the C_{18} suberin acids, namely the ones with a mid-chain unsaturation (C_{18} 9-unsaturated α,ω-diacid and ω-hydroxyacid), epoxide ring (C_{18} 9,10-epoxy α,ω-diacid and ω-hydroxyacid) and *vic*-diol group (C_{18} 9,10-diol α,ω-diacid and ω-hydroxyacid). Each chapter includes the article submitted to peer-review, concerning the stereochemistry of unsaturated acids (Chapter three) and of the epoxide and *vic*-diol acids (Chapter four). Finally, on chapter five "Conclusions and future perspectives", the main conclusions of this thesis are described, and some future work perspectives are discussed.

6. Work strategy and development

In this point of the introduction a brief summary is made of the strategy followed in the development of the present work, including mention to some of the "negative" results or "dead-end" experiments. The general workflow is outlined in Schemes 1 and 2.

The starting material for suberin extraction was cork powder from the Portuguese cork industry. In particular under-sized granulated cork, typically cork granules with size of less than 0.5 mm, was used. This material was sieved to extract the "40 to 60 mesh" fraction (0.425-0.250 mm) which was used for the work. The selected cork powder was solvent extracted (successively with dichloromethane, ethanol, and water) to remove the soluble extractives and air dried. After extractives removal, suberin was depolymerized using two ester breaking reactions, affording mixtures of suberin acids both as methyl esters (after the methanolysis reaction) or as free carboxylic acids (after the alkaline hydrolysis reaction).

In some cases, the suberin acids were recovered to an organic phase (separating glycerol and the reactants to the aqueous phase); in others, the mixture of suberin acids was directly extracted from the depolymerization products as part of the first isolation step.

A first cleaning step was attempted to remove the colored matter responsible for the suberin acids mixture typical dark-caramel brown color. Activated charcoal and diatomaceous earth were assayed with poor results.

Seven of the main cork suberin acids were targeted for isolation and purification, due to their quantitative representativeness in the suberin macromolecule and/or potential interest: the six C_{18} mid-chain substituted suberin monomers already discussed and the C_{22} saturated-chain ω-hydroxyacid. The general strategy followed to isolate and purify the targeted suberin acids involved two main stages: (i) separation by differential solvent solubility and (ii) purification by chromatographic techniques; in each stage contrasting polarity/affinity of the separating media was used in succession: non-

polar/polar solvents in the separation steps and normal phase/reversed phase in the chromatographic purification steps.

Scheme 1

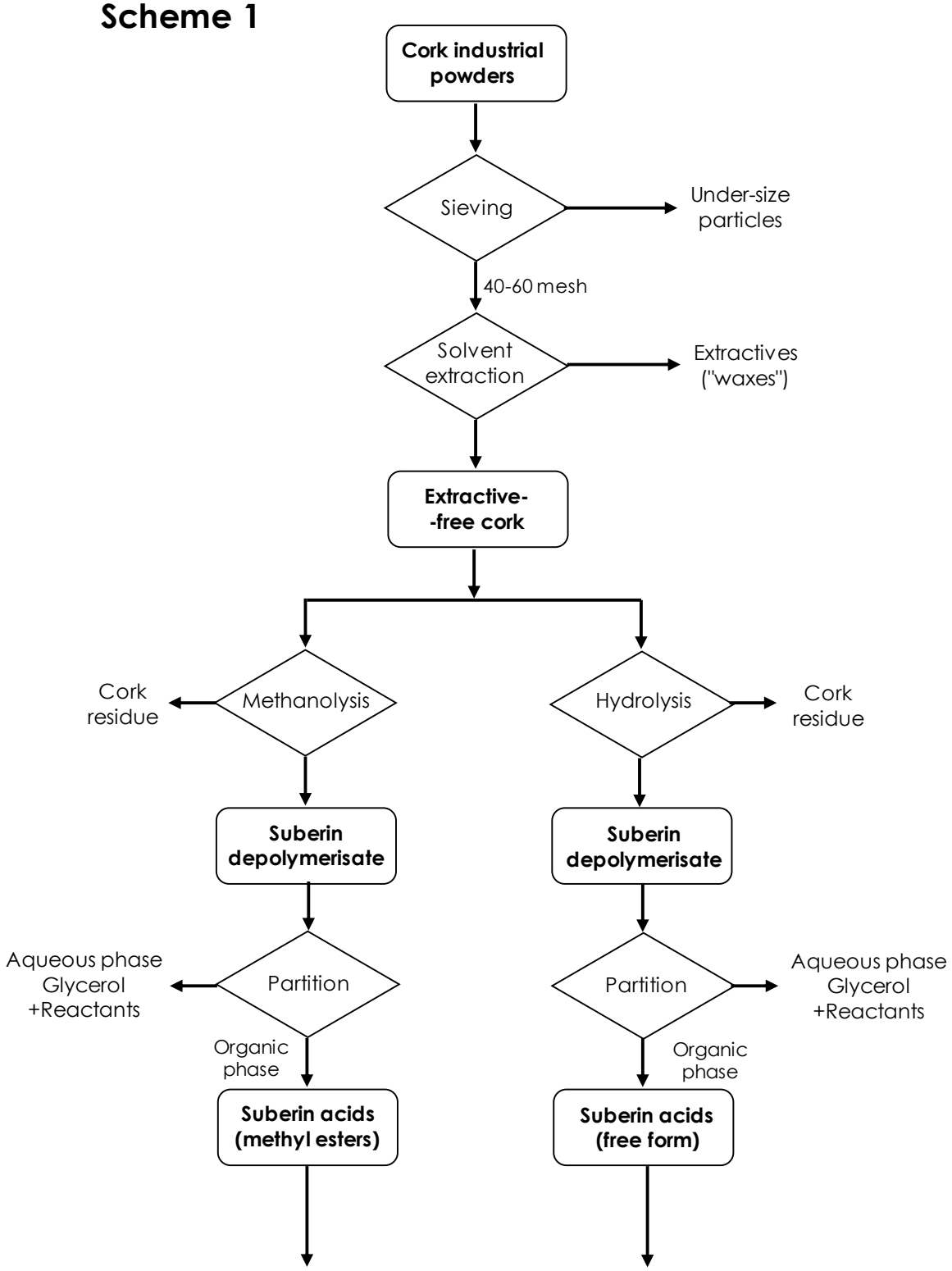

Scheme 1. General work-flow from the cork powders to suberin acids mixtures

Scheme 2

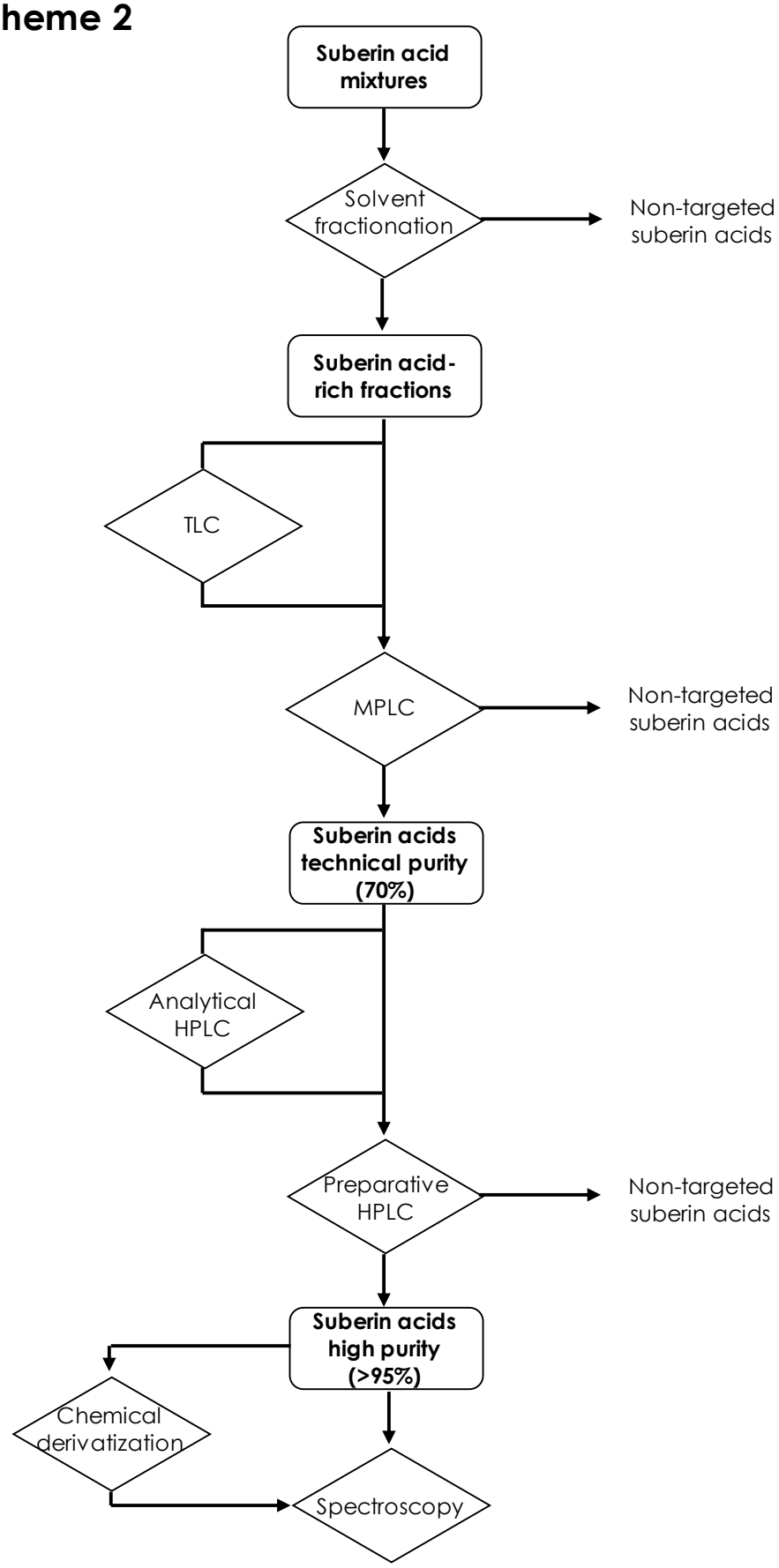

Scheme 2. General work-flow from suberin acids mixtures to individual structural and spectroscopic characterization

The first separation step was applied to the suberin acid mixtures using a non-polar solvent, followed by a polar one, solubilizing in both cases the suberin acid mixtures at temperatures close to the solvent boiling point, and separating precipitated from soluble matters at room temperature and/or cooling to a temperature close to 0 ºC. In this way a pre-separation based in polarity/solubility differences was achieved, and fractions "enriched" in the targeted suberin acids were obtained. Isolation sequences included all the above steps or were simpler whenever possible, depending on the specific acids or if they were in the form of methyl esters or free acids.

Each enriched fraction thus obtained including the targeted suberin acids was then submitted to two separation/purification chromatographic steps. The first step included medium pressure liquid chromatography (MPLC) in normal-phase. Before this column chromatography, solvent eluent mixtures were studied and optimized to achieve the desired separation in silica by thin layer chromatography (TLC) (Results not presented in the text). After this chromatographic step, suberin acid "isolates" were obtained, typically with technical grade purity (>70%). These suberin acids were then purified by preparative high-performance liquid chromatography (prep-HPLC) in reversed phase mode. The HPLC chromatographic methods were previously developed at analytical level (Results not presented in the text), and were afterwards scaled-up and optimized for the preparative separations. After this final purification step the targeted suberin acids were obtained with purities above 97% and, for some of them, with purities above 99.5%.

The highly pure suberin acids were afterwards characterized by spectroscopic techniques, namely Fourier transform infrared (FTIR), and Raman spectroscopy and nuclear magnetic resonance spectroscopy, including one-dimensional (1D) techniques (^{1}H, ^{13}C, ^{13}C DEPT) and two-dimensional (2D) homo and hetero correlation techniques (COSY, HSQC, HMBC). Besides, the suberin acids were analyzed by differential scanning calorimetry (DSC), and their thermal behavior, namely the melting point, extracted from the thermograms. The suberin acids were also analyzed by mass-spectrometry

(GC-EIMS), the ones obtained in the form of methyl esters as trimethylsilyl (TMS) ethers, and the ones isolated in the form of free acids as TMS ethers/TMS esters derivatives. To assign the position of the double bond in the $C_{18:1}$ 9-unsaturated suberin acids, their picolinyl esters and DMOX derivatives were produced (from the acids in the free form) and analyzed by GC-EIMS. Finally, the specific rotation of the C_{18} suberin acids with quiral centers, namely the C_{18} 9,10-epoxy and 9,10-diol, was also measured.

To assign the stereochemistry of the C_{18} mid-chain substituted suberin acids, the second main objective of the present work, the results from their spectroscopic characterization were used as a starting point. In most of the cases, however, the information from the FTIR, Raman and NMR spectra was not by itself sufficient to allow an ambiguous and definite assignment of the stereochemistry of these suberin acids. The analysis by NMR, probably the most powerful tool for stereochemical configuration determination, was in particular impaired by the high symmetry of all these molecules in relation to the substituent of interest at mid-chain. The protons of more diagnostic value, namely the methynes at C-9 and C-10, typically showed up as complex multiplets. To overcome this situation two approaches were followed: to co-analyze by the same spectroscopic techniques model compounds structurally very close to the suberin acids under study, with known and different stereochemistry, namely the C_{18} mono fatty acids with the same mid-chain substituent groups; and to synthesize derivatives modifying these mid-chain substituent groups, so that the relevant protons and carbons showed different chemical shifts depending on the stereochemistry of the original groups, and in that way allowing the assignment of their stereo-chemistry.

In the case of the $C_{18:1}$ 9-unsaturated suberin ω-hydroxyacid, a first attempt was made to resolve the signal of the two methyne protons of the double bond at C-9 and C-10, and in that way making possible the measurement of their coupling constant. To achieve this, an extremely deshielding group, pentafluorophenyldimethylsilyl (flophemesyl) – $C_8H_6F_5Si$ – (Figure 3) was linked to the hydroxyl moiety of the $C_{18:1}$ ω-hydroxyacid. However, although an

important deshielding effect was obtained through the molecule up to a distance of 10 carbon atoms away from the flophemesyl group, the protons of interest still had similar chemical shifts and appeared unresolved.

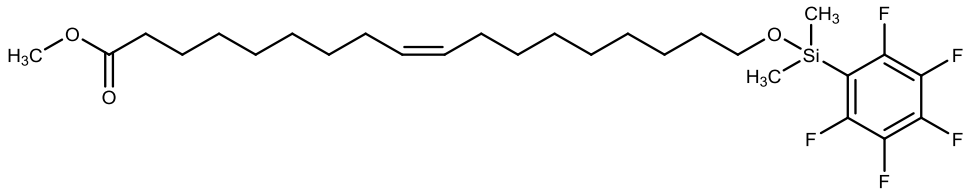

Figure 3. C_{18} *cis*-9-unsaturated ω-hydroxyacid methyl ester, flophemesyl ether

The second, and most successful approach to assign the *cis* or *trans* configuration of the $C_{18:1}$ suberin acids, was to compare the chemical shifts of their olefinic (at C-9 and C-10) and allylic (at C-8 and C-10) protons and ^{13}C carbons with the ones of similar model compounds with known stereochemistry. The results this way obtained were confirmed by the extraction of the coupling constants contributing to the olefinic multiplets by spectra simulation.

In the case of the analysis of the stereochemistry of the C_{18} 9,10-epoxy suberin acids, relevant information could be extracted directly from the spectroscopic data of the original compounds and comparing it with the results from the model compounds. However, because the conclusions weren't totally unambiguous, the suberin (and model compound) C_{18} 9,10-epoxyacids were converted to C_{18} 9,10-diols by stereospecific reactions, and in that form analyzed together with the C_{18} 9,10-diol suberin acids; in this way its original stereochemistry was inferred backwards.

The first approach to analyze the stereochemistry of the C_{18} 9,10-diol suberin acids, was to use chiral derivatization agents (CDA) together with NMR analysis. Two different pairs of CDAs were assayed: (*R*)-1-phenylethanamine and (*S*)-1-phenylethanamine, linked to 2-formylphenylboronic acid esterified to the *vic*-diol group (Figure 4 B); and (*R*)–($^{-}$)–α– and (S)–($^{+}$)–α–methoxyphenylacetic acid (MPA), bi-esterified to the two hydroxyls previously converted

to acyl chlorides (Figure 4 A). No NMR differences were observed between the *R* and *S* derivatives of the C_{18} 9,10-diol suberin acids in both cases. Therefore no information about the suberin *vic*-diols stereochemistry was obtained this way, probably due to the symmetry of the molecules in relation to the C-9 – C-10 sigma bond and the eventual free rotation around the latter.

The second approach was to find derivates that "fixed" the position of the vicinal hydroxyls, and in that way also "fixed" the relative positions of the diagnostic methyne protons equally linked to the C-9 and C-10 carbons, for NMR analysis. Two groups normally used for the protection of 1,2-diols were assayed to convert the *vic*-diols to a dioxolane acetal ring: isopropylidene acetals, through reaction with acetone (Figure 4 C), and benzylidene acetals, through reaction with benzaldehyde dimethyl acetal (Figure 4 D). In the NMR spectra of both derivatives, no evidence of the stereochemistry of the *vic*-diol groups in the suberin acids was possible to be extracted. However we decided to use one of these derivatives in model compounds (and in the hydrolyzed suberin epoxyacids) with structurally similar *vic*-diol groups, with known relative stereochemistry. The derivatives chosen were the benzylidene acetals, because they are less symmetrical than the isopropylidene acetals, and include a phenyl group, with potentially stronger deshielding effects. The protons and carbons of the methyne groups at C-9 and C-10 linked to the benzylidene acetal groups, showed significantly different chemical shifts depending on the relative stereochemistry of the original *vic*-diol (*erythro* or *threo*). In this way the relative stereochemistry of the C_{18} 9,10-epoxy and the C_{18} 9,10-diol suberin acids was assigned. The absolute stereochemistry of these same suberin acids was tentatively assigned by their specific rotation measured by polarimetry.

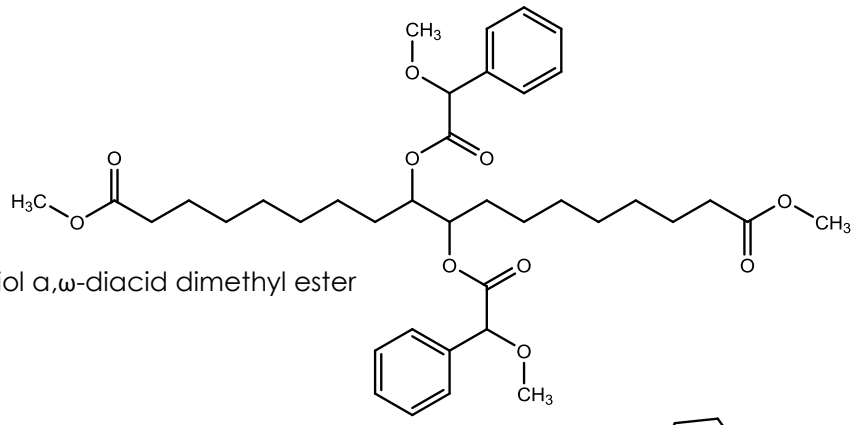

A) C_{18} 9,10-diol a,ω-diacid dimethyl ester bis MPA

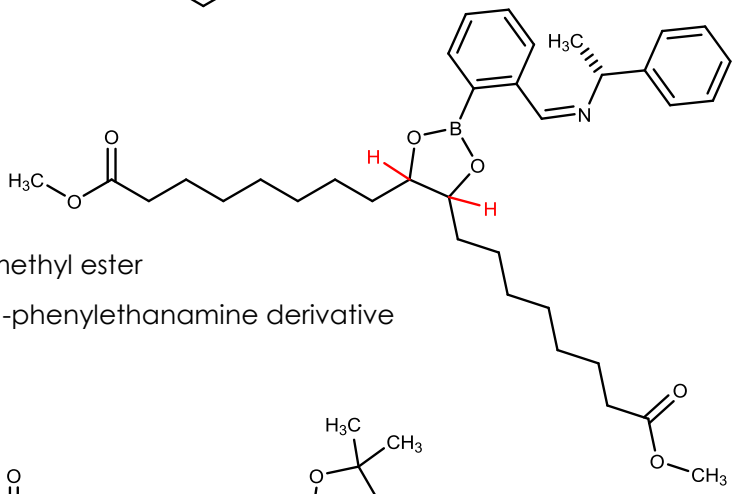

B) C_{18} 9,10-diol a,ω-diacid dimethyl ester 2-formylphenylboronate (*R*)-1-phenylethanamine derivative

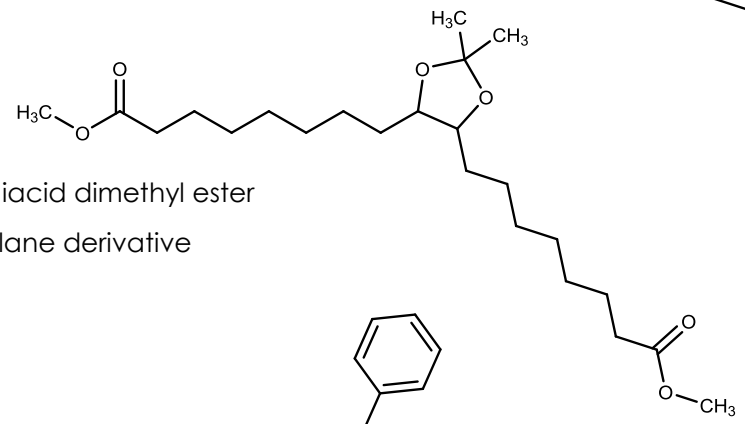

C) C_{18} 9,10-diol a,ω-diacid dimethyl ester isopropylidene-dioxolane derivative

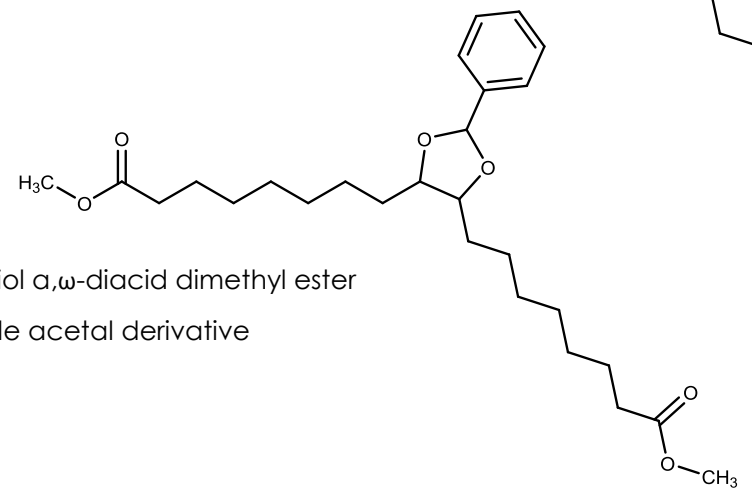

D) C_{18} 9,10-diol a,ω-diacid dimethyl ester benzaldehyde acetal derivative

Figure 4. C_{18} 9,10-diol a,ω-diacid derivatives assayed

7. References

[1] Evert, R. 2006. *Esau´s Plant Anatomy*. John Wiley & Sons: New Jersey.

[2] Kenrick, P., Crane, P. 1997. The origin and early evolution of plants on land. *Nature* **384**(4): 33-39.

[3] Kolattukudy, P. 2002. Cutin from plants. In: Doi, Y., Steinbüchel, A., editors. *Biopolymers - Polyesters I*. Wiley-VCH, Weinheim. pp. 1-40.

[4] Kolattukudy, P. 2002. Suberin from plants. In: Doi, Y., Steinbüchel, A., editors. *Biopolymers - Polyesters I*. Wiley-VCH, Weinheim. pp. 41-73.

[5] Pereira, H. 1988. Chemical composition and variability of cork from *Quercus suber* L. *Wood science and technology* **22**(3): 211-218.

[10] Sitte, P. 1955. Der Feinbau verkorten Zellwände. *Mikroskopie* **10**(5-6): 178-200.

[7] Marques, A., Pereira, H., Meier, D. Faix, O. 1996. Isolation and characterization of a guaiacyl lignin from saponified cork of *Quercus suber*. *Holzforschung* **50**(5): 393-400.

[8] Marques, A., Pereira, H., Meier, D. Faix, O. 1999. Structural characterization of cork lignin by thioacidolysis and permanganate oxidation *Holzforschung* **53**(2): 167-174.

[9] Bernards, M., Razem, F. 2001. The poly(phenolic) domain of potato suberin: a non-lignin cell wall bio-polymer *Phytochemistry* **57**(7): 1115-1122.

[10] Natividade, J. 1950. *Subericultura*. Direcção Geral das Florestas, Lisboa.

[11] Associação Portuguesa de Cortiça. 2010. *Cork statistics, cork statistic bureau*. http://apcor.pt/userfiles/File/Cork%20Statistics.pdf.

[12] Associação Portuguesa de Cortiça. 2012. *Comercialização de produtos portugueses da cortiça*. http://www.apcor.pt/artigo/comercializacao-cortica.htm

[13] Gil, L. 1997. Cork powder waste: an overview. *Biomass & Bioenergy* **13**(1-2): 59-61.

[14] Graça, J. 2006. *Caracterização dos pós de cortiça com vista à sua utilização como fonte de produtos químicos*. Relatório de execução material do projecto FCT POCTI/AGR/46419/2002. Instituto Superior de Agronomia, Lisboa.

[15] Guillemonat, A. 1949. Le liège matière première d'une industrie chimique. *Revue du bois e de ses applications* **4**(1): 4-6.

[16] United States Patent 2617814. 1952. *Methods of extracting fatty matters from cork*. Applicant: Société Suber [FR].

[17] Godinho, M., Martins, A., Belgacem, M., Gil, L., Cordeiro, N. 2001. Properties and processing of cork powder filled cellulose derivatives composites. *Macromolecular symposia* **169**: 223-228.

[18] Cordeiro, N., Blayo, A., Belgacem, N., Gandini, A., Neto, C., LeNest, J-F. 2000. Cork suberin as an additive in offset lithographic printing inks. *Industrial crops and products* **11**(1): 63-71.

[19] Evtiouguina, M., Gandini, A., Neto, C., Belgacem, N. 2001. Urethanes and polyurethanes based on oxypropylated cork: 1. Appraisal and reactivity of products. *Polymer international* **50**(10): 1150-1155.

[20] Evtiouguina, M. Barros-Timmons, A., Cruz-Pinto, J., Neto, C., Belgacem, M. Gandini, A. 2002. Oxypropylation of cork and the use of the ensuing polyols in polyurethane formulations. *Biomacromolecules* **3**(1): 57-62.

[21] Gandini, A., Neto, C., Silvestre, A. 2006. Suberin: A promising renewable resource for novel macromolecular materials. *Progress in polymer science* **31**(10): 878-892.

[22] Olsson, A., Lindström, M., Iversen, T. 2007. Lipase-catalyzed synthesis of an epoxy-functionalized polyester from the suberin monomer *cis*-9,10-epoxy-18-hydroxyoctadecanoic acid. *Biomacromolecules* **8**(2): 757-760.

[23] Pinto, P., Sousa, A., Silvestre, A., Neto, C., Gandini, A., Eckerman, C., Holmbom, B. 2009. *Quercus suber* and *Betula pendula* outer barks as renewa-

ble sources of oleochemicals: a comparative study. *Industrial crops and products* **29**(1): 126-132.

[24] International Patent WO/2010/093320 (A1). 2010. *A method for separating from suberin and/or cutin containing plants, a solid and/or oil fraction enriched in cis-9,10-epoxy-18-hydroxyoctadecanoic acid*. Applicant: Innventia AB [SE].

[25] Douliez, J-P., Barrault, J., Jerome, F., Heredia, A., Navailles, L., Nallet, F. 2005. Glycerol derivatives of cutin and suberin monomers: synthesis and self-assembly. *Biomacromolecules* **6**(1): 30-34.

[26] Huf, S., Krügener, S., Hirth, T., Rupp, S., Zibek, S. 2011. Biotechnological synthesis of long-chain dicarboxylic acids as building blocks for polymers. *European journal of lipid science and technology* **113**(5): 548-561.

[27] European Patent 0711746 (A1). 1996. *Process for preparing hydroxycarboxylic acids*. Applicant: Unilever [NL].

[28] Ashland. 2011. *Suberlift™*. http://online1.ispcorp.com/en-us/pages/ProductDetail.aspx?BU=Personal%20Care&l1=Function&l2=Vincience%20Actives&prodName=Suberlift%E2%84%A2&prdId=53157.

[29] GoodSkin Labs. 2012. *Eyeliplex-2™*. http://www.goodskinlabs.com/?q=website_admin/node/223/&menu=942.

[30] Peter Thomas Roth clinical skin care. 2012. *Firmx™ Growth factor extreme neuropeptide serum*. http://www.peterthomasroth.com/p-130-firmx-growth-factor-extreme-neuropeptide-serum.aspx.

[31] Seoane, E., Llinares, J., Arno, M. 1978. Síntesis estereoespecífica de *cis*- y *trans*-civetona. *Anales de química* **74B**: 654-657.

[32] Sanz, V., Seoane, E. 1982. Synthesis of ambrettolide from phloionolic acid. *Journal of the chemical society - Perkin transactions 1* **8**: 1837-1839.

[33] Horrobin, D. 2000. Essential fatty acid metabolism and its modification in atopic eczema. *American journal of clinical nutrition* **71**(1S): 367S-372S.

[34] Krizková, L., Lopes, M., Polónyi, J., Belicová, A., Dobias, J., Ebringer, L. 1999. Antimutagenicity of a suberin extract from *Quercus suber* in cork. *Mutation research* **446**(2): 225-230.

[35] Pardal, F., Salhi, S., Rousseau, B., Tessier, M., Claude, S., Fradet, A. 2008. Unsaturated polyamides from bio-based *Z*-octadec-9-enedioic acid. *Macromolecular chemistry and physics* **209**(1): 64-74.

[36] Aquaporin. 2010. http://www.aquaporin.dk.

[37] Graça, J., Santos, S. 2007. Suberin: a biopolyester of plants' skin. *Macromolecular bioscience* **7**(2): 128-135.

Chapter 1: What is known about suberin?

[Graça, J., Santos, S. 2007. Suberin: a biopolyester of plants' skin. *Macromolecular Bioscience*, **7**(2): 128-135]

1. Introduction

Suberin is a biopolymer present in specialized plant tissues, whenever confinement or protection against the surroundings is necessary [1,2]. Suberin is present in suberized cells, where it represents up to 50% of the chemical composition of its cell walls [3]. In the outermost tissues of plants, suberized cells play a vital role affording protection against environmental aggressions and pathogens and controlling temperature and water loss [1,2]. Some plants have significant quantities of suberized cells, namely the bark of a few tree species. The more familiar case is cork, the bark of the cork oak tree, used in cork stoppers and insulation and decorative products.

Suberin is a polyester biopolymer. A complex mixture of monomers with hydroxy and carboxylic acid functionalities is released upon suberin depolymerization. Most of the suberin monomers are aliphatic long-chain α,ω-diacids and ω-hydroxyacids, together with glycerol [4]. How these monomers are assembled at macromolecular level is poorly understood. The polyester aliphatic structure has extensive links to aromatic moieties, and some authors regard "suberin" as the overall aggregate of the polyaliphatic and polyaromatic domains [5,6]. Attempts to find uses for suberin are old, and have known a recent surge because of the development of new isolation techniques and the search for bio-based materials.

2. Suberin in plant tissues

Suberin is mainly found in the periderm of plants, such as tree barks and tuber skins. Suberized cells are also found in a number of other plant tissues, including the epidermis and hypodermis of roots, the endodermis, the bundle sheath of grasses and the sheath around crystal cells. The abscisic tissue of falling leaves and the plants' cicatricial tissue after wounding are also made of suberized cells [7,8]. Cork, the outer bark of the cork oak tree (*Quercus suber* L.), is one of the known plant tissues with the highest suberin content, up to 50% of its dry weight [3]. Cork is a renewable forest resource and is harvested

on a sustainable basis, every 9 to 10 years. Cork oak trees remain in production for at least 200 years [9].

3. Suberin in suberized cell walls

Suberized cell walls are generally very thin, less than 1 µm thick, and show a primary wall, a secondary wall, and sometimes a tertiary wall, which confines the cell lumen (Figure 1). In cork, these cell walls have, as structural components, suberin (50%), polyaromatics (30%), and polysaccharides (20%) [3]. Suberized cells also include significant quantities of extractives, deposited at the inner side of the cell wall (Figure 1).

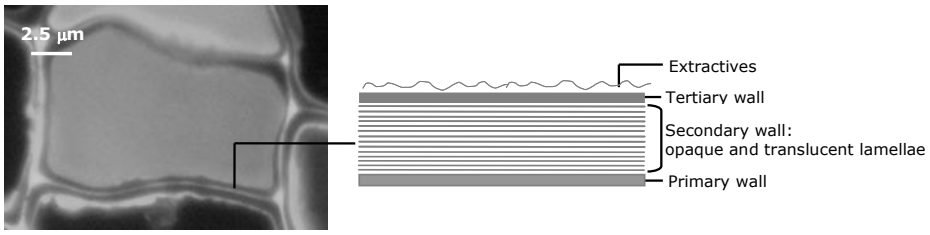

Figure 1. Cross-section of suberized cork cell (UV fluorescence microscopy)

Topochemical studies showed that the polysaccharides and part of the polyaromatics are located in the primary and tertiary walls [10]. The secondary wall, which accounts for most of the cell wall thickness, is where suberin and part of the polyaromatics are located. Some pioneering works have located part of the extractives associated with suberin within the secondary cell wall [11].

The suberin-containing secondary cell walls show a lamellate structure at ultrastructural level, as seen by transmission electron microscopy (TEM). After appropriate staining, these lamellae show alternate opaque and translucent contrast. In cork cell walls, the translucent lamellae have a regular thickness of ca 30 Å. Opaque lamellae have variable thickness of ca 70 to 100 Å. Between 30 and 60 lamellae have been counted in the suberized cell walls of

cork. Polarized light studies have shown that within the translucent lamellae there are ordered structures perpendicular to the plane of the lamellae [11].

4. Suberin monomeric composition

Suberin in situ is an insoluble polymer and its removal from suberized tissues is achieved by depolymerization reactions. Suberin depolymerization can be performed by any of the reactions that break ester bonds, like hydrolysis, alcoholyis or hydrogenolysis. The analysis of suberin monomers can be conveniently performed after methanolysis depolymerization, catalyzed by sodium methoxide [12]. The resulting depolymerizate mixture, after silylation, is then analyzed by gas chromatography coupled to mass spectrometry (GC-MS). The main suberin monomers are glycerol, long-chain a,ω-diacids, and long-chain ω-hydroxyacids. Small quantities of 1-alkanols and 1-alkanoic acids are also present among the suberin depolymerization products [12] (Table 1).

Glycerol is one of the main suberin monomers and can represent up to 26% of the total monomer mixture (Table 1). Long-chain suberin monomers have, as dominant chain-lengths, 16, 18 and 22 carbons [13,14]. C_{16} and C_{22} monomers have saturated alkyl chains. Most of the C_{18} monomers are ω-hydroxyacids and a,ω-diacids with mid-chain substituents, such as an unsaturation, an epoxide or a *vic*-diol group. In many suberins, a,ω-diacids are the dominant class of monomers, followed by ω-hydroxyacids [12-14]. 1-alkanols and 1-alkanoic acids, which cannot make the biopolymer grow because they have only one functional group, are generally present in smaller quantities. Some suberins have very low proportions of mid-chain oxygenated groups, while others have this type of monomer as the main constituent (Table 1).

Although the relative abundance of saturated and mid-chain substituted monomers varies depending on the plant species, the basic pattern of glycerol, a,ω-diacids and ω-hydroxyacids seems to be general in suberin

[12,15]. Table 1 shows the monomeric composition of suberin from several plant sources.

Table 1. Suberin composition (in percentage w/w of total) of *Pseudotsuga menziesii, Quercus suber*, and *Solanum tuberosum* periderms, determined after methanolysis depolymerization

		Composition		
		Pseudotsuga menziesii[12]	Quercus suber[12]	Solanum tuberosum[16]
Glycerol	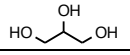	**26.0**	**14.2**	**22.0**
Phenolics	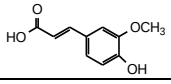	**0.8**	**0.8**	**1.0**
Ferulic acid		0.6	0.5	0.8
1-Alkanols (C_{18}–C_{26})	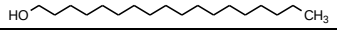	**0.6**	**0.4**	**2.5**
1-Alkanoic acids		**5.2**	**1.1**	**8.4**
C_{16}–C_{22}	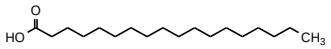	3.6	1.0	0.7
C_{23}–C_{30}		1.6	0.1	7.7
Saturated α,ω-diacids		**29.2**	**8.7**	**1.8**
Hexadecanedioic acid	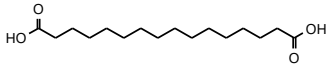	18.7	2.0	0.7
Docosanedioic acid		1.6	4.5	-
C_{18}, C_{20}, C_{24}, C_{26}		8.9	2.2	1.1
Substituted α,ω-diacids		**10.7**	**36.8**	**30.2**
Octadec-9-ene-1,18-dioic acid	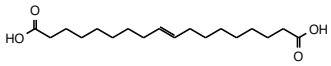	9.1	6.2	30.1
9-Epoxyoctadecane-1,18-dioic acid	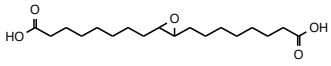	-	22.9	-
9,10-Dihydroxyoctadecane-1,18-dioic acid	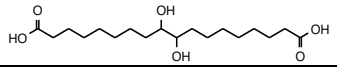	1.6	7.7	0.1
Total of α,ω-diacids		**39.9**	**45.5**	**32.0**
Saturated ω-hydroxyacids		**9.5**	**11.4**	**2.7**
16-Hydroxyhexadecanoic acid	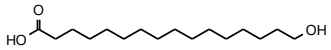	4.3	0.4	1.3
22-Hydroxydocosanoic acid		1.7	7.9	0.6
C_{18}, C_{20}, C_{24}–C_{28}		3.5	3.1	0.8
Substituted ω-hydroxyacids		**1.9**	**14.9**	**12.1**
18-Hydroxyoctadec-9-enoic acid	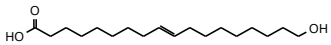	1.7	5.4	12.1
9-Epoxy-18-hydroxyoctadecanoic acid	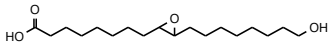	-	7.3	-
9,10,18-Trihydroxyoctadecanoic acid	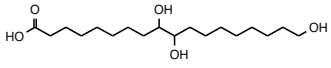	0.2	2.2	-
Total of ω-hydroxyacids		**11.4**	**26.3**	**14.8**
Others		2.2	1.0	-
Unidentified		13.9	10.7	19.3
Total		**100.0**	**100.0**	**100.0**

5. Suberin oligomeric blocks

Suberin oligomeric blocks are obtained by suberin partial depolymerization. This partial depolymerization can be done by methanolysis using calcium oxide and calcium hydroxide as catalysts, releasing ca 10% of suberin [4,16,17]. The oligomeric blocks have been identified by electrospray ionization coupled to tandem mass spectrometry in a triple-quadrupole (ESI-MS/MS), which allows the analysis of larger molecules. The identification of these structures was confirmed after the synthesis of model compounds. Table 2 presents some examples of the main oligomeric blocks found so far in suberin.

Three types of suberin oligomeric blocks with two and three ester-linked monomers have been identified (Table 2). (1) Linear esters: dimeric esters of linearly-linked ω-hydroxyacids and a,ω-diacids [17]. (2) Glyceryl esters: glycerol esterified to a,ω-diacids, to ω-hydroxyacids, and to 1-alkanoic acids, in the form of monoacylglycerols [4,15,16,18]; a,ω-diacids linked at both ends to glycerol units, in the form of diglycerol diacids [17,18]; glycerol linked to two a,ω-diacids in the form of diacylglycerols [18]; glycerol esterified as mono-acylglycerol to linear dimeric esters of a,ω-diacids and ω-hydroxyacids [18]. (3) Feruloyl esters: ferulic acid linked to ω-hydroxyacids [15,16,19,20], and this structure esterified to glycerol, in the form of a trimeric diester [20].

Table 2. Oligomeric blocks found in cork suberin

Linear esters[17]
9-epoxyoctadecane-1,18-dioic acid esterified to 9-epoxy-18-hydroxyoctadecanoic acid
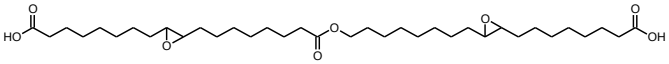
18-hydroxyoctadec-9-enoic acid esterified to 18-hydroxyoctadec-9-enoic acid
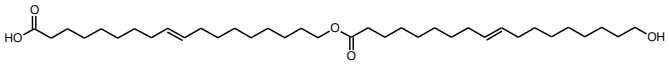
Glyceryl esters[4,15-18]
Glycerol esterified to octadec-9-ene-1,18-dioic acid
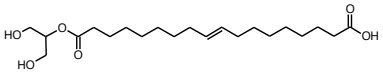
Glycerol esterified to 9-epoxyoctadecane-1,18-dioic acid esterified to glycerol
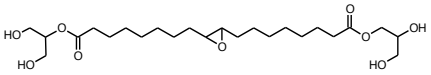
Octadec-9-ene-1,18-dioic acid esterified to glycerol esterified to 9-epoxyoctadecane-1,18-dioic acid
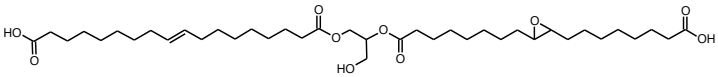
Glycerol esterified to 18-hydroxyoctadec-9-enoic acid esterified to 9-epoxyoctadecane-1,18-dioic acid
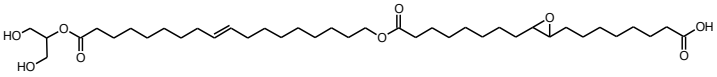
Glycerol esterified to octadec-9-ene-1,18-dioic acid esterified to 9-epoxy-18-hydroxyoctadecanoic acid
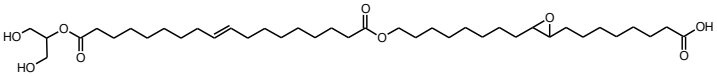
Feruloyl esters[15,16,19,20]
22-hydroxydocosanoic acid esterified to ferulic acid
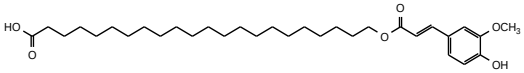
Glycerol esterified to 22-hydroxydocosanoic acid esterified to ferulic acid
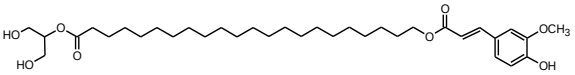

6. Suberin-associated polyaromatics

The suberin aliphatic polyester is closely associated with polymeric aromatics in suberized cell walls [5,6]. When the polyester is depolymerized, aromatic compounds are co-solubilized in different amounts, depending on the depolymerization technique used. GC-MS analysis of the suberin depolymerizates shows the presence of ferulic acid, although generally in small quantities. In the residue of the suberized materials, after suberin depolymeri-

zation, significant quantities of polyaromatics remain [21,22]. The nature of these polyaromatics and how they are associated with the suberin aliphatic polyester are still to be elucidated.

Two different populations of polyaromatics are apparent in suberized cell walls. Evidence from CP-MAS solid-state ^{13}C NMR spectroscopy led to the hypothesis that most of the suberin-associated polyaromatics were of a poly(ferulic acid) structure [21,23]. However, these polyaromatics were shown to be, in part, a lignin of the guaiacyl type, i.e. having as building monomer coniferyl alcohol [22,24]. Both coniferyl alcohol and ferulic acid are phenylpropanoids, mono-methoxylated in the phenolic ring. In addition, results from solid-state ^{13}C NMR spectroscopy showed the presence of two distinct phenylpropanoid populations in suberized cell walls, with distinguishable spin-lattice relaxation behavior [25]. One of these populations included guaiacyl and sinapyl (di-methoxylated) phenolic rings and was associated with polysaccharide-type glycosides [26].

Ferulic acid surely plays an important role in suberized cell walls. The partial depolymerization of suberin released dimeric blocks in which ferulic acid is ester-linked to the primary hydroxy group of ω-hydroxyacids [16,19] (Table 2). In addition, trimeric structures, which form when the above dimeric block is esterified to glycerol through the acid function of the ω-hydroxyacid, were found in cork suberin (Table 2). Together this led to the proposal that ferulic acid covalently links the suberin aliphatic polyester to the neighboring polyaromatics [20].

These results show that two types of polyaromatics may be present in suberized cell walls. One, associated with the polysaccharides in the primary (and tertiary) cell wall, will be a true lignin. The other, associated with the suberin polyester in the secondary cell wall, will be a polymer either based on ferulic acid, or a yet to be elucidated structure.

7. Suberin macromolecular structure

How are the a,ω-diacids, ω-hydroxyacids, and glycerol, assembled as a polyester macromolecule? How the macromolecule is spatially organized? Is there some kind of ordered arrangement? How does the macromolecular structure of suberin fit the lamellar ultrastructure of suberized cell walls? Current knowledge is manifestly insufficient to appropriately answer these questions, but some founded speculation is allowed. Evidence of suberin structure comes from two main sources: the oligomeric blocks obtained after partial depolymerization [4,17,18,20] and the observations on the intact biopolymer by solid-state NMR [21,27,28].

As a result of suberin partial depolymerization, several types of structural blocks have been found so far (Table 2). Although these oligomeric fragments were found in relatively small quantities, ca 10% of total suberin, they can give important insight into the polymer structure. The glycerol-a,ω-diacid-glycerol structure can be the basis of a three-dimensional polymeric network. The relative molar proportions of glycerol and a,ω-diacids as monomers show that this type of structure can be common in the suberin polyester. ω-hydroxyacids can also make linear chains grow by simultaneous esterification to glycerol and ferulic acid, ω-hydroxyacids will be part of the aliphatic polyester and will allow the linkage to the polyaromatics.

The solid-state NMR studies showed that there are two distinct aliphatic carbon populations in suberized cell walls, with different chemical shifts, different responses to delayed decoupling sequences, and different spin-lattice relaxation times [29,30]. A smaller part of the alkyl-chain methylenes showed flexibility, while the majority was motionally restricted [29,30]. The mobile carbons were present in short alkyl chains and were close to the polyaromatics [30]. The longer and more rigid alkyl chains will eventually correspond to the long-chain monomers while the dynamically flexible shorter chains will correspond to glycerol backbones.

Although there is a common pattern in suberin composition from different plant sources, some variability exists, namely in the monomers' mid-chain substituents. For instance, *Pseudotsuga* periderm suberin is dominated by saturated monomers, potato periderm suberin has a high proportion of unsaturated monomers, and cork suberin has a high proportion of mid-chain oxygenated monomers (Table 1). This means that some variability will exist in the suberin macromolecular structure. In the case of suberins rich in epoxide and *vic*-diol groups, relatively strong hydrogen bridges can be established at mid-chain. Eventually, at this level, even covalent bonds can exist, which further bridge the suberin monomers.

Together this knowledge led to the tentative suberin macromolecular model shown in Figure 2. In this model, the suberin aliphatic polyester will correspond to the translucent lamellae of suberized cell walls. The long-chain monomers will be oriented perpendicular to the lamellae plane, with their chains stretched. A rough correspondence between the alkyl chain length of the suberin monomers and the thickness of these lamellae was earlier recognized and it was proposed that they can be oriented this way [31]. A monolayer of α,ω-diacid long-chain monomers anchored on both sides by glycerol could be the basis of the suberin macromolecular structure. Although represented in two dimensions in the model, this structure can develop in three dimensions. This glycerol-aliphatic structure will be enveloped by polyaromatics, which will account for the opaque lamellae. At the interface of the lamellae, ferulic acid will assure the linkage between the suberin polyester and the polyaromatics. Linear chains made of ω-hydroxyacids, will cross through the polyaromatic layers and connect the several translucent lamellae of the suberin polyester. Intra or intermolecular bonds can exist at mid-chain level of the long-chain monomers, namely between the oxygen-containing substituted groups.

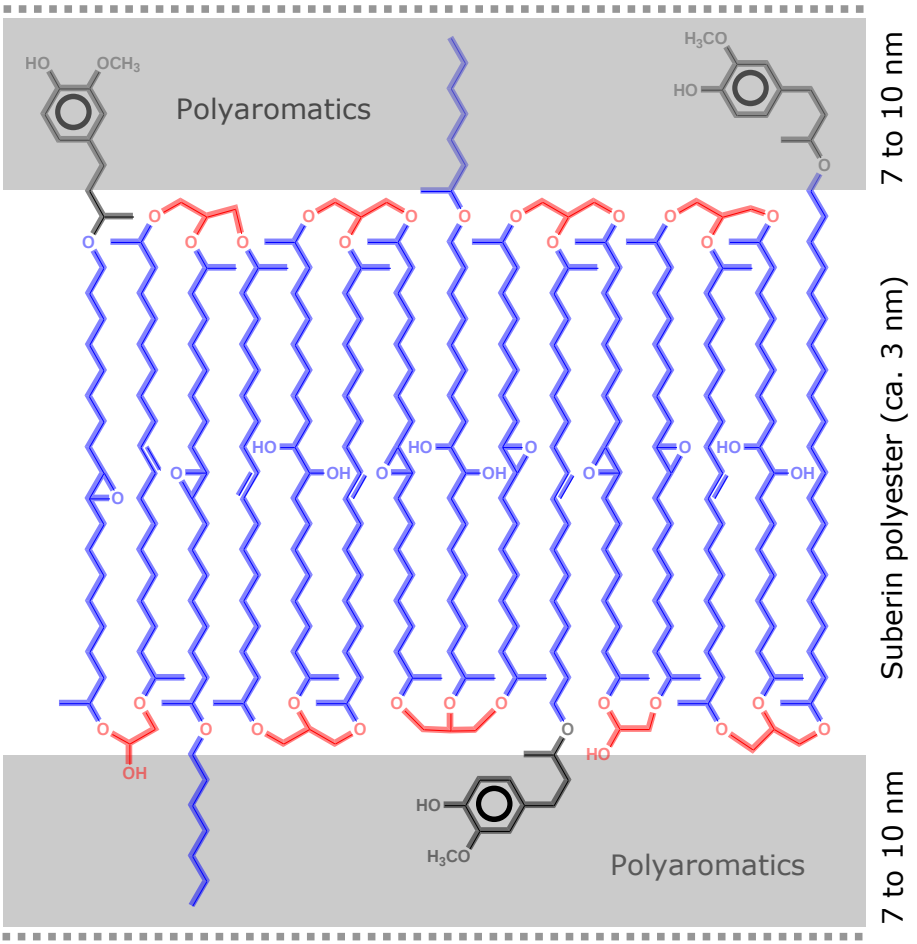

Figure 2. Proposed model of the suberin macromolecular structure

8. Suberin applications

The unique structure of suberin and the singularity of some of its constituent monomers enable valuable potential uses. Suberin is part of a very important material: cork. Cork is used in technologically demanding applications [32-34] because of the properties given by the suberized cell walls and the associated cellular structure: low density, low permeability to gases and water, low heat conductivity, high elasticity, non-perishability and chemically stability [32-34]. Cork is used worldwide in a myriad of products of which cork stoppers are the most common [35]. Cork composite materials have been successfully developed, by agglutinating cork granules with different binding agents. Cork panels for walls and floors are made with phenolic and

polyurethane resins. Cork mixed with different synthetic rubbers, such as Neoprene, Hypalon, and Vamac is used as sealant in motors [36]. In addition, cork granules mixed with epoxide resins are used as thermal shields in spacecraft [37]. Nowadays, 50% of the worlds cork is produced and industrially transformed in Portugal, with an annual export value of 10^9 euro [38].

Suberin-derived products also have potential use as pharmaceuticals, cosmetics and polymers. Suberin was found to inhibit mutagenesis [39] and to work as an absorbent of carcinogens [40]. A cork suberin hydrolysate was shown to act as an anti-ageing agent with smoothing anti-wrinkle action in human skin [41]. Promising results were obtained in the synthesis of polyurethane foams, after the oxypropylation of cork suberin [42,43]. Important amounts of plant wastes rich in suberin are available each year. The Portuguese cork industry produces about 40.000 ton/year of cork powders as a by-product. The bark of birch used in pulp production in northern countries can also be a significant source of suberin [44]. Most of these products are currently used for energy production. The potential of recovering the suberin monomers from these sources, namely α,ω-diacids and ω-hydroxyacids, has not yet been fully explored. Suberized plant tissues and suberin are expected in the future to be a source of specialty chemicals and serve as the basis for bio-inspired materials.

9. References

[1] Schreiber, L., Hartmann, K., Skrabs, M. Zeier, J. 1999. Apoplastic barriers in roots: chemical composition of endodermal and hypodermal cell walls. *Journal of experimental botany* **50**(337): 1267-1280.

[2] Groh, B. Hubner, C., Lendzian, K. 2002. Water and oxygen permeance of phellems isolated from trees: the role of waxes and lenticels. *Planta* **215**(5): 794-801.

[3] Pereira, H. 1988. Chemical composition and variability of cork from *Quercus suber* L. *Wood science and technology* **22**(3): 211-218.

[4] Graça, J. Pereira, H. 1997. Cork suberin: a glyceryl based polyester. *Holzforschung* **51**(3): 225-234.

[5] Bernards, M. 2002. Demystifying suberin. *Canadian journal of botany* **80**(3): 227-240.

[6] Kolattukudy, P. 2002. Suberin from plants. In: Doi, Y., Steinbüchel, A., editors. *Biopolymers - Polyesters I*. Wiley-VCH, Weinheim. pp. 41-73.

[7] Kolattukudy, P. 2001. Polyester in higher plants. In: Babel, W., Steinbüchel, A., editors. *Biopolyesters, biochemical engineering biotechnology*, Vol. 71. Springer-Verlag, Berlin. pp. 1-49.

[8] Franke, R., Briesen, I., Wojciechowski, T., Faust, A., Yephremov, A., Nawrath, C., Schreiber, L. 2005. Apoplastic polyesters in Arabidopsis surface tissues - A typical suberin and a particular cutin. *Phytochemistry* **66**(22): 2643-2658.

[9] Pereira, H., Graça, J., Baptista, C. 1992. The effect of growth rate on the structure and compressive properties of cork. *IAWA bulletin* **13**(4): 389-396.

[10] Sitte, P. 1955. Der Feinbau verkorten Zellwände. *Mikroskopie* **10**(5-6): 178-200.

[11] Sitte, P. 1962. Zum Feinbau der Suberinschichten im Flaschenkork. *Protoplasma* **54**(4): 555-559.

[12] Graça, J., Pereira, H. 2000. Methanolysis of bark suberins: analysis of glycerol and acid monomers. *Phytochemical analysis* **11**(1): 45-51.

[13] Holloway, P. 1983. Some variations in the composition of suberin from the cork layers of higher-plants. *Phytochemistry* **22**(2): 495-502.

[14] Kolattukudy, P., Kronman, K., Poulose, A. 1975. Determination of structure and composition of suberin from roots of carrot, parsnip, rutabaga, turnip, red beet, and sweet-potato by combined gas-liquid-chromatography and mass-spectrometry. *Plant physiology* **55**(3): 567-573.

[15] Graça, J., Pereira, H. 1999. Glyceryl-acyl and aryl-acyl dimers in *Pseudotsuga menziesii* bark suberin. *Holzforschung* **53**(4): 397-402.

[16] Graça, J., Pereira, H. 2000. Suberin structure in potato periderm: glycerol, long-chain monomers, and glyceryl and feruloyl dimers. *Journal of agricultural and food chemistry* **48**(11): 5476-5483.

[17] Graça, J., Santos, S. 2006. Linear aliphatic dimeric esters from cork suberin. *Biomacromolecules* **7**(6): 2003-2010.

[18] Graça, J., Santos, S. 2006. Glycerol-derived ester oligomers from cork suberin. *Chemistry and physics of lipids* **144**(1): 96-107.

[19] Graça, J., Pereira, H. 1998. Feruloyl esters of omega-hydroxyacids in cork suberin. *Journal of wood chemistry and technology* **18**(2): 207-217.

[20] Santos, S., Graça, J. 2006. Glycerol-omega-hydroxyacid-ferulic acid oligomers in cork suberin structure. *Holzforschung* **60**(2): 171-177.

[21] Bernards, M., Lopez, M., Zajicek, J., Lewis, G. 1995. Hydroxycinnamic acid-derived polymers constitute the polyaromatic domain of suberin. *Journal of biological chemistry* **270**(13): 7382-7386.

[22] Marques, A., Pereira, H., Meier, D., Faix, O. 1996. Isolation and characterization of a guaiacyl lignin from saponified cork of *Quercus suber* L. *Holzforschung* **50**(5): 393-400.

[23] Bernards, M., Razem, F. 2001. The poly(phenolic) domain of potato suberin: a non-lignin cell wall bio-polymer. *Phytochemistry* **57**(7): 1115-1122.

[24] Marques, A., Pereira, H., Meier, D., Faix, O. 1999. Structural characterization of cork lignin by thioacidolysis and permanganate oxidation. *Holzforschung* **53**(2): 167-174.

[25] Stark, R., Garbow, J. 1992. Nuclear-magnetic-resonance relaxation studies of plant polyester dynamics. 2. Suberized potato cell-wall. *Macromolecules* **25**(1): 149-154.

[26] Yan, B., Stark, R. 2000. Biosynthesis, molecular structure, and domain architecture of potato suberin: a C-13 NMR study using isotopically labeled precursors. *Journal of agricultural and food chemistry* **48**(8): 3298-3304.

[27] Garbow, J., Ferrantello, L., Stark, R. 1989. C-13 nuclear magnetic-resonance study of suberized potato cell-wall. *Plant physiology* **90**(3): 783-787.

[28] Neto, C., Rocha, J., Cordeiro, A., Esculcas, A., Rocha, S., Delgadillo, I., Jesus, J., Correia, A. 1995. C-13 solid-state nuclear-magnetic-resonance and Fourier-transform infrared studies of the thermal-decomposition of cork. *Solid state nuclear magnetic resonance* **4**(3): 143-151.

[29] Yan, B., Stark, R. 1998. A WISE NMR approach to heterogeneous biopolymer mixtures: dynamics and domains in wounded potato tissues. *Macromolecules* **31**(8): 2600-2605.

[30] Gil, A., Lopes, M., Rocha, J., Neto, C. 1997. A C-13 solid state nuclear magnetic resonance spectroscopic study of cork cell wall structure: the effect of suberin removal. *International journal of biological macromolecules* **20**(4): 293-305.

[31] Schmutz, A., Buchala, A., Ryser, U. 1996. Changing the dimensions of suberin lamellae of green cotton fibers with a specific inhibitor of the endoplasmic reticulum-associated fatty acid elongases. *Plant physiology* **110**(2): 403-411.

[32] Fortes, M., Nogueira, M. 1989. The Poisson effect in cork. *Materials science and engineering A: structural materials properties microstructure and processing* **122**(2): 227-232.

[33] Mano, J. 2002. The viscoelastic properties of cork. *Journal of materials science* **37**(2): 257-263.

[34] Gibson, L., Ashby, M. 1997. *Cellular solids: structure and properties*. Cambridge University Press, Cambridge.

[35] Silva, S., Sabino, M., Fernandes, E., Correlo, V., Boesel, L., Reis, R. 2005. Cork: properties, capabilities and applications. *International materials reviews* **50**(6): 345-365.

[36] Amorim group. 2012. *Cork contributes to an increase in motor vehicle safety levels*. http://www.amorim.com/en/cor_noticias_detail.php?aID=509.

[37] Guthrie, J., Battat, B., Severin, B. In: Material EASE. *Thermal protection systems for space vehicles.* www.p2pays.org/ref/34/33161.pdf.

[38] Associação Portuguesa da cortiça. 2012. *Comercialização de produtos portugueses de cortiça*. http://www.realcork.org/artigo/comercializacaocortica.htm.

[39] Krizková, L., Lopes, M., Polónyi, J., Belicová, A., Dobias, J., Ebringer, L. 1999. Antimutagenicity of a suberin extract from *Quercus suber* cork. *Mutation research-genetic toxicology and environmental mutagenesis* **446**(2): 225-230.

[40] Harris, P., Ferguson, L. 1999. Dietary fibers may protect or enhance carcinogenesis. *Mutation research-genetic toxicology and environmental mutagenesis* **443**(1-2): 95-110.

[41] Coquet, C., Bauza, E., Oberto, G., Berghi, A., Farnet, A., Ferre, E., Peyronel, D., Dal Farra, C., Domloge, N. 2005. *Quercus suber* cork extract displays a tensor and smoothing effect on human skin: An in vivo study. *Drugs under experimental and clinical research* **31**(3): 89-99.

[42] Cordeiro, N., Belgacem, M., Gandini, A., Neto, C. 1999. Urethanes and polyurethanes from suberin 2: synthesis and characterization. *Industrial crops and products* **10**(1): 1-10.

[43] Evtiouguina, M., Barros-Timmons, A., Cruz-Pinto, J., Neto, C., Belgacem, M., Gandini, A. 2002. Oxypropylation of cork and the use of the ensuing polyols in polyurethane formulations. *Biomacromolecules* **3**(1): 57-62.

[44] Ekman, R., Eckerman, C. 1985. Aliphatic carboxylic-acids from suberin in birch outer bark by hydrolysis, methanolysis, and alkali fusion. *Paperi ja puu-paper and timber* **67**(4): 255-273.

Chapter 2: Extraction and purification of suberin acids from cork

[The work developed in this Chapter was the basis of an International Patent submission (PCT/PT2012/000049): Process for the extraction and purification of suberin acids from cork. Applicant: Instituto Superior de Agronomia. Inventors: Santos, S., Graça, J.]

Chapter 3: Stereochemistry of monounsaturated cork suberin acids

[Santos, S., Graça, J. 2013. Stereochemistry of C_{18} monounsaturated cork suberin acids determined by spectroscopic techniques including ^{1}H NMR multiplet analysis of olefinic protons. *Phytochemical Analysis*, in review]

1. Abstract

Introduction – Suberin is a vital biopolyester responsible for the protection of secondary plant tissues, and yet its molecular structure remains unknown. The $C_{18:1}$ ω-hydroxyacid and the $C_{18:1}$ a,ω-diacid are major monomers in suberin structure, but their double bond *cis* or *trans* stereochemistry remains to be elucidated.

Objective – To develop a method based in NMR, together with other spectroscopic techniques, to directly assign in an unequivocal manner the configuration of the $C_{18:1}$ suberin acids.

Methodology – Pure $C_{18:1}$ ω-hydroxyacid and $C_{18:1}$ a,ω-diacid, isolated from cork suberin, and two structurally very close $C_{18:1}$ model compounds of known stereochemistry, *cis*-methyl oleate and *trans*-methyl elaidate, were analyzed by NMR spectroscopy, FTIR and Raman spectroscopy, DSC and GC-MS.

Results – GC-MS analysis showed that both acids were present in cork suberin as only one geometric isomer. The analysis of DMOX and picolinyl derivatives proved the double bond position to be at C-9. FTIR spectra were concordant with a *cis*-configuration for both suberin acids, but their definite stereochemical assignment came from the NMR analysis: (1) the chemical shifts of the allylic ^{13}C carbons were shielded comparatively to the *trans* model compound, and (2) the complex multiplets of the olefinic protons could only be simulated with $^{3}J_{HH}$ and long-range $^{4}J_{HH}$ coupling constants typical of a *cis* geometry.

Conclusion – The two $C_{18:1}$ suberin acids in cork are (*Z*)-18-hydroxyoctadec-9-enoic acid and (*Z*)-octadec-9-enedoic acid. Due to their relative importance, the configuration of these acids is determinant for the macromolecular structure of suberin.

Keywords: *cis*/*trans* configuration; cork suberin; ^{1}H NMR multiplet analysis; (*Z*)-18-hydroxyoctadec-9-enoic acid; (*Z*)-octadec-9-enedoic acid.

2. Introduction

Cork is a tissue found in the outer bark of plants with secondary growth and plays a major role protecting these plants from external aggressions, preventing water loss and affording insulation to internal tissues. 50% of the dry weight of cork cell walls is suberin, which is thus believed to be the main responsible for those barrier properties. Cork is commercially extracted from the cork-oak (*Quercus suber* L.), the only known tree able to produce thick layers of continuous cork tissue in a few years growth. Despite its fundamental role in trees life, suberin as a macromolecule is still very poorly understood.

Suberin is a polyester which after ester-breaking depolymerization releases a mixture of "monomers", mostly long-chain (C_{16} to C_{24}) α,ω-diacids and ω-hydroxyacids together with glycerol. The composition of suberin from different plant sources is variable, but is typically dominant by C_{18} α,ω-diacids and ω-hydroxyacids with mid-chain substituents, which can be an unsaturation, an epoxide or a vicinal-diol group [1,2].

Although the composition of the so far analyzed suberins differ in the relative proportion of C_{18} mid-chain substituted acids, the mono-unsaturated $C_{18:1}$ are always present in significant quantities. For instance, in cork suberin they amount up to 25% of all C_{18} mid-chain substituted acids, but there are cases, like in potato skin suberin, where this number grows close to 100% [3]. This level of importance means that the $C_{18:1}$ α,ω-diacid and ω-hydroxyacid monomers play a major role in the macromolecular structure of all suberins.

The objective of the present work is the determination of the double bond configuration of the two C_{18} monounsaturated suberin monomers: the 18-hydroxyoctadecenoic acid (ω-hydroxyacid), from now on referred as Hyd18:1, and the octadecene-1,18-dioic acid (α,ω-diacid), ahead referred as Di18:1. The only published works, which we are aware of, about the stereochemistry of these $C_{18:1}$ suberin acids, date back to the pioneering studies of Ribas and Seoane. These authors, through a stereospecific *syn*-hydroxylation, found indirect evidence that cork suberin Hyd18:1 and Di18:1

were present both as *cis* and *trans* isomers. However, as the authors themselves mentioned, these results would only be reliable if they could guarantee that the suberin acids with equivalent mid-chain diol groups, were removed prior to the *syn*-hydroxylation. In a later work, these same $C_{18:1}$ acids, but from potato skin suberin, were tentatively assigned as *cis*, based solely in the fact that they were liquid at room temperature [4].

The *cis* or *trans* stereoisomery can be determined in organic compounds by both chemical (as used in the Ribas and Seoane works described above) and physical methods [5]. Typically, in most of the physical approaches, either there are pure standards available or both *cis* and *trans* isomers exist to be compared. In the case of the unsaturated suberin acids analyzed here, two situations were to be faced: first, it was not known if one or both geometric isomers were present, and, if both, in what relative proportions, and there were no commercial standards available for reference; secondly, most of the most reliable and straightforward techniques to assign *cis* or *trans* configuration, namely by NMR, are dependent on the presence of different substituents close to the double bond. The difficulty here was that both Hyd18:1 and Di18:1 are highly symmetrical molecules in relation to the double bond, with identical alkyl substituents up to 7 carbons away.

To directly assign *cis* or *trans* configuration to the unsaturated suberin acids, we present here a NMR based method, with two approaches: the analysis of ^{1}H and ^{13}C chemical shifts of the olefinic protons and carbons; and the analysis of the splitting pattern of the complex multiplets that arise from the olefinic protons in the ^{1}H NMR spectra, extracting the coupling constants by computer simulation. Two $C_{18:1}$ model compounds, structurally similar to the $C_{18:1}$ suberin acid methyl esters, with known double bond stereochemistry were co-analyzed, namely *cis*-methyl oleate and *trans*-methyl elaidate. Besides the 1D NMR analyses, both $C_{18:1}$ suberin acids were fully characterized by 2D NMR, FTIR and Raman spectroscopy, EIMS and DSC, and the double bond position confirmed using picolinyl and DMOX derivatives. The data from these spectroscopic techniques which is relevant to the double bond

configuration analysis is presented and discussed; the remainder is presented as Supplementary Material. Furthermore, the implications of the stereochemistry of the $C_{18:1}$ ω-hydroxyacid and α,ω-diacid for the molecular structure of suberin are discussed.

3. Experimental

3.1. Chemicals and reagents

Methyl oleate and methyl elaidate with purity above 99% were obtained from Sigma-Aldrich and used as received. All solvents used were of HPLC grade (Merck, Germany).

3.2. Cork suberin C_{18} monounsaturated acids

The C_{18} monounsaturated bifunctional suberin fatty acids, in the form of methyl esters, methyl 18-hydroxyoctadecenoate (Hyd18:1_Me) and dimethyl 1,18-octadecenodioate (Di18:1_Me), were obtained from cork suberin after methanolysis depolymerization, followed by a multistep isolation and purification process, which is now part of a patent submission (data not shown). The purity of these suberin acids was checked by GC-MS (>99.9%) and their structure confirmed by mass spectrometry (EIMS) and 1D NMR (^{1}H, ^{13}C) and 2D correlation NMR (COSY, HSQC, HMBC).

3.3. *Cis/trans* separation by GC-MS analysis

3.3.1. Methyl oleate/methyl elaidate mixtures

A solution of an equimolar mixture of *cis*-methyl oleate and *trans*-methyl elaidate was prepared for GC-MS analysis as follows: 3 µL (ca 2.6 mg, 0.77 mmol) of methyl oleate was diluted in 340 µL of pyridine and 340 µL of *N,O*-Bis(trimethylsilyl)trifluoroacetamide (BSTFA); an identical solution was prepared

for methyl elaidate; an aliquot of 100 µL (ca 0.4 mg) of each of these solutions was taken and mixed in a vial to which 800 µL of pyridine was added.

3.3.2. Methyl 18-hydroxyoctadecenoate (Hyd18:1_Me) and dimethyl 1,18-octadecenodioate (Di18:1_Me)

Solutions of each of the two $C_{18:1}$ suberin acid methyl esters were prepared for GC-MS analysis as follows: 1.6 mg of Di18:1_Me (0.54 mmol) was solubilized in 202 µL of pyridine and 202 µL of BSTFA; 1.0 mg of Hyd18:1_Me (0.31 mmol) was solubilized in 130 µL of pyridine and 130 µL of BSTFA.

3.3.3. GC-MS analysis

The three previous solutions were injected on a 7890A gas chromatograph coupled to a 5975C mass spectrometer detector (Agilent Technologies, USA), in the following conditions: column DB5-MS (60 m, internal diameter 0.25 mm, film thickness 0.25 µm); oven temperature program was from 200 °C to 300 °C with a heating rate of 0.3 °C/min, with an helium flow rate of 1 ml/min. Injections were made in splitless mode, with an injector temperature of 300 °C. Mass spectrometer conditions: electron ionization 70 eV; source temperature 230 °C and quadrupole temperature 150 °C; transfer line temperature was kept at 310 °C.

3.4. Double bond position

3.4.1. Picolinyl esters

The procedure to synthesize the picolinyl esters was adapted from Gunstone (1999) [6]. 2.0 mg of each suberin acid (as free carboxylic acid) was reacted with 1 ml of oxalyl chloride, overnight at room temperature. The excess of oxalyl chloride was then removed in a warm water bath under a nitrogen flow. On a different flask, a solution of 3-hydroxymethylpyridine (HMP) was prepared by adding 34.8 mg of HMP with 1.7 ml of dichloromethane. The HMP

solution and both suberin acid chlorides were cooled down to 0 °C in an ice bath; 1 ml of the cooled HMP solution was added to each of the suberin acid chlorides, and after 30 min at 0 °C, the reaction mixtures were allowed to warm to room temperature during 2 h30. The excess of HMP was removed in a warm water bath under a nitrogen flow and the reaction products (the picolinyl esters) were dried in a vacuum oven, at 45 °C, over phosphorus pentoxide, overnight. Each picolinyl ester was then derivatized with pyridine and BSTFA (120 µl of each per mg), affording the TMS derivatives of un-reacted groups and analyzed by GC-MS.

3.4.2. DMOX derivatives

The procedure to synthesize the DMOX derivatives was adapted from Harvey (1992) [7]. 3.0 mg of each suberin acid (as free carboxylic acid) was reacted with 15.5 mg of 2-amino-2-methylpropanol during 6 h in an oil bath at 160 °C. Both reaction mixtures were allowed to cool to room temperature, were derivatized as described previously for the picolinyl esters, and analyzed by GC-MS.

3.4.3. GC-MS analysis

The TMS-derivatized solutions of the picolinyl esters and DMOX derivatives were injected on the GC-MS system previously described. The oven temperature program was: 5 min at 100 °C, followed by a temperature increase from 100 °C to 250 °C at a rate of 8 °C/min, and then from 250 °C to 300 °C at 3 °C/min; the final temperature was kept for 20 min. Injection and mass spectrometer conditions were as described above.

3.5. DSC analysis

DSC analyses were carried out on a Maia DSC 200 F3 differential scanning calorimeter (Netzsch, Germany). Before the analysis, the samples were dried

in vacuum and cooled to -50 °C with liquid nitrogen. Measurements were made on aluminium pans and the following quantities were used: 29.9 mg of Hyd18:1_Me, and 7.6 mg of Di18:1_Me. DSC measurements were carried out over a temperature range starting from -50 °C to 70 °C at a heating rate of 20 °C/min. Calibration was made with mercury (-37.1 °C), indium (157.3 °C), tin (232.5 °C) and bismuth (272.0 °C) at a heating rate of 1 °C/min with an expanded uncertainty of measurement error <0.5 °C.

3.6. FTIR analysis

FTIR absorption spectra (32 scans per spectrum) were acquired on an Alpha-P spectrometer (Bruker Optik, Germany) with a spectral resolution of 4 cm^{-1} and a wavenumber range from 4000 cm^{-1} to 400 cm^{-1}. The spectra were obtained by Attenuated Total Reflectance (ATR), with a diamond cell and the pressure clamp applied directly over the samples, which were liquid at room temperature.

3.7. Raman analysis

Vibrational Raman spectra were obtained in an apparatus consisting of a double monochromator Spex 1403 (Horiba, Japan), with an argon ion laser line at 514.5 nm, model 2016 (Spectra-Physics, USA) and a R928 photomultiplier detector (Hamamatsu Photonics, Japan). The spectra were acquired at room temperature, with 90 ° geometry, a resolution of 4 cm^{-1}, a time of integration of 1 sec and an exit power of 1 W. The liquid suberin acid methyl ester samples were placed in glass tubes and analyzed at room temperature.

3.8. NMR analysis

The NMR spectra were recorded on an Avance II+ 600 spectrometer (Bruker Biospin, Germany), operating at 600.13 MHz for protons and 150.96 MHz for carbons, equipped with a cryoprobe and pulse gradient units, capable of

producing magnetic field pulsed gradients in the z-direction of 56.0 G/cm. All NMR spectra were acquired in deuterated chloroform with 0.03% of TMS at a temperature of 300 K. The ^{1}H spectra chemical shifts were referenced to TMS (0.00 ppm) and the ^{13}C spectra to chloroform (77.00 ppm). The sample concentration used was 5 mg/500 µL placed in 3 mm or 5 mm diameter NMR tubes suitable for 600 MHz. The NMR spectra were further processed using MestReNova, version 7.1.2 (Mestrelab Research, Spain), and the multiplet simulation made with the "Spin simulation" feature of this software.

4. Results and discussion

4.1. *Cis/trans* separation by GC-MS analysis

The first question to be answered is whether the two suberin $C_{18:1}$ acids under study are mixtures of *cis* and *trans* isomers, or if they are present in suberin as only one isomer. Abundant literature exists on the separation of *cis* and *trans* fatty acid methyl esters by GC, and both polar and non-polar columns have been employed with success for that matter [8]. In the present work, a GC-MS method was developed to separate the two model compounds with different double bond configuration, *cis*-methyl oleate and *trans*-methyl elaidate, and applied to each of the $C_{18:1}$ suberin acids extracted from cork. A 1:1 mixture of the two standards was successfully separated in a 60 m DB5-MS non-polar column, with methyl oleate eluting 30 s earlier than methyl elaidate, with a resolution close to the baseline (see Figure SM1 in "Supplementary material"). In the exact same chromatographic conditions, each unsaturated suberin acid showed a single chromatographic peak (data not shown). Due to the structural similarity between the model compounds and the $C_{18:1}$ suberin acids, if the latter were present in both isomeric forms, it would be expected for them to show as two different peaks in the GC-MS chromatograms. Therefore, these results gave strong evidence that only one isomer, either *cis* or *trans,* was present both in Hyd18:1_Me and Di18:1_Me suberin acids.

4.2. Double bond position

The position of the double bond in the $C_{18:1}$ suberin acids from cork was for the first time (and only) assessed by chemical means, after permanganate *syn*-hydroxylation of the double bond, followed by cleavage of the ensuing diol by periodic acid oxidation. The elemental composition of the two resulting fragments was analyzed and based on those results the position of the double bond was proposed to be at C–9, for both Hyd18:1 [9] and Di18:1 [10]. To confirm this assignment, the double bond position was determined here by mass spectrometry, after derivatization of the suberin unsaturated acids (in the free form) to the corresponding picolinyl esters and 4,4-dimethyloxazoline (DMOX) derivatives [7]. In these derivatives, the presence of the nitrogen atom close to the carboxyl group of the monounsaturated long-chain acids, under typical electron ionization conditions, gives a characteristic pattern of molecule fragmentation which allows the recognition of the double bond position, particularly when it is mid-chain located [7]. In these conditions, the nitrogen-based derivatives afford clear-cut mass spectra and are commonly used for this purpose [7].

The GC-EIMS spectra of Hyd18:1 DMOX/TMS derivative and Di18:1 picolinyl/TMS derivative are presented in Figure 1 (A) and (B) respectively. The mass spectra of Hyd18:1 and Di18:1 TMS-derivatives, together with the mass spectra of Hyd18:1 picolinyl/TMS derivative, and Di18:1 DMOX/TMS and bis-DMOX derivatives, are shown as "Supplementary Material" (Figures SM2 to SM6, respectively). In both suberin acids the position of the double bond was proved to be at C-9. The Hyd18:1 DMOX/TMS spectrum (Figure 1A) showed the ions at *m*/z 113 and *m*/z 126 typical of the DMOX moiety, and the successive losses of 14 amu (CH_2 group) starting at *m*/z 320 (M-103) until *m*/z 222. The 14 amu sequence restarts at *m*/z 196 until the end of the alkyl chain, at *m*/z 98. The ions of *m*/z 222 and *m*/z 196 had a difference of 26 amu, thus indicating the double bond position at C-9. Another way to do the calculation is using the "12 mass rule" [11], looking for the mass interval of 12 amu, instead of 14 amu, which in this case is the diagnostic ion of *m*/z 208.

Previous work with Di18:1 *bis*-DMOX derivative, but extracted from the suberin of potato periderm, also led to the same assignment of the double bond position at C-9 [3].

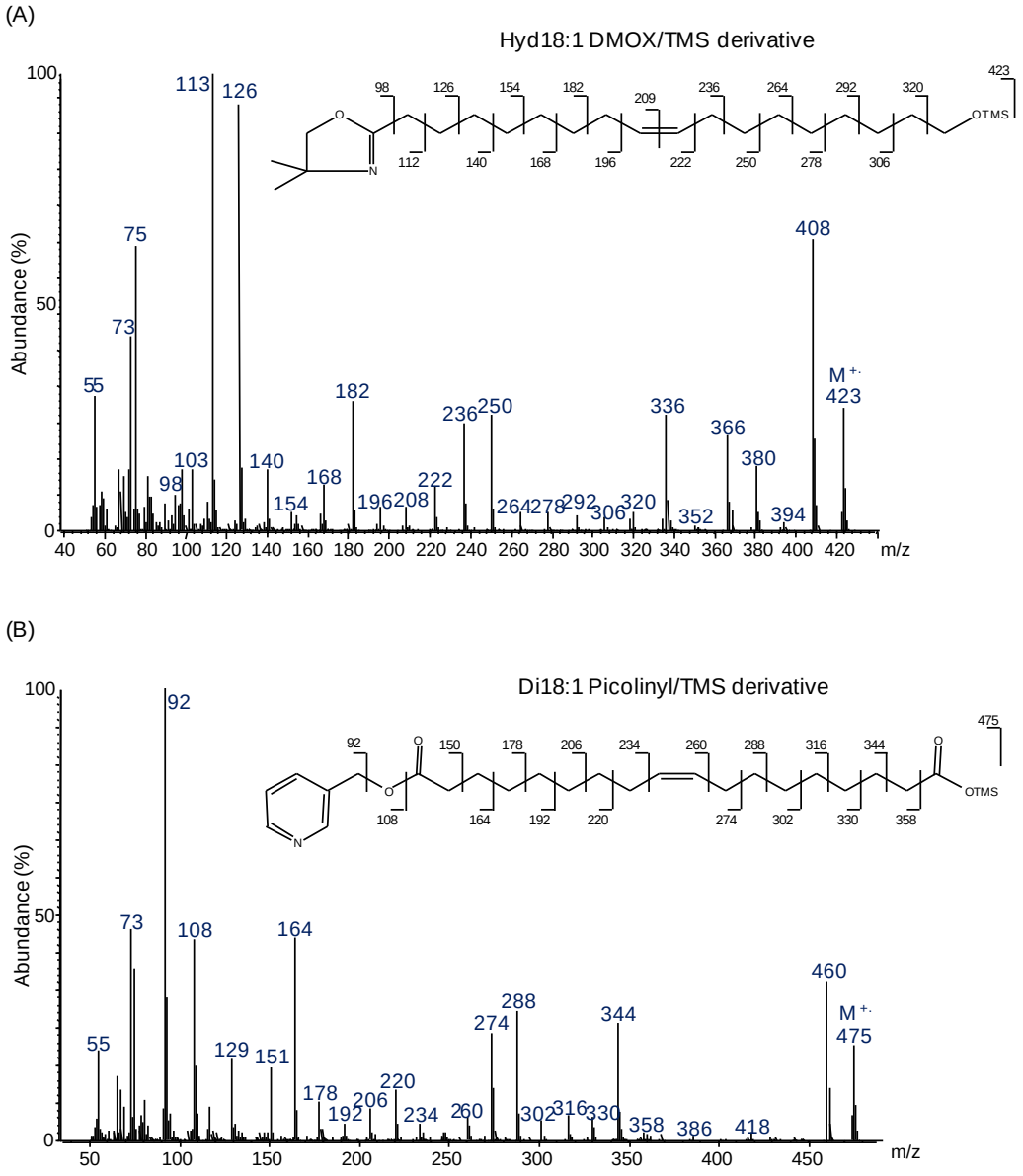

Figure 1. Assignment of the double bond position. Electron ionization mass spectrum and fragmentation pattern of: (A) (Z)-18-hydroxyoctadec-9-enoic acid (Hyd18:1) DMOX/TMS derivative; (B) (Z)-octadec-9-enedioic acid (Di18:1) picolinyl/TMS derivative

The spectrum of Di18:1 picolinyl ester, TMS-derivative (Figure 1B) showed intense ions at *m/z* 92, *m/z* 108, *m/z* 151 and *m/z* 164 indicative of the pyridine

ring presence. A series of 14 amu losses was found from *m*/z 358 (M-CO_2TMS) until *m*/z 260; this 14 amu loss sequence restarted at *m*/z 234, until the end of the alkyl chain. As with the case of the DMOX derivatives, this gap of 26 amu between *m*/z 260 and *m*/z 234, confirmed the double bond position at C-9.

4.3. DSC analysis: melting point and crystallization

Both $C_{18:1}$ suberin acid methyl esters, Hyd18:1_Me and Di18:1_Me, are viscous liquids at room temperature. No data exists regarding their melting points or other thermal behavior properties. As a rule, in fatty acid methyl esters structurally related to the ones considered here, *cis*-isomers have lower melting points than the equivalent *trans*-isomers, a fact attributed to an easier, more compact packing in the solid phase of the all-anti straight chains of the latter [12]. One of the most informative techniques for the determination of melting points and other phase transition properties is Differential Scanning Calorimetry (DSC). The thermal behavior by DSC of the *cis* and *trans* fatty acid methyl esters used in the present work as model compounds, methyl oleate and methyl elaidate, including their melting points, have already been studied [13]. A DSC analysis was made here for the Hyd18:1_Me and Di18:1_Me and their thermograms are presented in Figure 2 (A) and (B), respectively.

Of the two suberin acid methyl esters, Hyd18:1_Me showed the highest melting point, with an onset melting temperature of 6.1 °C, and a maximum melting temperature of 15.9 °C, when compared to the equivalent values for Di18:1_Me, -8.9 °C and -0.2 °C. The melting point (maximum peak temperature) determined by DSC for methyl oleate was -20.2 °C [13], a value lower than the ones observed for both $C_{18:1}$ suberin acids. This can be due to the difference in polarity of the terminal C-18 carbon head groups, and the comparatively higher strength of inter-molecular bonding they impart in the solid phase: the $–CH_3$ terminal C-18 group in methyl oleate is less polar than the group $–CO_2CH_3$ in Di18:1_Me, and the later is less polar then the $–CH_2–OH$ group present in Hyd18:1_Me. As expected, methyl elaidate had a much

higher DSC melting point, 9.9 °C, than methyl oleate [13], a value situated above the melting points found here for the two suberin acid methyl esters. In the case of methyl elaidate, the *trans* configuration increased the melting point temperature, eventually surpassing the polarity forces discussed above for the Di18:1_Me suberin acid. Together, these results for the melting point temperatures can therefore be indicative of a *cis* configuration for Di18:1_Me suberin acid, although no conclusion can be drawn regarding the Hyd18:1_Me.

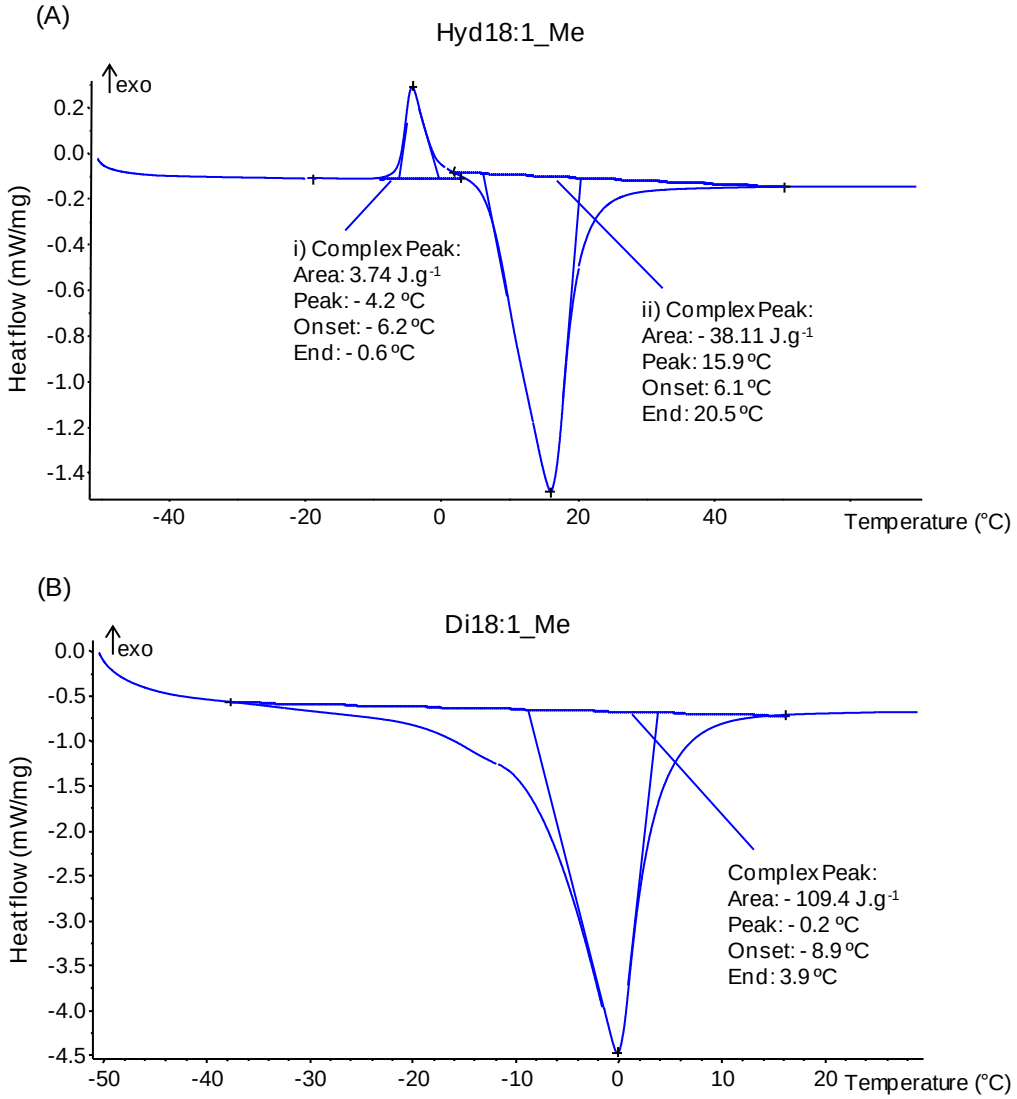

Figure 2. Differential scanning calorimetry (DSC) thermograms with indication of melting points (onset temperature, maximum peak and end temperature) and integrated areas of consumed (or released) heat of cork suberin acids: (A) methyl (Z)-18-hydroxyoctadecenoate (Hyd18:1_Me) and (B) dimethyl (Z)-1,18-octadecenodioate (Di18:1_Me)

An exothermic transition was observed in Hyd18:1_Me, peaking at -4.2 °C and immediately preceding the onset of the melting phase (Figure 2A). This shows that at least a partial crystallization occurred when molecular mobility was sufficient for structural rearrangement, before the change to the liquid phase. This crystallization phase was not observed in the case of Di18:1_Me, which may imply that the comparatively higher polarity of the free hydroxyl group in the terminal C-18 carbon of Hyd18:1_Me was important for the crystal formation. Both oleic and elaidic acids, either free or as methyl esters, are known to have different crystallization forms at different temperatures, associated with different conformations in the region of the double bond [12]. The implications of the eventual ordered packing arrangements of the $C_{18:1}$ acids in suberin structure are discussed below.

4.4. FTIR and Raman analysis

The simpler approach for the analysis of *cis*/*trans* isomerism of double bonds within hydrocarbon chains, as we are dealing here, is by using vibrational spectroscopy, in the form of FTIR absorption, or its complementary approach, Raman light scattering. The FTIR spectra of the two $C_{18:1}$ suberin acids, Hyd18:1_Me and Di18:1_Me and of the two model compounds, $C_{18:1}$ *cis*-methyl oleate and $C_{18:1}$ *trans*-methyl elaidate, are presented and compared in Figure 3. In this Figure, the most diagnostic bands for *cis*/*trans* assignment are highlighted. The Raman spectra of the Hyd18:1_Me and Di18:1_Me suberin acids, together with the complete list of tentative band assignments for all FTIR and Raman spectra are presented as "Supplementary material" (Figure SM7 and Tables SM1 and SM2, respectively). The band assignments were based in the general knowledge of the infrared and Raman characteristic frequencies [14] and in previous reviews and discussions of lipids and fatty acids IR and Raman spectra, including results for oleic and elaidic acids and their methyl esters [15-19].

The infrared bands of an isolated, non-conjugated double bond in a hydrocarbon chain, as in the $C_{18:1}$ fatty acids discussed here, derive mainly from the C–H and C–C vibration modes of the sp^2 C=C carbons. In the planar design of the –CH=CH– group, the H atoms and the heavier $–(CH_2)_n–$ groups can be substituted in a more symmetrical, *trans*, or more asymmetrical, *cis* configuration, therefore giving diagnostic vibrational bands that can eventually distinguish the two different geometries [20]. In this way, up to five modes of vibration can be used to differentiate *cis*/*trans* olefins, namely the =C–H stretching vibration, the C=C–H in-plane and out-of-plane deformation vibrations, and the C=C stretching and skeletal vibrations [20], each of them discussed below.

A weak to medium intensity absorption band at 3090-3010 cm^{-1} is typical of the =C–H stretching vibration. *Trans* isomers tend to absorb at a superior wavenumber than their equivalent *cis* isomers [14]. This fact can be verified in the *cis*-methyl oleate, where the =C–H stretching vibration is at 3005 cm^{-1} whilst in *trans*-methyl elaidate the same absorption band is at a higher frequency, 3016 cm^{-1} (Figure 3). In what respects the suberin acids Hyd18:1_Me and Di18:1_Me this same band is at 3002 cm^{-1} and 3003 cm^{-1}, respectively, values that are much closer to the one observed in the *cis* model compound. For the latter suberin acids, the equivalent vibration in Raman spectra band is at 3016 cm^{-1} for both of them (see "Supplementary Material", Figure SM7).

The FTIR band typical of the C=C stretching can be found in the 1680-1620 cm^{-1} window [14]. In this region, the *cis* isomers tend to absorb below 1665 cm^{-1} and the *trans* isomers above this frequency. The FTIR spectra of methyl oleate, Hyd18:1_Me and Di18:1_Me all show a very weak band close to 1655 cm^{-1}, well within the *cis* range. In the *trans*-methyl elaidate this band is not observed at all (Figure 3). In the Raman spectra, this C=C stretching vibration shows a much more intense band due to the double bond polarizability. Published results for methyl oleate and methyl elaidate illustrate the difference between *cis* and *trans* isomers, 1654 cm^{-1} and 1667 cm^{-1} [18], and 1656 cm^{-1} and 1670 cm^{-1} [21]. The Raman spectra of Hyd18:1_Me and Di18:1_Me showed strong

bands at 1662 and 1660 cm^{-1} respectively, which were assigned to this C=C stretching vibrations. Again, the results observed in the $C_{18:1}$ suberin acid methyl esters are closer to the values typical of a *cis* configuration.

Another possible diagnostic vibration band for *cis*/*trans* discrimination comes from the C=C–H– in-plane deformation, which although not assigned unambiguously in FTIR spectra, is relatively strong in Raman spectra of *cis* olefins. In published Raman spectra of methyl oleate, this band is present at ca 1267 cm^{-1} but not recognizable in methyl elaidate [18]. In the Hyd18:1_Me and Di18:1_Me Raman spectra, a medium to strong band assignable to this vibration is found at 1266 and 1270 cm^{-1} respectively (Figure SM7), therefore suggesting the *cis* configuration for these suberin acids.

In FTIR spectra, the relatively strong absorption band at 980-955 cm^{-1}, typical of the C=C–H out-of-plane (oop) deformation, is known to be unique of *trans* isomers [19]. As it can be seen in Figure 3, this band is prominent in the FTIR spectrum of methyl elaidate, at 967 cm^{-1}, but is not recognizable nor in methyl oleate neither in the $C_{18:1}$ suberin acids spectra. In the opposite, in Raman spectra, the most intense band for the C=C–H oop deformation is found in *cis*-isomers, and is weak in the corresponding *trans*-isomers. This band was found in methyl oleate at 882 cm^{-1}, but was not well defined in methyl elaidate [16]. In the Raman spectra of the $C_{18:1}$ suberin acids, this same band was also found at 882 cm^{-1} in Hyd18:1_Me and Di18:1_Me, in both cases again consistent with a *cis*-configuration.

Finally, two more FTIR absorption bands were used as indicative of *cis*-olefins, which were not observed in *trans*-methyl elaidate, but were present in *cis*-methyl oleate and in the two $C_{18:1}$ suberin acids. A weak band (shoulder) around 695 cm^{-1}, assigned to the wagging (oop) deformation vibrations of the C–H bond in *cis*–CH=CH– groups, and another weak band at ca 965 cm^{-1}, imputed to the skeletal vibrations of the same bond and group [14] (Figure 3). Taken all together, these results from the FTIR and Raman analysis strongly suggest that the $C_{18:1}$ acids from cork suberin have a *cis* configuration or at least that the later is largely dominant.

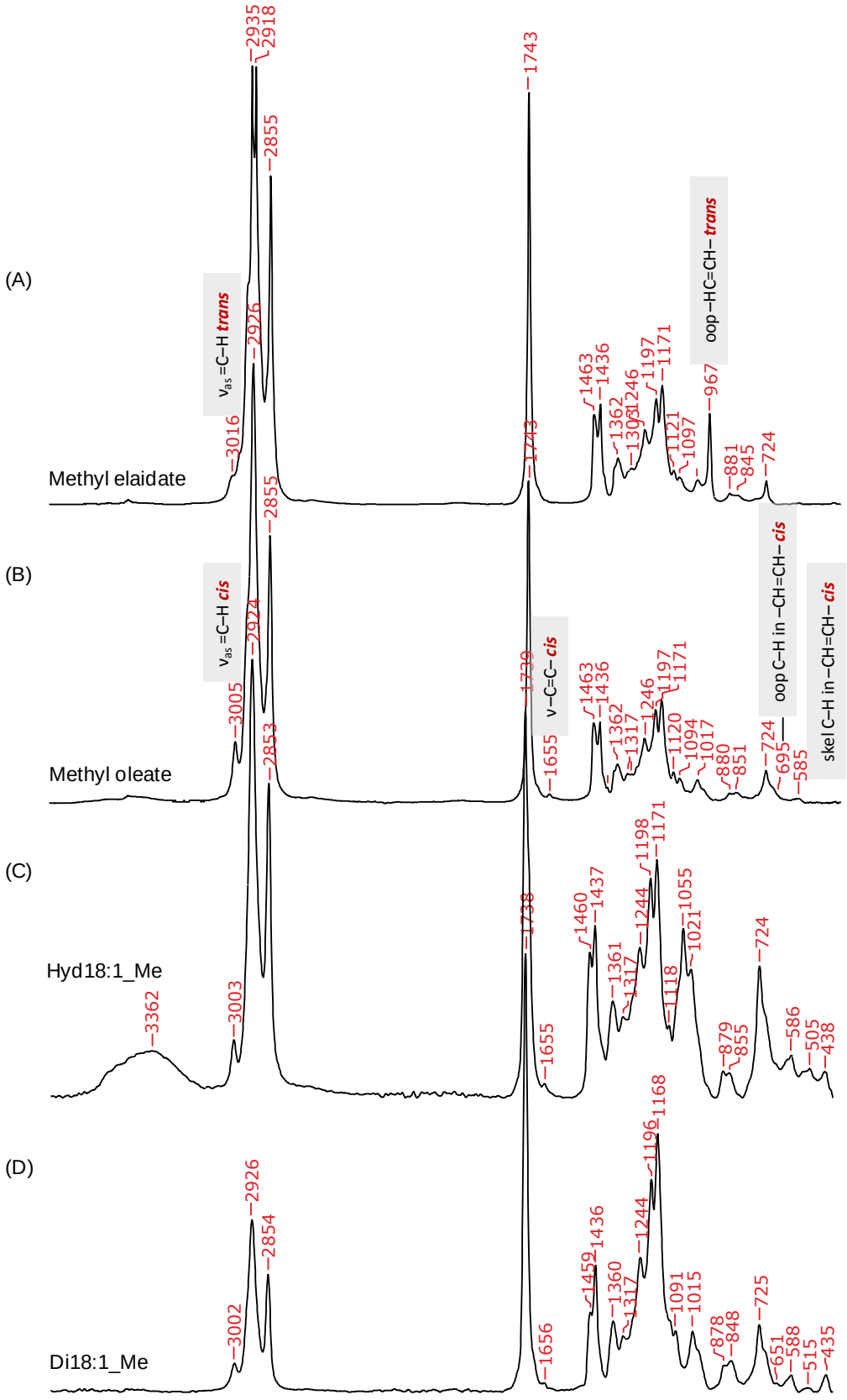

Figure 3. FTIR spectra of: model compounds (A) methyl (*E*)-octadec-9-enoate (methyl elaidate) and (B) methyl (Z)-octadec-9-enoate (methyl oleate); and cork suberin acids (C) methyl (Z)-18-hydroxyoctadecenoate (Hyd18:1_Me) and (D) dimethyl (Z)-1,18-octadecenodioate (Di18:1_Me). The main absorption bands assignable to *cis* or *trans* configuration are highlighted

4.5. NMR analysis

In disubstituted olefins, as we are dealing here, *cis*/*trans* configuration can eventually be determined by ^{1}H and ^{13}C NMR chemical shifts, J_{HH} and J_{HC} coupling constants, or through space correlation experiments based on the Nuclear Overhauser Effect [5]. Most of these approaches are however dependent on the presence of a substitution pattern in which the groups attached to the double bond, originate olefinic protons (or carbons) which have different and resolved chemical shifts. In –CH=CH– systems, the coupling constant varies from +4 to +12 Hz for *cis* isomers, and from +12 to +19 Hz, for the corresponding *trans* isomers [5]. In the case of the suberin acids and model compounds under study, both substituents are saturated methylene chains identical up to 7 methylene groups away, making the molecules highly symmetrical in relation to the double bond. The presence of these quasi-identical substituent groups originates a complex multiplet in the proton NMR spectra arising from both olefinic protons (Figure 4). Because the coupling constants cannot be directly extracted from these complex peaks, the stereochemistry of the double bond cannot be directly determined this way. However, the chemical shifts, particularly of the allylic ^{13}C carbons, and the determination of the above discussed J_{HH} olefinic coupling constants through spectra simulation, can prove the double bond configuration and are discussed below.

4.5.1. Chemical shifts and *cis*/*trans* configuration

The assignment of ^{1}H and ^{13}C chemical shifts of the suberin acid methyl esters, Hyd18:1_Me, and Di18:1_Me, and of the model compounds *cis*-methyl oleate and *trans*-methyl elaidate, are presented as Supplementary material (Tables SM3 and SM4), with the two latter compared with published results. The molecular schemes of the *cis* and *trans* double bonds are presented in Figure 5, with the olefinic (A and B) and allylic (X and Y) positions identified. The ^{1}H and ^{13}C chemical shifts of the olefinic and allylic positions are shown in Table 1.

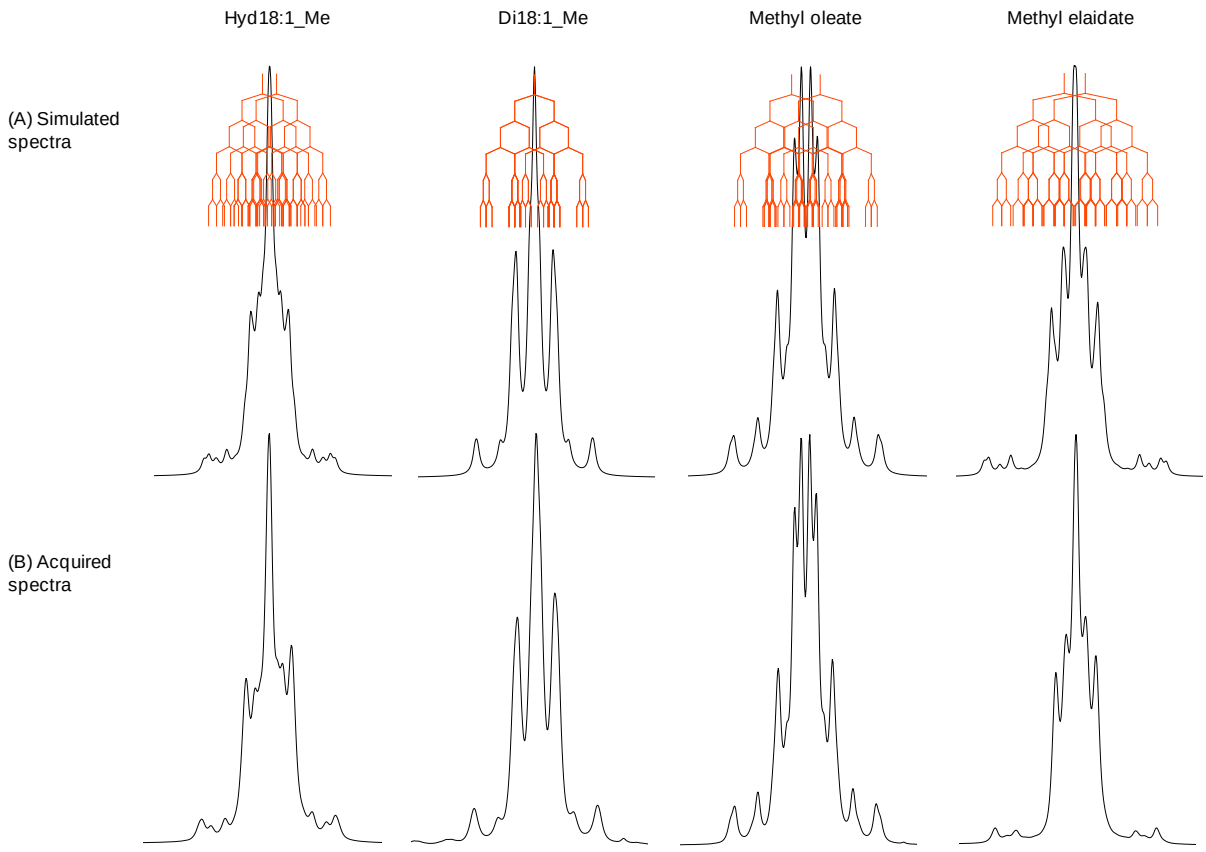

Figure 4. Olefinic protons NMR multiplets (A) simulated and (B) acquired of: methyl (Z)-18-hydroxyoctadecenoate (Hyd18:1_Me) and dimethyl (Z)-1,18-octadecenodioate (Di18:1_Me) from cork suberin; and model compounds methyl (Z)-octadec-9-enoate (methyl oleate) and methyl (*E*)-octadec-9-enoate (methyl elaidate)

In Table 1, the differences between the chemical shifts of the *cis* and *trans* model compounds, methyl oleate and methyl elaidate, $\Delta(ppm)=\delta^{cis}-\delta^{trans}$, are also given. In all the $C_{18:1}$ fatty acids analyzed here, both olefinic and allylic proton signals are unresolved multiplets, showing a complex pattern of spin-spin coupling (Figure 4). One approach to find eventual diagnostic differences between *cis* and *trans* isomers is the chemical shift of the olefinic and allylic protons and carbons. Comparing methyl oleate and methyl elaidate, a small difference of -0.03 ppm was observed in the olefinic protons, and of +0.05 ppm in the allylic protons (Table 1). The negative difference means that the *cis* olefinic protons are more shielded than the *trans* olefinic protons, and the positive difference indicates the opposite, that the *cis* allylic protons are more deshielded than the *trans* allylic protons. Differences of the same signal and order of magnitude were observed between other similarly alkyl disubsti-

tuted olefins, like in *cis*- and *trans*-2-pentene and *cis*- and *trans*-3-hexene [22]. These authors simulated these shielding and deshielding effects through theoretical calculations based on the magnetic anisotropy and steric effects associated with the double bond. They took into account the empirical formula of the shielding cone and the spatial distances and angles between the interacting nuclei. The calculations were made for *cis*- and *trans*-2-pentene and *cis*- and *trans*-3-hexene and other acyclic olefins assuming an *anti* conformation of the carbon chain. The calculated values were close to the observed ones, all showing a systematic shielding of the olefinic protons, and deshielding of the allylic protons in *cis* isomers [22]. Regarding the suberin acids, Hyd18:1_Me and Di18:1_Me, the chemical shifts of their olefinic and allylic protons were almost coincident with the ones observed in *cis*-methyl oleate (Table 1) and in this way, compatible with a *cis* stereochemistry.

Table 1. Chemical shifts (ppm) of the olefinic and allylic ^{1}H and ^{13}C in cork suberin acids methyl (*Z*)-18-hydroxyoctadecenoate (Hyd18:1_Me) and dimethyl (*Z*)-1,18-octadecenodioate (Di18:1_Me), and model compounds methyl (*Z*)-octadec-9-enoate (methyl oleate) and methyl (*E*)-octadec-9-enoate (methyl elaidate)

	Hyd18:1_Me	**Di18:1_Me**	***cis*-methyl oleate**	***trans*-methyl elaidate**	$\Delta=\delta^{cis}-\delta^{trans}$
^{1}H					
Olefinic H_9 & H_{10}	5.34	5.34	5.35	5.38	-0.03
Allylic H_8 & H_{11}	2.01	2.01	2.01	1.96	+0.05
^{13}C					
Olefinic					
C_9	129.74	129.79	129.74	130.20	-0.46
C_{10}	129.85	129.79	129.99	130.47	-0.48
Allylic					
C_8	27.11	27.11	27.20	32.59	-5.39
C_{11}	27.09	27.11	27.14	32.54	-5.40

More diagnostic to the *cis*/*trans* configuration assignment of these olefins with disubstituted long methylene chains can be the ^{13}C chemical shifts. Comparing *cis*-methyl oleate and *trans*-methyl elaidate, the difference between the chemical shifts of the olefinic carbons was relatively minor, on

average, -0.47 ppm, but a much bigger difference was observed in the allylic carbons, ca -5.40 ppm, showing a significant upfield shift for the *cis* isomer (Table 1). This comparative shielding of the *cis*-allylic carbons is probably due to the so-called γ-effect. This empirical effect has been attributed to the van der Waals spatial interactions, which can happen between substituent groups located at three-bond distance [23]. In the *cis* double bond configuration, this effect is much more important due to the forced proximity of the two bulkier methylene allylic groups; in *trans* isomers each methylene faces a much smaller hydrogen atom, significantly diminishing the γ-effect. This same shielding of the *cis*-allylic carbon was observed comparing *cis*- and *trans*-2-butene, with the same value measured for the chemical shift difference, -5.40 ppm [24].

This negative difference between the chemical shifts of *cis* and *trans* allylic carbons was found to be systematic in other $C_{18:1}$ olefinic fatty acids. However, the chemical shifts of the allylic carbons were variable depending on the double bond position, in ranges for *cis* and *trans* isomers that partly overlap [25]. This means that as long as only one isomer is available, the absolute value of its allylic carbons chemical shifts may not allow an unambiguous assignment of a *cis* or *trans* configuration. Nevertheless, when the double bond is close to the middle of the C_{18} chain, the chemical shifts of the allylic carbons were found to lay in a very short range close to 27 ppm for the *cis* isomer, and 32 ppm for the *trans* isomer [25], making in these cases possible the direct assignment of a *cis* or *trans* configuration. This reasoning can be applied to both 9-unsaturated $C_{18:1}$ suberin acids, Hyd18:1_Me and Di18:1_Me, which showed allylic carbon chemical shifts of ca 27 ppm (Table 1), therefore concordant with a *cis* configuration.

4.5.2. Coupling constants and *cis*/*trans* configuration

Another approach to directly assign *cis* or *trans* configuration in $C_{18:1}$ fatty acids by NMR, is through the analysis of spin-spin coupling patterns of their

olefinic and allylic protons. Coupling constants can differ both in magnitude and in signal, and measure how strongly a nucleus is influenced by the spin state of another neighbor nuclei, through polarization of the bonding electrons [23]. Thus, the higher the interaction between the bonding electronic orbitals, the stronger is the spin information transmitted and, consequently, the higher is the absolute value of the coupling constant between two interacting nuclei. If two coupled nuclei have their lowest energy level when their spins are paired (anti-parallel), by definition their coupling constant is positive; on the other hand, if their spins are aligned in the lowest energy level, the coupling constant is negative [23]. In second-order spin systems, the sign of the coupling constant has frequently a major effect on the splitting pattern [26], a fact observed in the olefinic multiplets discussed here.

In alkyl disubstituted olefins as the $C_{18:1}$ acids under analysis, up to four coupling constants can be observed associated with the double bond: the $^3J_{HH}$ olefinic coupling between the olefinic protons; the $^3J_{HH}$ coupling between the olefinic and allylic vicinal protons; the $^4J_{HH}$, long-range allylic coupling, between the olefinic and the allylic distal protons; and the $^5J_{HH}$, long-range homoallylic coupling between the allylic protons (Figure 5). The $^3J_{HH}$ between the two olefinic protons is the main diagnostic coupling constant used for *cis*/*trans* configuration assignment. The magnitude of this coupling constant depends on the small overlapping extent of the orbitals of the two =C–H bonds under consideration, which is highest when they are parallel [27]. The orbital parallelism, and therefore the magnitude of this $^3J_{HH}$ depends on the values of the =C–H bonds dihedral angle (φ) and the H–C=C bond (valence) angles (α and α´, Figure 5). Considering the dihedral angle, the maximum orbital interaction occurs in the *trans* configuration, due to the anti-parallel arrangement of the =C–H orbitals [27], coincident with φ = 180°. In the *cis* configuration, where the dihedral angle is 0°, there is a somewhat lower orbital interaction, compared to 180°, as illustrated by the Karplus equation. Considering the bond angles (Figure 5), in the *cis* configuration both =C–H groups are on the same side and angled away in the plane of the double

bond, making their orbitals less parallel; in the *trans* case, the =C–H groups are in opposite sides but parallel to each other, and therefore have comparatively bigger coupling constants. These differences in geometry explain why $^{3}J_{HH}$ coupling constants between the two olefinic protons are higher in *trans* isomers compared to *cis* isomers. Typical values for this $^{3}J_{HH}$ vary from +4 to +12 Hz for *cis* isomers, and from +12 to +19 Hz, for the corresponding *trans* isomers [5].

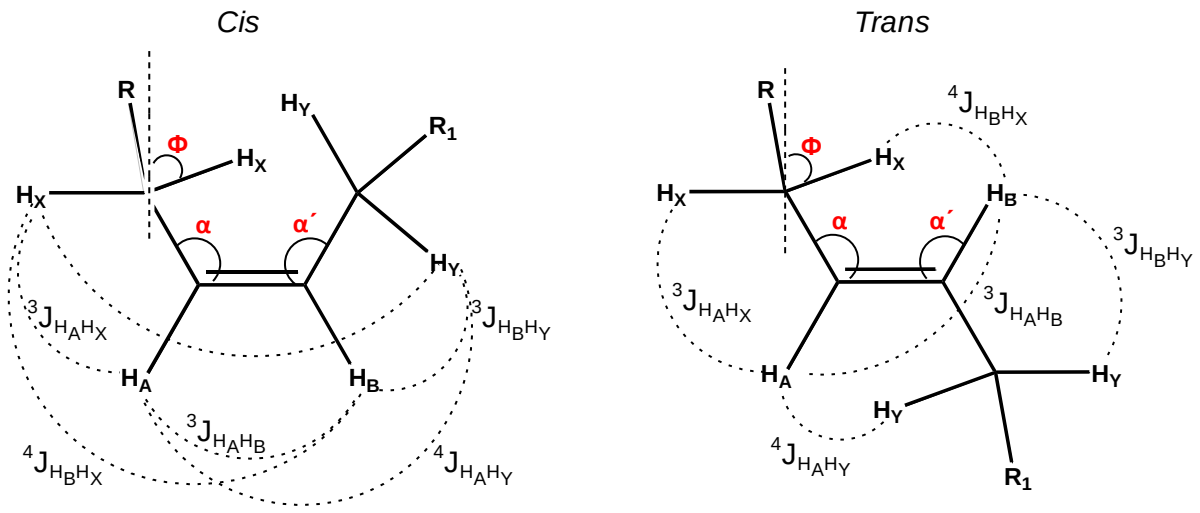

Φ = torsional angle; α and α´= bond (valence) angle; A and B: olefinic protons; X and Y: allylic protons; $^{3}J_{HAHB}$ = olefinic coupling; $^{3}J_{HAHX}$ = olefinic/allylic coupling; $^{3}J_{HBHY}$ = olefinic/allylic coupling; $^{4}J_{HBHX}$ = allylic coupling; $^{4}J_{HAHY}$ = allylic coupling

Figure 5. Molecular schemes of double bonds of *cis* and *trans* configuration with reference to the coupling constants.

R = $[CH_2]_6 – CO_2CH_3$

Suberin acids: $R_1 = [CH_2]_7 – OH$: methyl (*Z*)-18-hydroxyoctadecenoate (Hyd18:1_Me)

$R_1 = [CH_2]_6 – CO_2CH_3$: dimethyl (*Z*)-1,18-octadecenodioate (Di18:1_Me)

Model compounds: $R_1 = [CH_2]_6 – CH_3$: methyl (*Z*)-octadec-9-enoate (methyl oleate)

$R_1 = [CH_2]_6 – CH_3$: methyl (*E*)-octadec-9-enoate (methyl elaidate)

In alkyl disubstituted olefins, the second most important coupling constant in magnitude is the $^{3}J_{HH}$ between the olefinic and allylic vicinal protons (Figure 5). However, as the conformation of the allylic protons can change, a *cis* or *trans* double bond configuration doesn't show a major effect on this coupling constant, which has a typical averaged value of about +7 Hz [23]. On the

other hand, although smaller in magnitude, the $^4J_{HH}$ long-range allylic coupling was found to have a significant impact in the olefinic multiplet splitting pattern, even when small changes were considered. These long-range couplings are found in systems with double bonds, in which π-electrons help to transmit the spin information, so that there is a J(σ) and J(π) contribution to the coupling constant [27]. There is a stereochemical requirement in order for partial bond overlap to occur and consequently for these long-range couplings to take place. Taking in consideration the torsional angle (Φ) of the allylic C–H bond (as defined in Figure 5), J(π) maximizes for Φ = 0 or 180°, conformations in which the allylic C–H σ bond is parallel with the *p* orbitals of the C–C π bond. On the other hand, J(σ) maximizes for Φ = 90 or 270°, conformations in which the allylic C–H σ bond is parallel with the sp^2 orbitals of the C–C σ bond. The sign of the J(π) component of the $^4J_{HH}$ allylic coupling is negative, whilst the sign of the J(σ) component is positive [23], and therefore the signal of the actually observed $^4J_{HH}$ allylic coupling constant, reflects the preferred conformations. Typically, in alkyl disubstituted olefins, the observed values for the $^4J_{HH}$ allylic coupling constant in *trans* configuration are higher in absolute value compared to the *cis* isomer [28].

Finally, a $^5J_{HH}$ long-range homoallylic coupling can also be observed in these alkene systems but, due to the greater distance, it has a lower value than the allylic $^4J_{HH}$. Again, this type of coupling has to obey stereochemical requirements, only occurring if the two allylic C–H σ bonds are parallel to the plane of the C–C π bond [23]. However, in the simulation of the olefinic protons multiplets discussed below, variations in the $^5J_{HH}$ homoallylic coupling constants were shown to have little effect in the splitting pattern. For this reason they were not included in the simulations.

In this work we simulated the ^{1}H NMR complex second-order olefinic multiplets of methyl oleate, methyl elaidate, Hyd18:1_Me and Di18:1_Me (Figure 4, Table 2) in order to extract the double bond-derived coupling constants. In Figure 4, the original acquired multiplets are compared to the simulated multiplets together with the respective splitting diagrams. The spin systems, the chemical

shifts and the coupling constants used in the olefinic multiplets simulation of suberin acids and model compounds are shown in Table 2. Although in the four analyzed fatty acids the double bond substituents are mostly identical alkyl chains, $–[CH_2]_7–$, and the only possible structural difference is a *cis* or *trans* configuration, the olefinic multiplets were strikingly different in their splitting patterns (Figure 4). To simulate these multiplets, two spin systems were used. One, ABX_2Y_2, for non-symmetrical (in relation to the double bond) structures, namely the two model fatty acids and Hyd18:1_Me. The other, an AA'X_2X_2' system was used for Di18:1_Me, although one would expect it to have an A_2X_4 spin system, due to the complete symmetry of the molecule. If the latter case applied, that would mean that the olefinic protons of Di18:1_Me would show as a well defined quintet, which was not the case (Figure 4). We must conclude that some conformational effect makes the two olefinic protons in Di18:1_Me somehow magnetically non-equivalent.

Table 2. Simulation of olefinic proton NMR multiplets: spin systems, chemical shifts (ppm) and coupling constants (Hz) used in the simulation. Cork suberin acids methyl (*Z*)-18-hydroxyoctadecenoate (Hyd18:1_Me) and dimethyl (*Z*)-1,18-octadecenodioate (Di18:1_Me), and model compounds methyl (*Z*)-octadec-9-enoate (methyl oleate) and methyl (*E*)-octadec-9-enoate (methyl elaidate)

	Hyd18:1_Me	**Di18:1_Me**	***cis*-methyl oleate**	***trans*-methyl elaidate**
Spin system	ABX_2Y_2	$AA'X_2X_2'$	ABX_2Y_2	ABX_2Y_2
Chemical shifts				
A	5.3525	5.35	5.356	5.388
B	5.3460	5.35	5.344	5.379
X	2.0150	2.01	2.015	2.015
Y	2.0050	2.01	2.005	2.005
Coupling constants				
$^3J_{HH}$ olefinic	10.5	10.5	11.0	16.0
$^3J_{HH}$ olefinic/allylic	H_AH_X = 6.5 H_BH_Y = 6.5	H_AH_X = 7.3 H_BH_Y = 7.0	7.5	H_AH_X = 8.0 H_BH_Y = 7.9
$^4J_{HH}$ allylic	-2.0	-1.5	-1.5	H_AH_Y = -2.3 H_BH_X = -2.6

To match the acquired multiplets, the $^{3}J_{HH}$ olefinic, $^{3}J_{HH}$ olefinic-allylic and $^{4}J_{HH}$ allylic coupling constants were assayed within the known ranges for *cis* and *trans* isomers. The simulation, that took into account the 600 MHz resolution used in the acquired spectra, showed that relatively minor variations in the coupling constants had a major impact in the multiplet patterns (Table 2). In what respects the model compounds used, methyl oleate and methyl elaidate, a simulation of their olefinic protons has already been published [29], but both the multiplet patterns and some of the coupling constants presented are very different from the ones acquired and simulated in the present work. This can be probably due to the low resolution (60 MHz) on which the spectra were acquired, and also to different values used for the coupling constants, with the biggest differences for the *trans* isomer.

In our simulation, the $^{3}J_{HH}$ olefinic coupling constants used were in the *cis* range for methyl oleate, Di18:1_Me and Hyd18:1_Me, and within the *trans* range for methyl elaidate. In what respects the $^{3}J_{HH}$ olefinic-allylic coupling constants, values ranging from 6.5-8.0 Hz were used, with no apparent relation to *cis* or *trans* configuration. A significant role was played by the $^{4}J_{HH}$ allylic coupling constants, including their magnitude and signal. In fact, only negative coupling constants could approach the observed splitting patterns of the olefinic protons. As discussed above, *trans* isomers have higher $^{4}J_{HH}$ allylic coupling constants in absolute value, which is confirmed by the values used to simulate the *trans*-methyl elaidate olefinic multiplet, compared to the ones used in *cis*-methyl oleate and both $C_{18:1}$ suberin acids (Table 2). All the coupling constants used in the simulations to match the acquired ^{1}H olefinic multiplets of Di18:1_Me and Hyd18:1_Me were coincident with the values assignable to the *cis* configuration, thus definitely proving the stereochemistry of these suberin acids.

5. The configuration of $C_{18:1}$ suberin acids and the molecular structure of suberin

The suberin macromolecular assembly and how it relates to the ultrastructure of cork cell walls is almost completely unknown. Suberin composition is typically dominated by 9,10 mid-chain substituted C_{18} aliphatic acids, including 9-unsaturated, 9-epoxy and 9,10-diol monomers [2]. One key factor to understand the molecular packing of suberin is the stereochemistry of these mid-chain substituted C_{18} suberin acids, which can have different configurations, and therefore different spatial orientations. Although the composition of suberin from different plant sources is quite variable in terms of these long-chain aliphatic acids [1], the $C_{18:1}$ 9-unsaturated a,ω-bifunctional acids, the Hyd18:1 and Di18:1 discussed above, are common to all of them. These two monounsaturated acids are present in significant quantities in all suberins studied so far, sometimes in overwhelming proportions, such as in potato periderm, where they represent more than 70% of all long-chain monomers [3]. This means that the configuration of these olefinic acids and its associated preferable spatial conformations will be determinant for the suberin macromolecular structure.

We have shown here that both these $C_{18:1}$ suberin acids have a *cis* configuration, at least in the case of cork suberin. This is in agreement with the actually proposed pathway for the biosynthesis of the $C_{18:1}$ suberin acids, starting from oleic acid, and by successive oxidation of the terminal C-18 carbon, originating first the ω-hydroxyacid, Hyd18:1, and then the corresponding a,ω-diacid, Di18:1 [1]. The fact that the $C_{18:1}$ suberin acids are all *cis*, will condition their spatial preferred arrangements in the solid phase, as it is known to occur in fats [12]. Abundant literature exists about the molecular packing in the solid phase of oleic acid and its glycerol esters in fats, namely as triacylglycerol (triolein), one of its natural forms in plants. Triolein is known to have up to three different crystalline forms in the solid phase, each associated with different conformations around the double bond of the oleic acid units [12]. This means that the *cis*-9-unsaturation plays a major role in those crystal struc-

tures. We should remember that in suberin, the $C_{18:1}$ acids also exist as glycerol esters [2]. Besides, we have shown here that one of them, the $C_{18:1}$ ω-hydroxy-acid (Hyd18:1), even as a methyl ester, had at least one crystalline form. All together this shows that some ordered structure can exist in suberin and that the $C_{18:1}$ 9-unsaturated acids probably play a major role in such a molecular arrangement, which will eventually explain the unique properties of cork cell walls.

The $C_{18:1}$ 9-unsaturated suberin acids can have a number of valuable potential uses, taking advantage of their fatty-like behavior, derived from their long hydrocarbon chains and mid-chain *cis*-unsaturation, together with their bifunctionality at both chain ends. Taking into account that Hyd18:1 and Di18:1 are two of the main constituents of cork suberin, the latter can also be regarded as a natural and renewable source to obtain these compounds.

6. References

[1] Kollatukudy, P. 2002. Suberin from plants. In: Doi, Y., Steinbüchel, A., editors. *Biopolymers - Polyesters I*. Wiley-VCH, Weinheim. pp. 1-40.

[2] Graça, J., Santos, S. 2007. Suberin: a biopolyester of plants' skin. *Macromolecular bioscience* **7**(2): 128-135.

[3] Graça, J., Pereira, H. 2000. Suberin structure in potato periderm: glycerol, long-chain monomers, and glyceryl and feruloyl dimers. *Journal of agricultural and food chemistry* **48**(11): 5476-5483.

[4] Rodríguez-Miguens, B., Ribas-Marqués, I. 1972. Investigaciones químicas sobre el corcho de *Solanum tuberosum* L. (patata). *Anales de química* **68**: 303-308.

[5] Eliel, E., Wilen, S. 1994. *Stereochemistry of organic compounds*. John Wiley & Sons, New York.

[6] Gunstone, F. 1999. *Lipid synthesis and manufacture*. Sheffield Academic Press, Sheffield.

[7] Harvey, D. 1992. Mass spectrometry of picolinyl and other nitrogen-containing derivatives of lipids. In: Christie, W., editor. *Advances in Lipid Methodology – One*. The Oily Press, Dundee. pp. 19-80.

[8] Eder, K. 1995. Gas chromatographic analysis of fatty-acid methyl-esters. *Journal of chromatography B - Biomedical applications* **671**(1-2): 113-131.

[9] Ribas, I., Seoane, E. 1954. Química del corcho. XII. Ácido 18-hidroxi-9-octadecenoico y derivados. *Anales de la real sociedad Española de física y química/Ser.B, química* **50B**: 971-976.

[10] Ribas, I., Seoane, E. 1954. Química del corcho. XI. Ácidos no saturados. *Anales de la real sociedad Española de física y química/Ser.B, química* **50B**: 963-970.

[11] Zhang, J., Yu, Q., Liu, B., Huang, Z. 1988. Chemical modification in mass spectrometry IV-2-alkenyl-4,4-dimethyloxazolines as derivatives for the double

bond location of long-chain olefinic acids. *Biomedical and environmental mass spectrometry* **15**(1): 33-44.

[12] Larsson, K., Quinn, P., Sato, K., Tiberg, F. 2006. *Lipids: structure, physical properties and functionality*. The Oily Press, Bridgewater.

[13] Knothe, G., Dunn, R. 2009. A comprehensive evaluation of the melting points of fatty acids and esters determined by differential scanning calorimetry. *Journal of the American oil chemists' society* **86**(9): 843-856.

[14] Socrates, G. 2001. *Infrared and Raman characteristic group frequencies - Tables and charts 3rd Edition*. John Wiley & Sons, Chichester.

[15] Lerma-García, M., Simo-Alfonso, E., Bendini, A., Cerretani, L. 2011. Rapid evaluation of oxidized fatty acid concentration in virgin olive oil using Fourier-transform infrared spectroscopy and multiple linear regression. *Food chemistry* **124**(2): 679-684.

[16] Beattie, J., Bell, S., Moss, B. 2004. A critical evaluation of Raman spectroscopy for the analysis of lipids: fatty acid methyl esters. *Lipids* **39**(5): 407-419.

[17] Guillén, M., Cabo, N. 1998. Relationships between the composition of edible oils and lard and the ratio of the absorbance of specific bands of their Fourier transform infrared spectra. Role of some bands of the fingerprint region. *Journal of agricultural and food chemistry* **46**(5): 1788-1793.

[18] Sadeghi-Jorabchi, H., Wilson, R., Belton, P., Edwardswebb, J., Coxon, D. 1991. Quantitative analysis of oils and fats by Fourier transform Raman spectroscopy. *Spectrochimica acta part A: Molecular and biomolecular spectroscopy* **47**(9-10): 1449-1458.

[19] Chapman, D. 1965. *Infra-red and Raman spectroscopy*. Methuen and CO Ltd., London.

[20] Günzler, H., Gremlich, H-U. 2002. *IR Spectroscopy*. Wiley-VCH, Weinheim.

[21] Bailey, G., Horvat, R. 1972. Raman spectroscopic analysis of the *cis/trans* isomer composition of edible vegetable oils. *Journal of the American oil chemists' society* **49**(8): 494-498.

[22] Abraham, R., Canton, M., Griffiths, L. 2001. Proton chemical shifts in NMR: Part 17. Chemical shifts in alkenes and anisotropic and steric effects of the double bond. *Magnetic resonance in chemistry* **39**(8): 421-431.

[23] Günther, H. 2001. *NMR Spectroscopy*. John Wiley & Sons, New York.

[24] Allman, R. 2010. CMR: Peak splitting. In: Allman, R., editor. *Nuclear magnetic resonance*. http://www.wavesignal.com/forensics/NMR.html.

[25] Gunstone, F. 1993. The composition of hydrogenated fats by high-resolution C-13 nuclear-magnetic-resonance spectroscopy. *Journal of the American oil chemists' society* **70**(10): 965-970.

[26] Reich, H. 2012. 5.3 Spin-spin splitting: J-coupling. In: University of Wisconsin, editor. *University of Wisconsin, department of chemistry*. http://www.chem.wisc.edu/areas/reich/nmr/05-hmr-03-jcoupl.htm.

[27] Pavia, D., Lampman, G., Kriz, G., Vyvyan, J. 2009. *Introduction to spectroscopy*. Brooks/Cole, Belmont.

[28] Rummens, F., Haan, J. 1970. Spectroscopic studies on olefins - III: NMR of *cis*- and *trans*-disubstituted olefins. *Organic magnetic resonance* **2**(4): 351-355

[29] Schaumburg, K., Bernstein, H. 1968. Calculation of the NMR spectrum of double-bond protons in aliphatic systems. *Lipids* **3**(3): 193-198.

7. Supplementary material

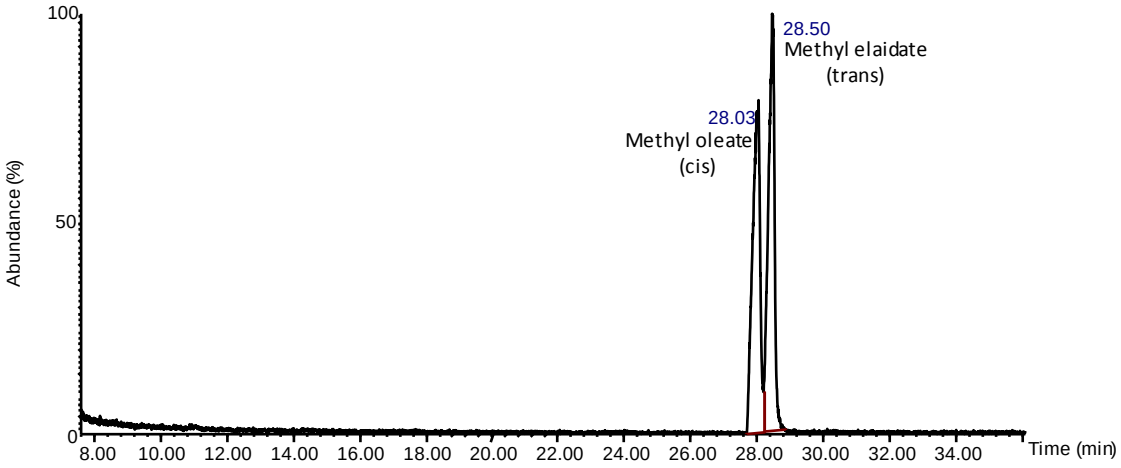

Figure SM1. GC-MS ion chromatogram of a 1:1 mixture of methyl oleate (Rt=28.03min) and methyl elaidate (Rt=28.50min) separated on a DB5-MS GC column

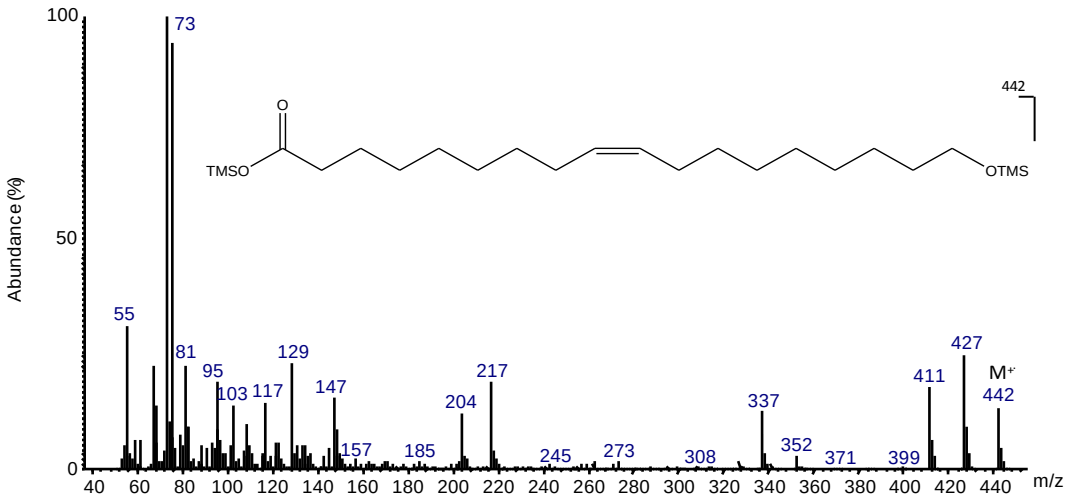

Figure SM2. Electron ionization mass spectrum of the (Z)-18-hydroxyoctadec-9-enoic acid (Hyd18:1) bis-TMS derivative, extracted from cork suberin

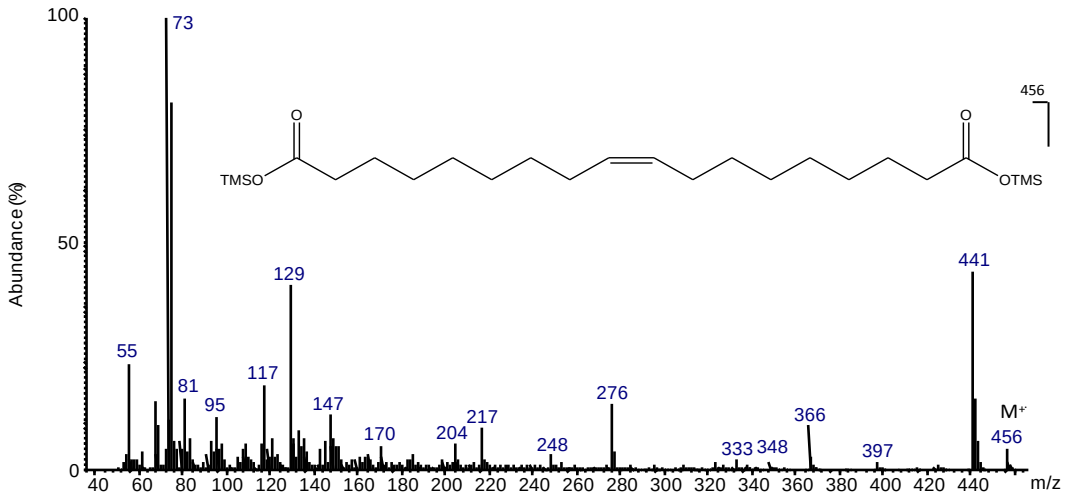

Figure SM3. Electron ionization mass spectrum of the (Z)-octadec-9-enedioic acid (Di18:1) bis-TMS derivative, extracted from cork suberin

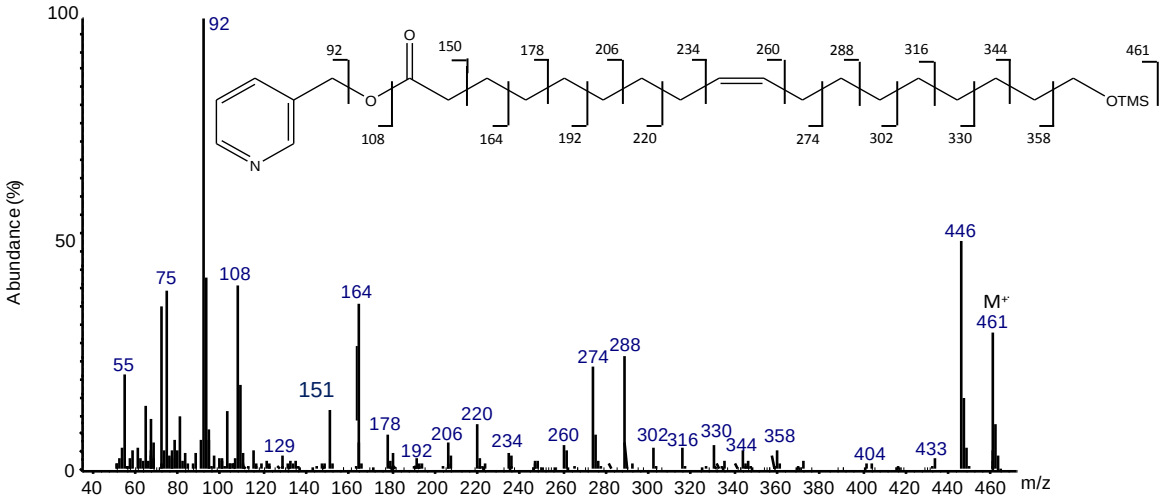

Figure SM4. Electron ionization mass spectrum of the picolinyl ester, TMS ether derivative of (Z)-18-hydroxyoctadec-9-enoic acid (Hyd18:1), extracted from cork suberin

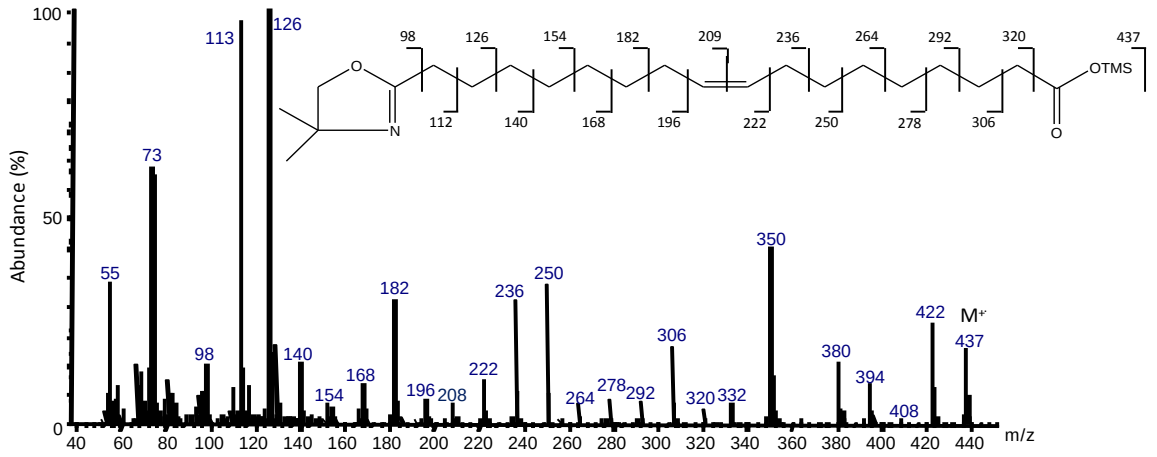

Figure SM5. Electron ionization mass spectrum of the DMOX/TMS derivative of (Z)-octadec-9-enedioic acid (Di18:1), extracted from cork suberin

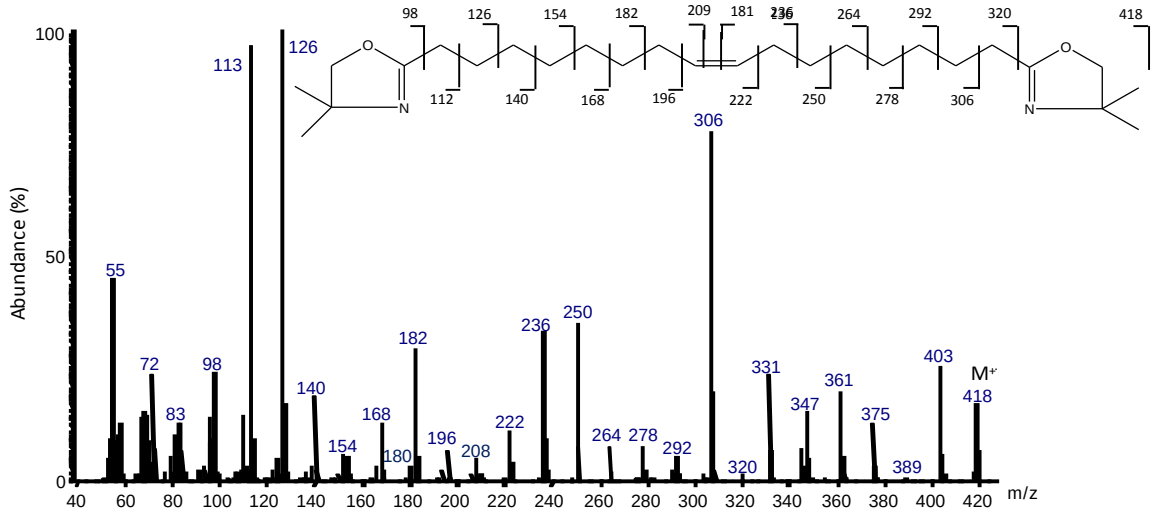

Figure SM6. Electron ionization mass spectrum of the *bis*-DMOX derivative of (Z)-octadec-9-enedioic acid (Di18:1), extracted from cork suberin

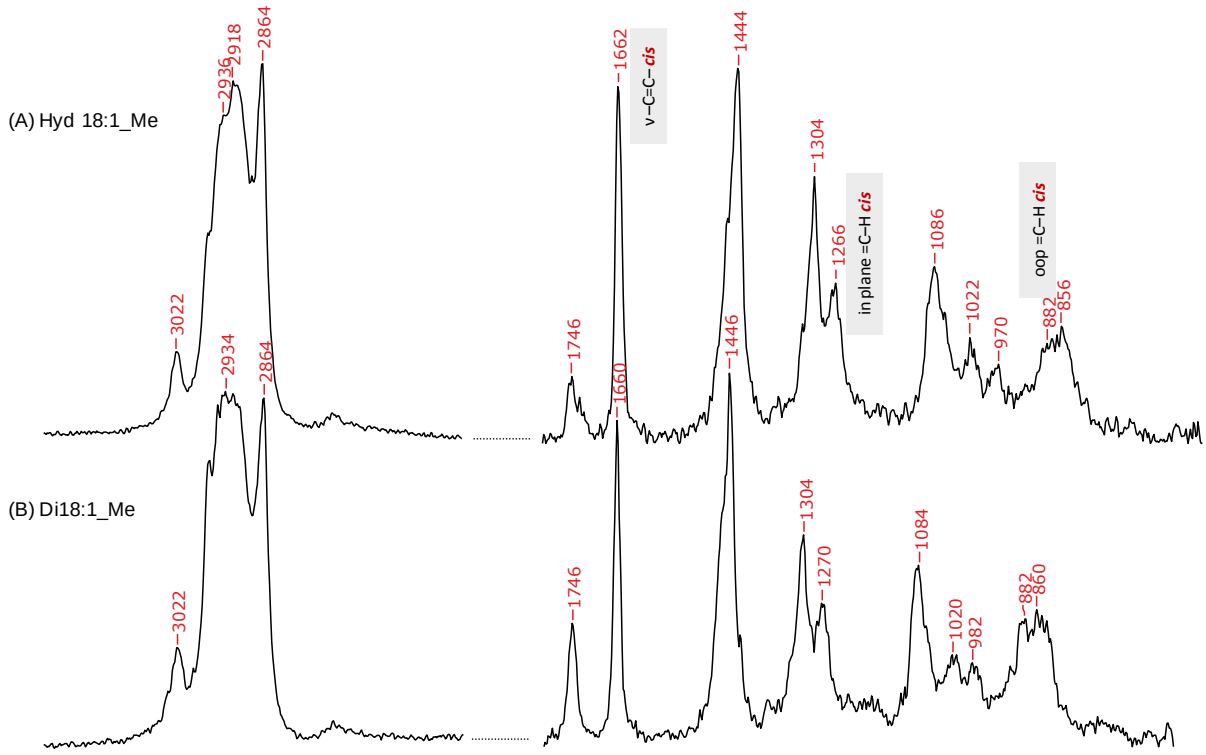

Figure SM7. Raman spectra of cork suberin $C_{18:1}$ monounsaturated acids: (A) Hyd18:1_Me [methyl (Z)-18-hydroxyoctadecenoate]; (B) Di18:1_Me [dimethyl (Z)-1,18-octadecenodioate], with the main diagnostic *cis* absorption bands highlighted

Table SM1: FTIR frequencies (cm^{-1}) in methyl (*E*)-octadec-9-enoate (methyl elaidate), methyl (*Z*)-octadec-9-enoate (methyl oleate), methyl (*Z*)-18-hydroxyoctadecenoate (Hyd18:1_Me) and dimethyl (*Z*)-1,18-octadecenodioate (Di18:1_Me), with tentative band assignments [a]

v max					Assignment	
Methyl Elaidate	**Methyl Oleate**	**Hyd18:1_Me**	**Di18:1_Me**	**Band intensity**	**Group**	**Mode**
		3362		w (broad)	H bonded alcohols	O–H str [3]
3016				w	–HC=CH– ***trans***	asym C–H str [1]
	3005	3003	3002	w/m	–HC=CH– ***cis***	asym C–H str [1]
2960	2960			m	aliphatic $–CH_3$ (shoulder)	asym C–H str [1]
2935 2918	2926	2924	2926	vs	$–(CH_2)_n–$	asym C–H str [3]
2855	2855	2853	2854	s	$–(CH_2)_n–$	sym C–H str [3]
1743	1743	1739	1738	vs	$–CO_2CH_3$	C=O str [3]
	1655	1655	1656	vw	–HC=CH– ***cis***	C=C str [3]
1463	1463	1460	1459	m	$–(CH_2)_n–$ aliphatic $–CH_3$ (shoulder)	C–H scis [1] asym C–H def [4]
1436	1436	1437	1436	w/m	$–CO_2CH_3$	sym C–H def [3]
1377	1377			w	aliphatic $–CH_3$ (shoulder)	sym C–H def [1]
1362	1362	1361	1360	w	α-CH_2	C–H wag [2]
1317	1317	1317	1317	w	$–(CH_2)_n–$	C–H wag or twist [2]
1303	1303			w	$–(CH_2)_n–$	C–H wag or twist [2]
1246	1246	1244	1244	w/m	$–CH_2–CO_2CH_3$	C–C skel coupled with α-CH_2 def [2]
1197	1197	1198	1196	w/m	$–CH_2–CO_2CH_3$ $–(CH_2)_n–$	C–C skel coupled with α-CH_2 def [2] C–H twist [2]
1171	1171	1171	1168	m/s	$–CO_2CH_3$	asym C–O–C str [3]
1121	1120			vw	$–CO_2CH_3$	C–H rock [3]
1097	1094	1091	1091	vw	$–(CH_2)_n–$ $–CO_2CH_3$	C–C skel [3] C–H rock [3]
		1055		m	$–CH_2CH_2OH$ in primary alcohols	C–O in –C–C–O– str [3]
1018	1017	1021	1015	w	$–CO_2CH_3$ $–CH_2–CO_2CH_3$	C–H rock [3] C–C skel coupled with α-CH_2 def [2]
967				w/m	–HC=CH– ***trans***	C=C oop bend [3]
881	880	879	878	vw/w	$–CO_2CH_3$	C–H wag [3] or rock [2] (?)
845	851	855	848	vw/w	(Sat) –CH=CH– (Sat´) $–CO_2CH_3$	C–H wag [3] C–H rock [2]
724	724	723	725	w/m	$–(CH_2)_n–$	C–H rock [3]
	694	695	695	w	–CH=CH– ***cis***	C–H wag [3]
	585	586	588	w	–CH=CH– ***cis***	C–H skel [3]
			515	w	$–CO_2CH_3$	C–H def [3]
		505		w	$–CH_2–OH$ in primary alcohols	C–O def [3]
		438	435	w	C–C –CH=CH– (?)	C–C skel [3] C–H skel and torsional [3]

Note: [a] asym: asymmetric; def: deformation (bending); m: medium; oop: out-of-plane; rock: rocking; scis: scissoring; skel: skeletal; str: stretching; s: strong; sym: symmetric; twist: twisting; v: very; wag: wagging; w: weak; v max: maximum wavelength (cm^{-1}).

Table SM2: Raman frequencies (cm^{-1}) of methyl (Z)-18-hydroxyoctadecenoate (Hyd18:1_Me) and dimethyl (Z)-1,18-octadecenodioate (Di18:1_Me), with tentative band assignments [a]

v max			Assignment	
Hyd18:1_Me	**Di18:1_Me**	**Band intensity**	**Group**	**Mode**
3022	3022	m	–HC=CH–	asym C–H str [3]
2964-2910	2962-2912	vs	$–(CH_2)–$	asym C–H str [3]
2864	2864	vs	$–(CH_2)–$	sym C–H str [3]
1746	1746	m	$–CO_2CH_3$	C=O str [3]
1662	1660	vs	–HC=CH– ***cis***	C=C str [3]
1462	1458	s	$–(CH_2)–$ aliphatic $–CH_3$ (shoulder)	C–H scis [1] asym C–H def [4]
1444	1446	vs	$–CO_2CH_3$	sym C–H def [3]
1326	1325	w/m	$–(CH_2)_n–$	C–H wag or twist [2]
1304	1304	s	$–(CH_2)_n–$	C–H twist [5]
1266	1270	m	–HC=CH– ***cis***	C–H in plane [5]
1086	1084	m	$–(CH_2)_n–$ $–(CH_2)_n–$	C–C skel [3] C–C–C str [3]
1068	1070	w/m	$–(CH_2)_n–$	asym C–C–C str [5]
1022	1020	w	$–CH_2–CO_2CH_3$	C–C skel coupled with α-CH_2 def [2]
980	982	w	$–(CH_2)_n–$	asym C–C–C–C str [3]
882	882	w/m	–HC=CH– ***cis*** $–(CH_2)_n–$ $–CO_2CH_3$	C–H oop [3] C–C and C–C–C–C skel [3] C–H wag [3]
856	860	w/m	$–(CH_2)_n–$ (Sat) –CH=CH– (Sat´) $–CO_2CH_3$	C–C and C–C–C–C skel [3] C–H wag [3] C–H rock [2]

Note: [a] asym: asymmetric; def: deformation (bending); m: medium; oop: out-of-plane; rock: rocking; scis: scissoring; skel: skeletal; str: stretching; s: strong; sym: symmetric ; twist: twisting; v: very; wag: wagging; w: weak; v max: maximum wavelength (cm^{-1}).

Table 1 references:

[1] Guillen MD, Cabo N. 1998. Relationships between the composition of edible oils and lard and the ratio of the absorbance of specific bands of their Fourier transform infrared spectra. Role of some bands of the fingerprint region. *J Agric Food Chem* **46**(5): 1788-1793.
[2] Chapman D. 1965. *The structure of lipids*. Methuen and CO Ltd.: London; 52-128.
[3] Socrates G. 2001. *Infrared and Raman characteristic group frequencies - Tables and charts 3rd Edition*. John Wiley & Sons; England.
[4] Lerma-García MJ, Simo-Alfonso EF, Bendini A, Cerretani L. 2011. Rapid evaluation of oxidised fatty acid concentration in virgin olive oil using Fourier-transform infrared spectroscopy and multiple linear regression. *Food Chem* **124**(2): 679-684.

Table 2 references:

[1] Guillen MD, Cabo N. 1998. Relationships between the composition of edible oils and lard and the ratio of the absorbance of specific bands of their Fourier transform infrared spectra. Role of some bands of the fingerprint region. *J Agric Food Chem* **46**(5): 1788-1793.
[2] Chapman D. 1965. *The structure of lipids*. Methuen and CO Ltd.: London; 52-128.
[3] Socrates G. 2001. *Infrared and Raman characteristic group frequencies - Tables and charts 3rd Edition*. John Wiley & Sons; England.
[4] Lerma-García MJ, Simo-Alfonso EF, Bendini A, Cerretani L. 2011. Rapid evaluation of oxidised fatty acid concentration in virgin olive oil using Fourier-transform infrared spectroscopy and multiple linear regression. *Food Chem* **124**(2): 679-684.
[5] Beattie JR, Bell, SEJ, Moss BW. 2004. A critical evaluation of Raman spectroscopy for the analysis of lipids: Fatty acid methyl esters. *Lipids* **39**(5): 407-419.

Table SM3. ^{1}H and ^{13}C chemical shifts (ppm) of the suberin acids methyl (*Z*)-18-hydroxyoctadecenoate (Hyd18:1_Me) and dimethyl (*Z*)-1,18-octadecenodioate (Di18:1_Me), and of the model compounds methyl (*Z*)-octadec-9-enoate (methyl oleate) and methyl (*E*)-octadec-9-enoate (methyl elaidate), the two latter compared with literature data

	Hyd18:1_Me		**Di18:1_Me**		**Methyl oleate**		**Methyl elaidate**		**Methyl oleate [1]**	**Methyl oleate [2]**	**Methyl elaidate [1]**
	^{1}H	**^{13}C**	**^{1}H**	**^{13}C**	**^{1}H**	**^{13}C**	**^{1}H**	**^{13}C**	**^{13}C**	**^{13}C**	**^{13}C**
OCH_3	3.66	51.37	3.66	51.35	3.67	51.43	3.67	51.43	51.40	51.31	51.31
1	-	174.30	-	174.22	-	174.31	-	174.33	174.27	173.91	174.15
2	2.30	34.04	2.30	34.04	2.30	34.10	2.30	34.10	34.10	34.09	34.06
3	1.62	24.88	1.62	24.90	1.62	24.93	1.62	24.94	24.96	24.96	24.95
4	1.30-1.33	29.00-29.66	1.30-1.33	29.03-29.62	1.27-1.34	29.08-29.75	1.26-1.34	28.92-29.64	29.16	29.13	28.94
5	1.30-1.33	29.00-29.66	1.30-1.33	29.03-29.62	1.27-1.34	29.08-29.75	1.26-1.34	28.92-29.64	29.16	29.13	29.13
6	1.30-1.33	29.00-29.66	1.30-1.33	29.03-29.62	1.27-1.34	29.08-29.75	1.26-1.34	28.92-29.64	29.16	29.09	29.13
7	1.33/1.34	29.00-29.66	1.30-1.33	29.03-29.62	1.27-1.34	29.08-29.75	1.26-1.34	28.92-29.64	29.71	29.68	29.19
8	2.01	27.11	2.01	27.11	2.01	27.20	1.96	32.59	27.22	27.22	32.61
9	5.34	129.74	5.34	129.79	5.35	129.74	5.38	130.20	129.74	129.56	130.18
10	5.34	129.85	5.34	129.79	5.35	129.99	5.38	130.47	129.98	129.80	130.44
11	2.01	27.09	2.01	27.11	2.01	27.14	1.96	32.54	27.18	27.18	32.56
12	1.33/1.34	29.00-29.66	1.30-1.33	29.03-29.62	1.27-1.34	29.08-29.75	1.26-1.34	28.92-29.64	29.79	29.76	29.33
13	1.30-1.33	29.00-29.66	1.30-1.33	29.03-29.62	1.27-1.34	29.08-29.75	1.26-1.34	28.92-29.64	29.34	29.33	29.51
14	1.30-1.33	29.00-29.66	1.30-1.33	29.03-29.62	1.27-1.34	29.08-29.75	1.26-1.34	28.92-29.64	29.54	29.52	29.57
15	1.30-1.33	29.00-29.66	1.30-1.33	29.03-29.62	1.27-1.34	29.08-29.75	1.26-1.34	28.92-29.64	29.34	29.33	29.66
16	1.33/1.34	25.69	1.62	24.90	1.27-1.34	31.89	1.26-1.34	31.89	31.93	31.90	31.92
17	1.56	32.74	2.30	34.04	1.27-1.34	22.67	1.26-1.34	22.67	22.71	22.70	22.68
18	3.63	62.91	-	174.22	0.88	14.10	0.88	14.10	14.12	14.09	14.07
OCH_3'	-	-	3.66	51.35	-	-	-	-	-	-	-

References:

[1] Frighetto N, Silveira LPC, Reis AMF, Magalhães GE, Rúveda AE. 1978. Dienoic acids, synthesis and ^{13}C NMR spectral analysis. *Chem. Phys. Lipids* **22**(2): 115–120.

[2] Tulloch AP, Mazurek M. 1976. C-13 Nuclear magnetic-resonance spectroscopy of saturated, unsaturated, and oxygenated fatty-acid methyl-esters. *Lipids* **11**(3): 228-234.

Table SM4. Olefinic and allylic (C_8 to C_{11}) ^{1}H and ^{13}C chemical shifts (ppm) of the suberin acids methyl (*Z*)-18-hydroxyoctadecenoate (Hyd18:1_Me) and dimethyl (*Z*)-1,18-octadecenodioate (Di18:1_Me), and of the model compounds methyl (*Z*)-octadec-9-enoate (methyl oleate) and methyl (*E*)-octadec-9-enoate (methyl elaidate), the two latter compared with literature data

	Hyd18:1_Me		Di18:1_Me		methyl oleate		methyl elaidate		methyl oleate 1	methyl oleate 2	methyl oleate 3	methyl oleate 4	methyl oleate 5	methyl elaidate 1	methyl elaidate 3	methyl elaidate 4	methyl elaidate 5
	^{1}H	^{13}C	^{1}H	^{13}C	^{1}H	^{13}C	^{1}H	^{13}C	^{13}C	^{13}C	^{13}C	^{13}C	^{13}C	^{13}C	^{13}C	^{13}C	^{13}C
C_8	2.01	27.11	2.01	27.11	2.01	27.20	1.96	32.59	27.22	27.22	-	27.2	-	32.61	-	32.5	-
C_9	5.34	129.74	5.34	129.79	5.35	129.74	5.38	130.20	129.74	129.56	129.78	129.8	129.71	130.18	130.23	130.3	130.07
C_{10}	5.34	129.85	5.34	129.79	5.35	129.99	5.38	130.47	129.98	129.80	130.09	130.0	130.03	130.44	130.54	130.5	130.60
C_{11}	2.01	27.09	2.01	27.11	2.01	27.14	1.96	32.54	27.18	27.18	-	27.3	-	32.56	-	32.6	-

References:

[1] Frighetto N, Silveira LPC, Reis AMF, Magalhães GE, Rúveda AE. 1978. Dienoic acids, synthesis and ^{13}C NMR spectral analysis. *Chem. Phys. Lipids* **22**(2): 115–120.

[2] Tulloch AP, Mazurek M. 1976. C-13 Nuclear magnetic-resonance spectroscopy of saturated, unsaturated, and oxygenated fatty-acid methyl-esters. *Lipids* **11**(3): 228-234.

[3] Gunstone FD, Pollard MR. 1977. Fatty-acids part 50 - C-13-Nuclear magnetic-resonance studies of olefinic fatty-acids and esters. *Chem. Phys. Lipids* **18**(1): 115-129.

[4] Pfeffer PE, Luddy EF. 1977. Analytical C-13 NMR - Rapid, nondestructive method for determining *cis*, *trans* composition of catalytically treated unsaturated lipid mixtures. *J Am Oil Chem Soc* **54**(9): 380-386.

[5] Miyake Y, Yokomizo K. 1998. Determination of *cis*- and *trans*-18:1 fatty acid isomers in hydrogenated vegetable oils by high-resolution carbon nuclear magnetic resonance. *J Am Oil Chem Soc* **75**(7): 801-805.

Chapter 4: Stereochemistry of 9,10-epoxy and 9,10-diol cork suberin acids

[Santos, S., Cabral, V., Graça, J. 2013. Cork suberin molecular structure: stereochemistry of the C_{18} epoxy and *vic*-diol ω-hydroxyacids and a,ω-diacids analyzed by NMR. *Journal of Agricultural and Food Chemistry*, **61**(29): 7038–7047]

1. Abstract

Suberin is the biopolyester that protects the secondary tissues of plants against environmental variability and aggressions. The backbone of cork suberin are the C_{18} ω-hydroxyacids and a,ω-diacids 9,10-substituted with an unsaturation, an epoxide ring or a *vic*-diol group. Although determinant for suberin molecular structure, few studies were made on their stereochemistry, sometimes with contradictory results. NMR techniques were developed here to assign the configuration of the C_{18} 9,10-epoxy and 9,10-diol suberin acids based in the ^{1}H and ^{13}C chemical shifts, either analyzed as such or after conversion into benzylidene acetal derivatives. The relative stereochemistry was proved to be *cis* in the C_{18} 9,10-epoxy and *threo* in the C_{18} 9,10-diol suberin acids. These suberin monomers are probably present as racemic mixtures, as shown by polarimetry. The revealed stereochemistry allows the suberin macromolecule to be built as an ordered array of mid-chain kinked C_{18} acids, reinforced by intra-molecular hydrogen bonding.

Keywords: suberin, cork, C_{18} 9,10-epoxy suberin acids, C_{18} 9,10-diol suberin acids, *vic*-diols stereochemistry determined by NMR, benzylidene acetal derivatives.

2. Introduction

Suberin is a lipid macromolecule found in suberized plant cell walls, which act as a frontier barrier towards environmental variability and aggressions. Suberized cells comprise most of the periderm, the tissue that envelops plant organs of secondary growth, like tree trunks or potato tubers. Suberized cells also develop as wound tissue in plants, after injury or leaf fall ("abscission"), and in internal organs where water flow control is needed, like in the root endodermis ("Casparian bands"). The barrier and insulation properties of suberin, which are vital for plants survival, derive ultimately from its molecular and

supramolecular structure in suberized cell walls. In spite of its importance, and the significant quantity of knowledge already gathered [1,2], many doubts remain about how suberin is build up as a macromolecule.

Suberin is known to be a glycerolipid polyester, meaning that it is assembled from glycerol and fatty acid-derived units, inter-linked by ester bonds. When these ester bonds are broken, suberin depolymerization occurs releasing its "monomers". Besides glycerol, the major constituents of suberin are long-chain aliphatic acids, which typically account for 80% or more of its depolymerization products, and are collectively named as "suberin acids". Within the latter, two families of a,ω-bifunctional fatty acids are largely dominant: ω-hydroxyacids and a,ω-diacids. The fact that ω-hydroxyacids and a,ω-diacids have either hydroxyl or carboxylic acid linking groups at both chain ends, allows the macromolecular polyester to grow, making suberin fundamentally different from other glycerolipids or waxes, which are based in monofunctional fatty acids.

Although suberins studied so far from different plant species and tissues all show the basic composition pattern of glycerol, ω-hydroxyacids and a,ω-diacids, they can be quite variable in the specific suberin acids they are made of. Suberin ω-hydroxyacids and a,ω-diacids typically have even-numbered carbon chain lengths between C_{16} and C_{24} [1,2]. There are suberins with significant amounts of C_{16} acids, and others where C_{22} or longer acids are relevant monomers [1]. However, all suberins analyzed had C_{18} suberin acids in significant amounts, meaning that they play a major role in its macromolecular structure. These C_{18} suberin acids are specific because they all have a mid-chain "functional" group, at carbons C-9 and C-10: this can be a double-bond, or an oxygen-containing substituent group, either an epoxide ring or two hydroxyl groups in vicinal positions (*vic*-diol). Because these secondary substituents impart chirality to the carbons they are attached to, these suberin acids can have different stereochemical configurations. Understanding the stereochemistry of the C_{18} suberin acids is important for two main reasons: first, the molecular packing of the C_{18} monomers, including eventual ordered

arrangements or intra-molecular bonds they might have, are dependent on their spatial configuration and conformation, thus determining the macromolecular structure of suberin; second, because these suberin acids are potentially interesting for a number of valuable industrial uses, their stereochemistry will also determine their properties, reactivity and possible applications.

The focus of the present work is the stereochemistry of the C_{18} suberin acids with oxygen-containing substituents, namely 9,10-epoxy and 9,10-diol groups, found in cork suberin (the stereochemical analysis of the C_{18} 9-unsaturated has been presented and discussed in Chapter three).

Cork suberin is paradigmatic and interesting for this study for several reasons. First, cork is the epitome of the suberized plant tissues: cork is the outer-bark of the cork-oak tree (*Quercus suber* L.), and is harvested in a sustainable manner, reaching several centimeters of thickness in each growth cycle of 9 years. This commercial cork is an important material, used worldwide in an enormous number of artifacts and technical uses, for some of them without an alternative substitute. The second reason is because cork suberin has a complex composition including significant amounts of C_{18} 9,10-epoxy and 9,10-diol suberin acids, together representing ca 44% of the suberin mass [3,4]. Finally, in the perspective of an eventual extraction of these suberin acids for industrial use, availability is assured: cork is produced each year in thousands of tons [5], with suberin accounting for about 45% of its dry weight.

Cork suberin includes two C_{18} 9,10-epoxy acids and two C_{18} 9,10-diol acids, both ω-hydroxyacids and a,ω-diacids. Each of them has two asymmetric carbons and therefore can exist in the form of up to four different stereoisomers (Figure 1). We can consider their relative and their absolute stereochemistry. The C_{18} epoxy-ω-hydroxyacid, 9,10-epoxy-18-hydroxyoctadecanoic (from now on referred as Hyd18Epox) and the C_{18} epoxy-a,ω-diacid, 9,10-epoxy-octadecane-1,18-dioic (Di18Epox), can have a *cis* or *trans* relative configuration, each one with two possible absolute configurations, (*S*,*R* or *R*,*S* for the *cis* isomer and *S*,*S* or *R*,*R* for the *trans* isomer) (Figure 1). In the specific case of the Di18Epox, where both substituents regarding the epoxide ring are

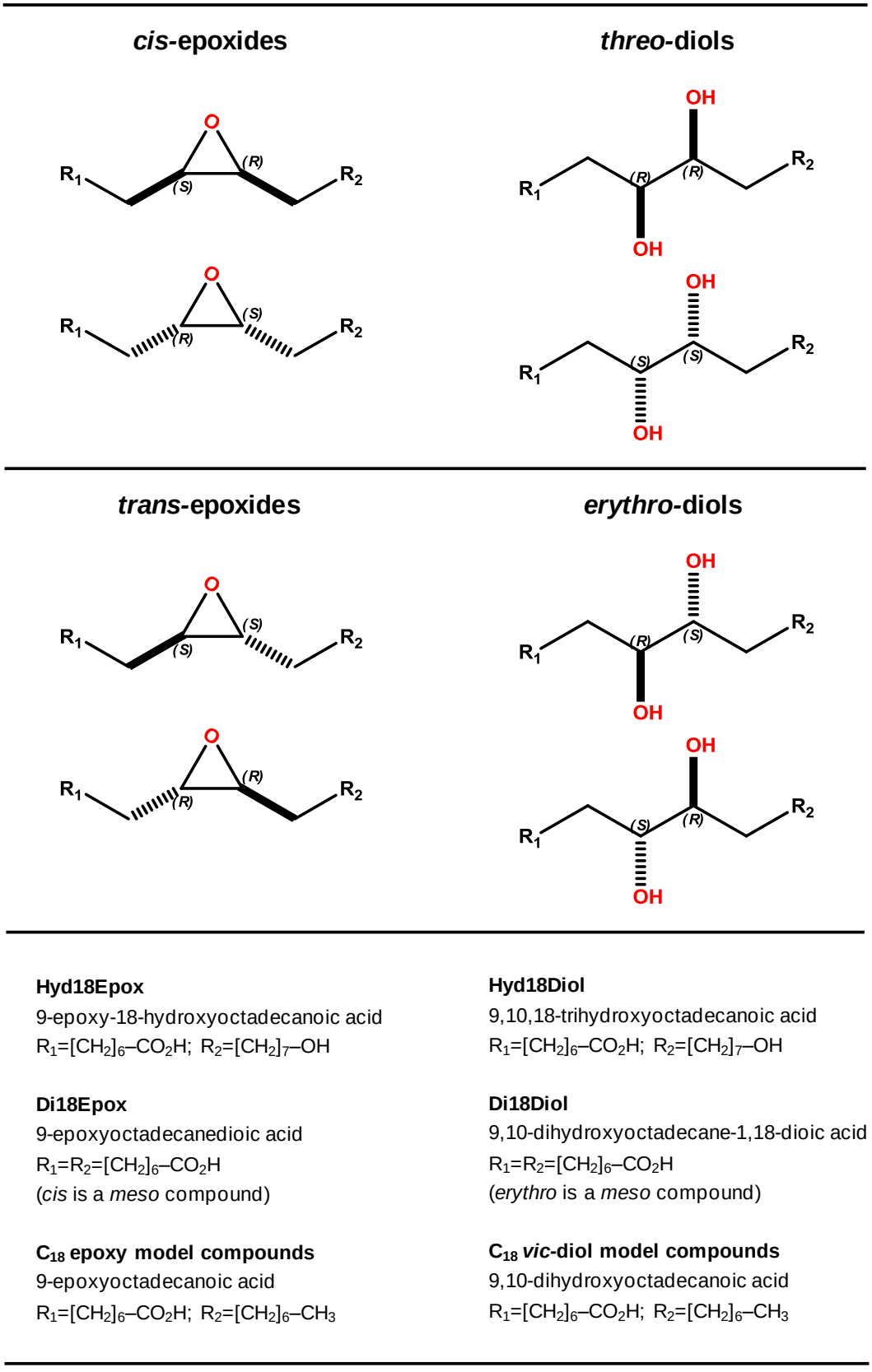

Hyd18Epox
9-epoxy-18-hydroxyoctadecanoic acid
R_1=$[CH_2]_6$–CO_2H; R_2=$[CH_2]_7$–OH

Hyd18Diol
9,10,18-trihydroxyoctadecanoic acid
R_1=$[CH_2]_6$–CO_2H; R_2=$[CH_2]_7$–OH

Di18Epox
9-epoxyoctadecanedioic acid
R_1=R_2=$[CH_2]_6$–CO_2H
(*cis* is a *meso* compound)

Di18Diol
9,10-dihydroxyoctadecane-1,18-dioic acid
R_1=R_2=$[CH_2]_6$–CO_2H
(*erythro* is a *meso* compound)

C_{18} epoxy model compounds
9-epoxyoctadecanoic acid
R_1=$[CH_2]_6$–CO_2H; R_2=$[CH_2]_6$–CH_3

C_{18} *vic*-diol model compounds
9,10-dihydroxyoctadecanoic acid
R_1=$[CH_2]_6$–CO_2H; R_2=$[CH_2]_6$–CH_3

Figure 1. Structural representation of the stereochemistry of the C_{18} 9,10-epoxy and C_{18} 9,10-diol acids: possible relative (*cis*/*trans* and *erythro*/*threo*) and absolute configurations

identical, the *cis* isomer is a *meso* compound, since its two possible enantiomeric forms are identical (Figure 1). In what respects the C_{18} 9,10-diol suberin acids, namely the ω-hydroxyacid, 9,10,18-trihydroxyoctadecanoic (Hyd18Diol) and the a,ω-diacid, 9,10-dihydroxyoctadecane-1,18-dioic (Di18Diol), their relative stereochemistry can be described using the Fischer projection, as *threo* (*R*,*R* or *S*,*S*) or *erythro* (*R*,*S* or *S*,*R*) (Figure 1). Again, in the case of Di18Diol, where both substituents attached to the *vic*-diol group are identical, the *erythro* isomer is *meso*, because the *R*,*S* and *S*,*R* forms are indistinguishable (Figure 1).

Except for a few pioneering works dating back to the middle of the last century, the stereochemistry of these C_{18} 9,10-epoxy and 9,10-diol acids in suberin have never been thoroughly studied. The relative configuration of the Hyd18Diol acid (by then also known as "phloionolic acid"), was firstly studied by Seoane and co-workers [6-9]. These authors compared the melting point (104 °C) of the Hyd18Diol isolated from cork, with the melting point of the presumed *erythro* isomer (133 °C), obtained by the stereospecific *syn*-hydroxylation of the C_{18} 9-unsaturated ω-hydroxyacid (18-hydroxyoctadec-9-enoic acid, also obtained from cork, and believed to be of *cis* configuration by infrared analysis). Because the latter melting point value was higher than the former, and following the empiric rule that *erythro* isomers have higher melting points then the corresponding *threo* isomers, the *threo* configuration was assigned to the Hyd18Diol obtained from cork suberin [7,9].

A similar approach and reasoning was used for the assignment of the relative stereochemistry of the Di18Diol, formerly named "phloionic acid". The Di18Diol was isolated from cork suberin (melting point 121 °C), converted to its isomeric form *iso*-Di18Diol (melting point 159 °C), and retro-synthesized to its original form through stereospecific reactions; as above, based on the melting points difference, and the *cis* or *trans* configuration of the unsaturated intermediates (as determined by infrared analysis), a *threo* configuration was assigned to the Di18Diol suberin acid [10]. However, in a more recent publication both *threo* and *erythro* Hyd18Diol and Di18Diol were identified as cork suberin

monomers, although it was not mentioned how the configuration was assigned [11]. In this latter work, cork suberin was depolymerized by methanolysis and the solubilized suberin monomers analyzed by GC-MS, with the assigned *threo* and *erythro* forms chromatographically resolved; on average, for both *vic*-diols, the *threo* and *erythro* forms were found in almost identical amounts [11].

The C_{18} 9,10-epoxy acids, Hyd18Epox and Di18Epox, were for the first time recognized in 1973 as constituents of cork suberin by Holloway and Deas [12]. The presence of epoxyacids in suberin and the position of the epoxide ring in the alkyl chains were determined by GC-MS, after the conversion of the epoxide groups by ethanolysis to the corresponding ethoxyhydrins, followed by TMS derivatization [12]. The only known study about the stereochemistry of these epoxyacids is the work of Seoane and co-workers in 1977 [13]. These authors isolated the Hyd18Epox and Di18Epox acids from cork suberin and hydrolyzed the epoxide rings to *vic*-diols; the latter showed spectroscopic and melting point values similar to the Hyd18Diol and Di18Diol suberin acids, respectively, to which these same authors had previously assigned a *threo* configuration, as discussed above; due to the stereospecific *anti*-hydroxylation reaction used in the hydrolysis, a *cis* configuration was assigned to the epoxide suberin acids [13].

In order to get unambiguous and definite results on the stereochemistry of the C_{18} 9,10-epoxy and C_{18} 9,10-diol suberin acids from cork, in the present work we assessed this question using NMR-based techniques. NMR has been successfully used for the determination of both the relative and absolute stereochemistry of organic compounds [14-16]. The general strategies include the use of chiral solvents or additives, without covalent linking to the stereoisomer(s) under analysis; the use of chiral derivatizing agents (CDA), with covalent linkage to the substrates, sometimes using the two enantiomers of the CDA; or the use of the nuclear Overhauser effect (NOE) through space interactions between nuclei, which can show the atoms relative positions, particularly in rigid systems. In many situations, for the configuration to be

unambiguously assigned, both enantiomers have to be available so that the differences of the chemical shifts in the chiral-induced environments can be compared.

In the case of the two C_{18} 9,10-epoxy and the two C_{18} 9,10-diol suberin acids under consideration here, their stereochemistry analysis by NMR faced a number of situations: each compound has two stereogenic carbons that can, in the case of the 9,10-diols, rotate around the sigma bond linking them, therefore with many possible spatial conformations; the chemical neighborhood on both sides of the chiral centers are identical methylene chains up to seven carbons away, giving symmetrical effects in many approaches; there is no previous safe knowledge if one or two of the possible relative configurations are present, and, if both, in what relative proportions, neither if each of the former include one or two of its possible enantiomers (Figure 1). To allow us an unambiguous assignment of their relative configuration, the approach followed here was to compare the more diagnostic ^{1}H and ^{13}C chemical shifts of the C_{18} 9,10-epoxy and 9,10-diol suberin acids with the ones of model compounds with known relative stereochemistry. The model compounds used include the C_{18} 9,10-epoxy and 9,10-diol substituted octadecanoic (stearic) acids, structurally identical to the suberin acids in what concerns the stereogenic carbons and their vicinity (Figure 1). Identical C_{18} *vic*-diol model compounds were used, but starting from C_{18} 9-unsaturated and 9,10-epoxy compounds with known configuration, and transforming them into *vic*-diols with determined stereochemistry through stereospecific reactions, to check the validity of the latter.

The NMR analysis was applied to the suberin acids and model compounds as such, but also carried out after converting the *vic*-diols into benzylidene acetals (BzAc), a group which is normally used to protect secondary *vic*-diols. The analysis of the suberin epoxyacids stereochemistry was also done using this same derivative, after conversion of the epoxides into *vic*-diols through a stereospecific reaction. The advantage of the use of BzAc derivatives is that they form a ring with the *vic*-diol, which has restricted conformational mobility,

thus keeping the carbons and protons of interest for the NMR stereochemistry analysis in relatively fixed positions. Finally, after determining the relative configuration of the 9,10-epoxy and 9,10-diol suberin acids, they were analyzed by polarimetry, to check its enantiomeric composition and to tentatively assign their absolute configuration.

3. Experimental

3.1. Cork C_{18} 9,10-epoxy and C_{18} 9,10-diol suberin acids

The two C_{18} 9,10-epoxy and the two C_{18} 9,10-diol suberin acids, ω-hydroxy-acids (identified by the prefix Hyd) and a,ω-diacids (Di), in the form of methyl esters, were obtained from cork after a methanolysis depolymerization reaction. These compounds were isolated and purified through a process of successive extraction and purification steps (method under patent submission) and obtained with the following purities as determined by GC-MS analysis: 9-epoxyoctadecanedioic acid, dimethyl ester (Di18Epox_Me), 95%; 9-epoxy-18-hydroxyoctadecanoic acid, methyl ester (Hyd18Epox_Me), 97%; 9,10-dihydroxyoctadecanedioic acid, dimethyl ester (Di18Diol_Me), 99%; and 9,10,18-trihydroxyoctadecanoic acid, methyl ester (Hyd18Diol_Me), 99%. The four C_{18} suberin acids were characterized by mass spectrometry (EIMS), FTIR and 1D NMR (^{1}H, ^{13}C) and 2D NMR (COSY, HSQC, HMBC) spectroscopy.

3.2. Model compounds

C_{18} 9,10-epoxy and C_{18} 9,10-diol monoacids of known relative stereochemistry, were used as model compounds, and purchased as pure standards: *cis*-9,10-epoxyoctadecanoic acid, 99%, from Sigma-Aldrich (Lisboa, Portugal); rac-*trans*-9,10-epoxyoctadecanoic acid, 98%, and rac-*threo*-9,10-dihydroxy-octadecanoic acid, 98%, from Santa Cruz Biotechnology (Heidelberg, Germany); *erythro*-9,10-dihydroxyoctadecanoic, 97%, from Larodan Fine Chemicals (Malmoe, Sweden). The C_{18} 9-unsaturated monoacids, *cis*-oleic

acid methyl ester and *trans*-elaidic acid methyl ester, 99%, were purchased from Sigma-Aldrich. Two other compounds with a *vic*-diol group substituted in an alkyl chain of known relative stereochemistry, were used, namely: *erythro*-5,6-dodecanediol, 98%, and *threo*-5,6-dodecanediol, 96%, purchased from TCI Europe (Zwijndrecht, Belgium). All solvents were of HPLC grade and obtained from Merck (Lisboa, Portugal).

3.3. GC-MS analysis

3.3.1. Separation of *cis*/*trans* isomeric pairs

Cis- and *trans*-9,10-epoxyoctadecanoic acid mixtures were prepared for GC-MS analysis from equimolar solutions of each of the two acids as follows: 1.0 mg (0.3 mmol) of *cis*-9,10-epoxyoctadecanoic acid was diluted in 130 µL of pyridine and 130 µL of *N,O*-Bis(trimethylsilyl)trifluoroacetamide (BSTFA); an identical solution was prepared for *trans*-9,10-epoxyoctadecanoic acid; aliquots of 100 µL of each solution were mixed on a vial to which 800 µL of pyridine was added.

3.3.2. Separation of *erythro*/*threo* isomeric pairs

Solutions for GC-MS analysis of equimolar mixtures of *threo*- and *erythro*-9,10-dihydroxyoctadecanoic acid, and *threo*- and *erythro*-5,6-dodecanediol were prepared as previously described.

3.3.3. Analysis of suberin acids

Solutions of each of the suberin acids, 9-epoxyoctadecanedioic acid, dimethyl ester (Di18Epox_Me), 9-epoxy-18-hydroxyoctadecanoic acid, methyl ester (Hyd18Epox_Me), 9,10-dihydroxyoctadecanedioic acid, dimethyl ester (Di18Diol_Me), and 9,10,18-trihydroxyoctadecanoic acid, methyl ester (Hyd18Diol_Me) were prepared for GC-MS analysis by dissolving and derivatizing 1.0 mg of each suberin acid in 130 µL of pyridine and 130 µL of BSTFA.

3.3.4. GC-MS conditions

All the above solutions were injected in a 7890A gas chromatographer coupled to a 5975C mass spectrometer detector (Agilent Technologies, USA), in the following chromatographic conditions: column DB5-MS (60 m, internal diameter 0.25 mm, film thickness 0.25 μm); oven program: initial temperature 200 °C, followed by a temperature increase to 250 °C at 8 °C/min, and then to 300 °C at 3 °C/min; the final temperature was kept for 15 min; injections were made in splitless mode, with an injector temperature of 300 °C. Mass spectrometer conditions: electron ionization 70 eV; source temperature 230 °C and quadrupole temperature 150 °C; transfer line temperature was kept at 310 °C.

3.4. Hydroxylation of the C_{18} 9-unsaturated monoacids into C_{18} 9,10-diols

Model *vic*-diols of determined stereochemistry were obtained through a stereospecific *syn*-hydroxylation of the C_{18} 9-unsaturated monoacid model compounds, *cis*-oleic acid methyl ester (converted to the *erythro*-9,10-diol) and *trans*-elaidic acid methyl ester (converted to the *threo*-9,10-diol), by a permanganate oxidation following a procedure adapted from Bhushan et al., 1984 [17].

3.4.1. Cetyltrimethylammonium permanganate (CTAP) preparation

5.0 g (31.7 mmol) of potassium permanganate was dissolved in 160 ml of water. In another flask, 12.6 g (34.7 mmol) of cetyltrimethylammonium bromide (CTAB) was dissolved in 155 ml of water during 1 h with stirring. This CTAB solution was added slowly and dropwise to the potassium permanganate solution for 1 h, with strong stirring. The mixture was allowed to further react for 30 min and the resulting violet precipitate recovered by filtration on a G3-porosity glass filter and washed with water. This residue (CTAP) was dried on a vacuum oven over phosphorus pentoxide. 10.2 g of dry CTAP was grounded to a fine powder and kept in a refrigerator.

3.4.2. Hydroxylation reaction

1.0 g (3.4 mmol) of *cis*-oleic acid methyl ester was dissolved in 10 ml of dichloromethane, to which a solution of 6.8 g (16.9 mmol) of CTAP dissolved in 102 ml of dichloromethane was added dropwise and the mixture allowed to react for 100 h at room temperature. The reaction mixture was filtered on a G3-porosity glass filter, 50 ml of dichloromethane added to the filtered solution, and the organic solution washed with 3x150 ml of water. After the dichloromethane removal in a rotary evaporator, *erythro*-9,10-dihydroxyoctadecanoic acid methyl ester was recovered in a reaction yield of 37%. The same procedure was followed to hydrolyze *trans*-elaidic acid methyl ester: 0.9 g (3.0 mmol) was dissolved in 9 ml of dichloromethane and 6.1 g (15.2 mmol) of CTAP dissolved in 92 ml of dichloromethane was added. The recovered organic phase included *threo*-9,10-dihydroxyoctadecanoic acid methyl ester in a reaction yield of 90%.

3.4.3. Purification of the C_{18} 9,10-diols obtained from the hydroxylation of the C_{18} 9-unsaturated monoacids

Each of the 9,10-diols obtained was purified by medium pressure liquid chromatography (MPLC) as follows: the solid material recovered from the organic phases was dissolved in chloroform/ethyl acetate 7:3 and applied to a VersaFlash™ silica column, 40x75 mm, and eluted with the same solvent at a flow rate of 50 ml/min. From the mixture enriched in *erythro*-9,10-dihydroxyoctadecanoic acid methyl ester, a fraction with 82.0 mg of the latter was recovered in a purity of 99%. From the mixture enriched in *threo*-9,10-dihydroxyoctadecanoic acid methyl ester, 131.5 mg of the latter was recovered in a purity of 99%.

3.5. Hydrolysis of the C_{18} 9,10-epoxyacids into C_{18} 9,10-diol acids

A stereospecific *anti*-hydroxylation converting the epoxides into *vic*-diols, namely the *cis*-9,10-epoxides into *threo*-9,10-diols and the *trans*-9,10-epoxides

into *erythro*-9,10-diols, was applied to the C_{18} 9,10-epoxy model compounds (*cis*- and *trans*-9,10-epoxyoctadecanoic acids), and to the C_{18} 9,10-epoxy suberin acids (Hyd18Epox_Me and Di18Epox_Me). The *anti*-hydroxylation reaction was carried out by an acid-catalyzed hydrolysis, described as follows: 50.1 mg (0.2 mmol) of *cis*-9,10-epoxyoctadecanoic acid was dissolved in 5 ml of tetrahydrofuran and 5 ml of water, and 500 µL of sulfuric acid was added dropwise. The mixture reacted at room temperature for 72 h with stirring, and after the reaction completion, 20 ml of water and 20 ml of dichloromethane were added and the organic phase recovered. After solvent removal, 42 mg of *threo*-9,10-dihydroxyoctadecanoic acid in a purity of 72% was recovered from the organic phase, and further purified in 0.5 mm TLC silica plates with hexane/isopropyl alcohol/formic acid 70:30:1. The band with R_f = 0.8 was collected, extracted with methanol/dichloromethane 1:1, giving 12.0 mg of *threo*-9,10-dihydroxyoctadecanoic acid methyl ester with a purity of 90%. The same procedure was applied to: 10.0 mg (0.03 mmol) of *trans*-9,10-epoxyoctadecanoic acid with a final recovery of 10.0 mg of *erythro*-9,10-dihydroxyoctadecanoic acid (88% pure); 17.8 mg (0.05 mmol) of Hyd18Epox_Me, resulting in 16.0 mg of recovered organic phase with Hyd18Diol in 98% purity, which was methylated afterwards as described below; 62.8 mg (0.2 mmol) of Di18Epox_Me resulting in 44.7 mg of Di18Diol in 97% purity, also further methylated.

3.6. Methylation of the free acids

Some of the purchased model compounds, as well as their synthesized derivatives, in the form of free acids, were methylated (to avoid signal overlapping in the NMR spectra) in methanol with 1% sulfuric acid, for 3 h, in reflux at 80 ºC.

3.7. Derivatization of *vic*-diol groups into benzylidene acetals (BzAc)

All *vic*-diol compounds were converted to the corresponding BzAc derivatives, including: the C_{18} 9,10-diol suberin acids (Di18Diol_Me and Hyd18Diol_Me); the equivalent C_{18} 9,10-diols obtained from the *anti*-hydroxylation of the C_{18} 9,10-epoxy suberin acids (Di18Epox_Me and Hyd18Epox_Me); the purchased *erythro*- and *threo*- C_{18} 9,10-dihydroxyoctadecanoic acids; the two latter obtained from (i) the *syn*-hydroxylation of the model compounds *cis*-oleic acid methyl ester and *trans*-elaidic acid methyl ester and (ii) from the *anti*-hydroxylation of the model compounds *trans*- and *cis*- C_{18} 9,10-epoxy-octadecanoic acids; the model compounds C_{12} *erythro*-5,6-dodecanediol and C_{12} *threo*-5,6-dodecanediol.

3.7.1. BzAc derivatization reaction

To prepare the BzAc derivatives, a procedure adapted from McElhanon et al., 1997 [18] was used. To a known quantity of each *vic*-diol compound, benzaldehyde dimethyl acetal (a,a-dimethoxytoluene) and *p*-toluenesulfonic acid monohydrate were added in molar proportions of 100x and 0.1x, respectively. Dimethylformamide was added up to a total volume of 3 ml/0.1 mmols of the *vic*-diol compound. A few beads of molecular sieve were added and the solution mixture was allowed to react in an oil bath at 100 ºC for 24 h, in reflux with stirring. The reaction mixture was then partitioned in 20 ml water/20 ml dichloromethane, the organic phase recovered, and analyzed by GC-MS to control the reaction yield.

3.7.2. Purification steps

The *vic*-diol BzAc derivatives were isolated and purified from the corresponding organic phases by MPLC (in the same system described above) and, when necessary, also by TLC to a minimum of 98% purity. Di18Diol_Me BzAcs (one from the suberin acid Di18Diol_Me and the other from the hydrolysis of the suberin acid Di18Epox_Me) were purified in hexane/ethyl acetate 9:1;

Hyd18Diol_Me BzAcs (one from the suberin acid Hyd18Diol_Me and the other from the hydrolysis of the suberin acid Hyd18Epox_Me) were purified in chloroform/ethyl acetate 9:1; *threo*-9,10-dihydroxyoctadecanoic acid_Me BzAcs (one from the model compound *threo*-9,10-dihydroxyoctadecanoic acid_Me, a second from the hydroxylation of *cis*-oleic acid methyl ester, and a third from the hydrolysis of the *cis*-9,10-epoxyoctadecanoic acid) were purified in chloroform/ethyl acetate 7:3; *erythro*-9,10-dihydroxyoctadecanoic acid_Me BzAcs (one from the model compound *erythro*-9,10-dihydroxyoctadecanoic acid_Me, a second from the hydroxylation of *trans*-elaidic acid methyl ester, and a third from the hydrolysis of the model compound *trans*-9,10-epoxyoctadecanoic acid) were purified in chloroform/ethyl acetate 7:3 (the latter two BzAc derivatives were lost in the purification steps and were not used for the NMR analysis); *threo*-5,6-dodecanediol BzAc and *erythro*-5,6-dodecanediol BzAc were purified in hexane/ethyl acetate 9:1.

3.8. DSC analysis

For melting point determination, the suberin acids Hyd18Epox_Me, Di18Epox_Me, and Di18Diol_Me were analyzed by Differential Scanning Calorimetry (DSC). The thermograms were acquired on a Maia DSC 200 F3 (Netzsch, Germany) in a temperature range from -50 ºC to +90 ºC, with a heating rate of 20 ºC/min. The suberin acid samples, previously dried in a vacuum oven, were weighed in aluminium pans (5.0 mg of Hyd18Epox_Me, 5.8 mg of Di18Epox_Me, and 9.6 mg of Di18Diol_Me), and cooled to -50 ºC with liquid nitrogen. DSC was calibrated with an expanded uncertainty of measurement error <0.5 ºC.

3.9. FTIR analysis

FTIR spectra were acquired from the four suberin acids and from the 9,10-epoxy and the *vic*-diol model compounds, either in Attenuated Total Reflection (ATR) mode or transmission mode, depending on its physical state

at room temperature, in an Alpha-P spectrometer (Bruker Optik, Germany). ATR spectra were obtained from liquid and semi-solid samples in a diamond cell with a pressure clamp; transmission spectra were obtained from solid samples in potassium bromide pellets after grounding to a fine powder (1.5 mg of sample with 200 mg of potassium bromide). 32 scans were acquired per spectrum with a resolution of 4 cm^{-1} in a wavenumber range from 4000 cm^{-1} to 400 cm^{-1}.

3.10. Raman analysis

Raman spectra were obtained from the cork suberin 9,10-epoxyacids, Di18Epox_Me and Hyd18Epox_Me and from the 9,10-diol cork suberin acid, Di18Diol_Me in a system comprising a double monochromator Spex 1403 (Horiba, Japan), with an argon ion laser line at 514.5 nm, model 2016 (Spectra-Physics, USA) and a R928 photomultiplier detector (Hamamatsu Photonics, Japan). The spectra were acquired at room temperature in a 90 ° geometry, with a spectral resolution of 4 cm^{-1}.

3.11. NMR analysis

NMR spectra, including the 1D ^{1}H and ^{13}C, together with 2D correlation experiences (COSY, HSQC, HMBC) were obtained from the suberin acids, model compounds, synthesized *vic*-diols, and all BzAc derivatives. The NMR spectra were acquired on an Avance II+ 600 spectrometer (Bruker Biospin, Germany), with frequency resonances of 600.13 MHz for protons and 150.96 MHz for carbons, equipped with a cryoprobe and pulse gradient units, able to produce magnetic field pulsed gradients in the z-direction of 56.0 G/cm. All samples were solubilized in deuterated chloroform with 0.03% of TMS, with an approximate concentration of 5 mg/500 µL, and the spectra acquired at a temperature of 300 K. The TMS signal (0.00 ppm) was used to calibrate the chemical shifts in ^{1}H spectra, and chloroform (77.00 ppm) was used as refe-

rence in ^{13}C spectra. The NMR spectra were processed in MestReNova, version 8.0.1 (Mestrelab Research, Spain).

3.12. Polarimetry analysis

The specific rotation of the suberin acids, Hyd18Epox_Me, Di18Epox_Me, Hyd18Diol_Me, and Di18Diol_Me was measured in a Perkin-Elmer 241 MC Polarimeter, equipped with a sodium lamp (589 nm) and a 1 ml quartz cell with 1 dm of length. Sample concentration was between 5 and 10 mg/ml in dichloromethane and the measurements acquired at room temperature (ca 25 °C).

4. Results and discussion

4.1. Spectroscopic analysis and stereochemistry of the C_{18} 9,10-epoxy suberin acids

4.1.1. GC-MS and DSC analysis

The two C_{18} 9,10-epoxyacids were obtained from cork as methyl esters, after suberin depolymerization, with purities as determined by GC-MS of 95% for Di18Epox_Me and 96% for Hyd18Epox_Me. Their melting points and fusion enthalpies were determined by DSC, respectively 40.7 °C and 57.4 kJ/mol for Hyd18Epox_Me and 21.7 °C and 46.2 kJ/mol for Di18Epox_Me. Literature values for the melting point of Hyd18Epox_Me is 38 °C and Di18Epox_Me is reported as an oil at room temperature [13]. A first approach to check if these epoxyacids were present in cork suberin both as *cis* and *trans* isomers, or only in one of the two possible relative configurations, was made by GC-MS analysis, comparing with model compounds. The latter, the C_{18} *cis*-9,10-epoxyoctadecanoic acid and the C_{18} *trans*-9,10-epoxyocta-decanoic acid, both as methyl esters, were mixed and base line separated in the chromatographic conditions described in "Experimental". Each of the two suberin C_{18} 9,10-epoxyacids was then analyzed in the same chromatographic conditions, including solution concentration and injection volume,

but only one peak was recognizable in the chromatograms. This gave evidence that the two suberin epoxyacids, Di18Epox and Hyd18Epox, exist in cork suberin probably in only one of the forms, either *cis* or *trans*.

4.1.2. FTIR and Raman analysis

The *cis* or *trans* configuration of epoxide rings can be tentatively assessed by vibrational spectroscopy, namely FTIR and Raman. The diagnostic bands used for this purpose derive from the epoxide ring vibrations: in epoxides substituted in alkyl chains, typically, for *cis*-isomers this band is observed in the range of 785-865 cm^{-1} and for *trans*-isomers at 860-950 cm^{-1} [19]. In the *cis* and *trans* model compounds analyzed these bands were conspicuous: in the C_{18} *cis*-epoxyacid it was found at 847 cm^{-1} and in the C_{18} *trans*-epoxyacid, at 877 cm^{-1} (see Supplementary material, Figure SM1). In what respects the two suberin epoxyacids, a relatively strong band at 844 cm^{-1} was observed in the Hyd18Epox_Me, and a medium to weak band at 837 cm^{-1} was present in the Di18Epox_Me (Figure SM2). The former can probably be assignable to a *cis*-epoxide ring vibration, but the latter, due to its weak intensity, is not so clear. However, in both suberin acids (and also in the two model compounds) there are a number of weak intensity bands in the window assignable to the ring vibrations of *cis* and *trans* epoxides, and therefore no unambiguous conclusion can be drawn about their configuration based only in the FTIR analysis. The Raman spectra were also inconclusive: both Hyd18Epox_Me and Di18Epox_Me showed absorption bands in the window that includes the *cis* and *trans* epoxide ring vibrations; however, some of these bands are probably assignable to skeletal vibrations of the alkyl chains, which are stronger in Raman compared to FTIR.

4.1.3. NMR analysis

The second approach for the stereochemistry assignment of the suberin epoxyacids was using NMR spectroscopy. The two suberin acids,

Di18Epox_Me and Hyd18Epox_Me, and the two model compounds of known relative configuration, C_{18} *cis*-epoxyacid and C_{18} *trans*-epoxyacid were analyzed by NMR including ^{1}H, ^{13}C, and 2D correlation techniques, namely COSY, HSQC and HMBC. The chemical shifts of the relevant protons and carbons for the discussion of the *cis*/*trans* configuration, namely of the epoxide methines (C-9 and C-10) and of the adjacent methylenes (C-8 and C-11) are presented in Table 1. The first information obtainable from NMR spectra relevant for the configuration assignment would be the coupling constants between the epoxide methine protons. However, in the proton spectra of Hyd18Epox_Me, Di18Epox_Me and also of C_{18} *cis*-9,10-epoxyoctadecanoic acid model compound, the methine protons of the epoxide group, showed up as broad unresolved multiplets. In the case of the C_{18} *trans*-9,10-epoxyoctadecanoic acid model compound, these protons appeared as a triplet-like multiplet. However, due to the lack of symmetry in the multiplet, and the presence of peak shoulders, it was clearly not a first order spin system. Some essays were done to simulate these epoxide proton multiplets and eventually measure the coupling constants, which were relatively successful for the *trans* model compound (data not shown), but the lack of defined peaks in the *cis* model compound and cork suberin epoxyacids did not allow a reliable simulation.

More relevant information could be obtained from the chemical shifts of the epoxide methine groups. A significant difference was found in the chemical shifts of the methine epoxide protons, between the *cis* and *trans* isomers in the analyzed model compounds, $\Delta H^{\delta cis-\delta trans}$ = +0.25 ppm (Table 1). This comparative shielding of the *trans* epoxide methine protons was also observed in a number of other *cis*/*trans* isomers of C_{18} epoxy fatty acids, with the epoxide group in different chain positions [20,21]. This systematic upfield effect might be imputable to the fact that the methine protons in *trans* isomers are spatially closer to the methylene protons located on the other side of the epoxide ring, in comparison to the *cis* isomers, where such proximity doesn't exist (Figure 2). This spatial proximity of the opposite methylene protons is probably responsi-

ble for the shielding of the epoxide protons in *trans* isomers. In this way, having in mind the structural similarity of the model compounds with the suberin epoxyacids, the chemical shifts of their methine epoxide protons can be seen as indicative of a *cis* configuration: 2.89 ppm both for Di18Epox_Me and for Hyd18Epox_Me, very close to 2.91 ppm of the C_{18} *cis*-9,10-epoxyoctadecanoic acid model compound (Table 1).

Table 1. Chemical shifts (ppm) of ^{1}H and ^{13}C methines and adjacent methylenes in C_{18} 9,10-epoxyacids, from cork suberin and model compounds

	Epoxide methines (C-9 & C-10)		Adjacent methylenes (C-8 & C-11)	
C_{18} 9,10-epoxy suberin acids	^{1}H	^{13}C	^{1}H	^{13}C
cis-Di18Epox_Me	2.89	57.07	1.49	27.74
cis-Hyd18Epox_Me	2.89	57.16 & 57.19	1.50	27.78 & 27.79
C_{18} 9,10-epoxy model compounds				
cis-9,10-epoxyoctadecanoic acid	2.91	57.23 & 57.28	1.50	27.77 & 27.81
trans-9,10-epoxyoctadecanoic acid	2.66	58.90 & 58.95	1.51	32.07 & 32.11
$\delta^{cis\text{-epox}} - \delta^{trans\text{-epox}}$	+0.25	–1.67 & –1.67	–0.01	–4.30 & –4.30

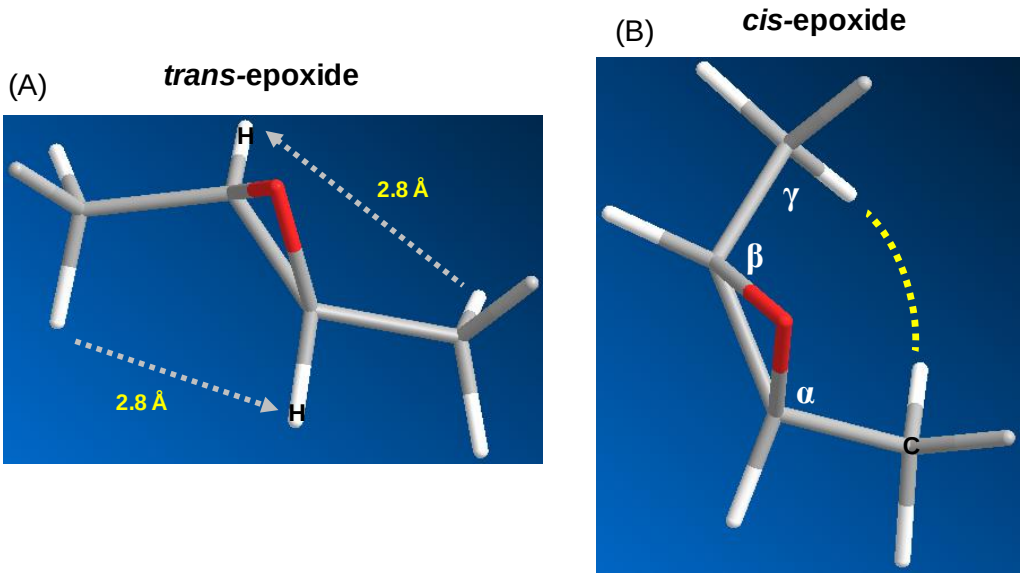

Figure 2. NMR chemical shift effects in *cis*- and *trans*-epoxides: (A), in *trans*-epoxyacids, shielding of the epoxide methine protons (marked) by the opposite methylenes and (B), in *cis*-epoxyacids, shielding of the adjacent methylene carbons (one marked) due to the γ-effect of the "substituent" group three carbons away (the opposite adjacent methylene)

In the ^{13}C NMR spectra it was also observed a significant difference between the chemical shifts in the *cis* and *trans* model compounds, particularly in the carbons of the methylenes adjacent to the epoxide ring (C-8 and C-11). In fact, the *cis* methylene carbons were comparatively more shielded, with a $\Delta C^{\delta cis-\delta trans} = -4.30$ ppm (Table 1). Differences of this order of magnitude were also found in the equivalent methylene carbons in several other C_{18} epoxyacids, between *cis* and *trans* isomers [22]. This higher shielding observed in the C-8 and C-11 carbons in *cis* isomers might be attributed to the so-called "gamma-effect", an empirical observation in which the chemical shift of a carbon is affected by a spatially close substituent located three bonds away [23]. In *cis*-epoxides "the substituent group" is the methylene group on the opposite side of the epoxide ring, gamma-positioned to the carbon under consideration; this spatial proximity, and the van der Waals interactions believed to be behind the "gamma-effect", only exist in *cis*-isomers (Figure 2). Theoretical calculations taking into account bond length compression or stretching, or angular distortions, imparted by the steric effects of the substituent groups in the chemical shift, were able to predict to some extent the comparative shielding of gamma-carbons in similar alkyl-substituted *cis*-epoxides, when compared to *trans*-epoxides [24].

The chemical shifts of the epoxide methine carbons (C-9 and C-10) and of the epoxide vicinal carbons (C-8 and C-11) both in Hyd18Epox_Me and Di18Epox_Me were very similar to the *cis* model compound (Table 1), thus reinforcing the hypothesis that the suberin epoxyacids have a *cis* configuration.

4.2. Spectroscopic analysis and stereochemistry of the C_{18} 9,10-diol suberin acids

4.2.1. GC-MS and DSC analysis

The C_{18} 9,10-diol cork suberin acids were extracted from cork suberin and purified up to 95%, in the case of Di18Diol_Me, and 97% in the case of

Hyd18Diol_Me, as controlled by GC-MS. The melting point of Di18Diol_Me, measured by DSC, was 75.0 °C, with a fusion enthalpy of 42.5 kJ/mol. As presented in the "Introduction", each of the two 9,10-diol suberin acids can have two relative configurations (Figure 1), namely *erythro* and *threo*. The possibility of separating these two diastereomers by GC was tested with model compounds, structurally very close to the C_{18} 9,10-diol suberin acids, and with known stereochemistry, namely the C_{18} *threo*-9,10-dihydroxyoctadecanoic acid and C_{18} *erythro*-9,10-dihydroxyoctadecanoic acid, both standards as racemic mixtures. A 1:1 mixture of these two latter model compounds was successfully separated by GC with base line resolution, with a difference in the retention times of 12 sec (data not shown). Each of the C_{18} 9,10-diol suberin acids, analyzed exactly in the same GC conditions, afforded a single peak, suggesting that only one of the two possible relative configurations, either *threo* or *erythro*, is present in cork suberin.

4.2.2. NMR analysis

The C_{18} 9,10-diol suberin acids were analyzed by NMR, together with two pairs of *threo/erythro* model compounds, namely the C_{18} *threo*- and *erythro*-9,10-dihydroxyoctadecanoic acids and the C_{12} *threo*- and *erythro*-5,6-dodecanediols. The chemical shifts of the diagnostic protons and carbons, namely the C-9 and C-10 (C-5 and C-6 in the case of C_{12} diols) methines where the hydroxyl groups are linked, which are relevant for the configuration discussion, are presented in Table 2. The differences in these chemical shifts between the *threo* and *erythro* model compounds are presented in Table 3.

A systematic difference was observed between the chemical shifts of the *erythro* and *threo* methine protons in the *vic*-diol model compounds, with a $\Delta H^{\delta erythro-\delta threo}$ of +0.19 ppm (Table 3). To understand this difference we have to consider the possible conformations of the *vic*-diol group, due to the rotation around the sigma bond between the two hydroxyl-substituted carbons, and therefore the different magnetic environments of the methine

protons (Figure 3). An immediate approach would be to consider the coupling constants between the two methine protons, taking advantage of the Karplus equation. However their signals appear as complex multiplets in the ^{1}H NMR spectra (Figure 3), and therefore the coupling constants can't be directly extracted.

Table 2. Chemical shifts (ppm) of ^{1}H and ^{13}C methines in *vic*-diols of cork suberin acids (C-9 & C-10) and model compounds (C-9 & C-10 or C-5 & C-6), with the *vic*-diol as a free group, and as benzylidene acetal (BzAc) derivative

	free *vic*-diol group		benzylidene acetal (BzAc) derivative [F]			
C_{18} 9,10-diol suberin acids	^{1}H	^{13}C	^{1}H	^{13}C	H_{BzAc}	C_{BzAc}
threo-Di18Diol_Me	3.40	74.46	3.75	81.52 & 82.80	5.86	102.59
threo-Hyd18Diol_Me	3.41	74.46 & 74.48	3.75	81.52 & 81.54 82.80 & 82.83	5.86	102.60
threo-Di18Diol_Me [A]	3.40	74.48	3.75	81.52 & 82.80	5.86	102.59
threo-Hyd18Diol_Me [B]	3.40	74.47 & 74.49	3.75	81.52 & 81.53 82.80 & 82.82	5.86	102.59
C_{18} 9,10-diol model compounds						
threo-9,10-dihydroxyoctadecanoic acid	3.38	74.35 & 74.40	3.74	81.55 & 81.57 82.82 & 82.85	5.86	102.56
erythro-9,10-dihydroxyoctadecanoic acid methyl ester	3.60	74.71 & 74.76	4.11	78.74 & 78.77 79.20 & 79.28	5.77	103.05
threo-9,10-dihydroxyoctadecanoic acid methyl ester [C]	3.41	74.48 & 74.54	3.75	81.53 & 81.56 82.80 & 82.86	5.86	102.58
erythro-9,10-dihydroxyoctadecanoic acid methyl ester [D]	3.60	74.63 & 74.70	-	-	-	-
threo-9,10-dihydroxyoctadecanoic acid [E]	-	-	3.75	81.53 & 81.56 82.80 & 82.85	5.86	102.58
C_{12} 5,6-diol model compounds						
threo-5,6-dodecanediol	3.41	74.51 & 74.53	3.76	81.55 & 81.57 82.84 & 82.85	5.87	102.57
eryhtro-5,6-dodecanediol	3.60	74.68 & 74.70	4.12	79.28	5.77	103.08

Notes:

[A] obtained from the hydrolysis of the cork suberin acid C_{18} *cis*-Di18Epox_Me; [B] obtained from the hydrolysis of the cork suberin acid C_{18} *cis*-Hyd18Epox_Me; [C] obtained from the *syn*-hydroxylation of the model compound C_{18} *trans*-elaidic acid methyl ester; [D] obtained from the *syn*-hydroxylation of the model compound C_{18} *cis*-oleic acid methyl ester; [E] obtained from the hydrolysis of the model compound C_{18} *cis*-9,10-epoxyoctadecanoic acid; [F] H_{BzAc} and C_{BzAc} are the ^{1}H and ^{13}C chemical shifts of the acetal methine in the benzylidene group.

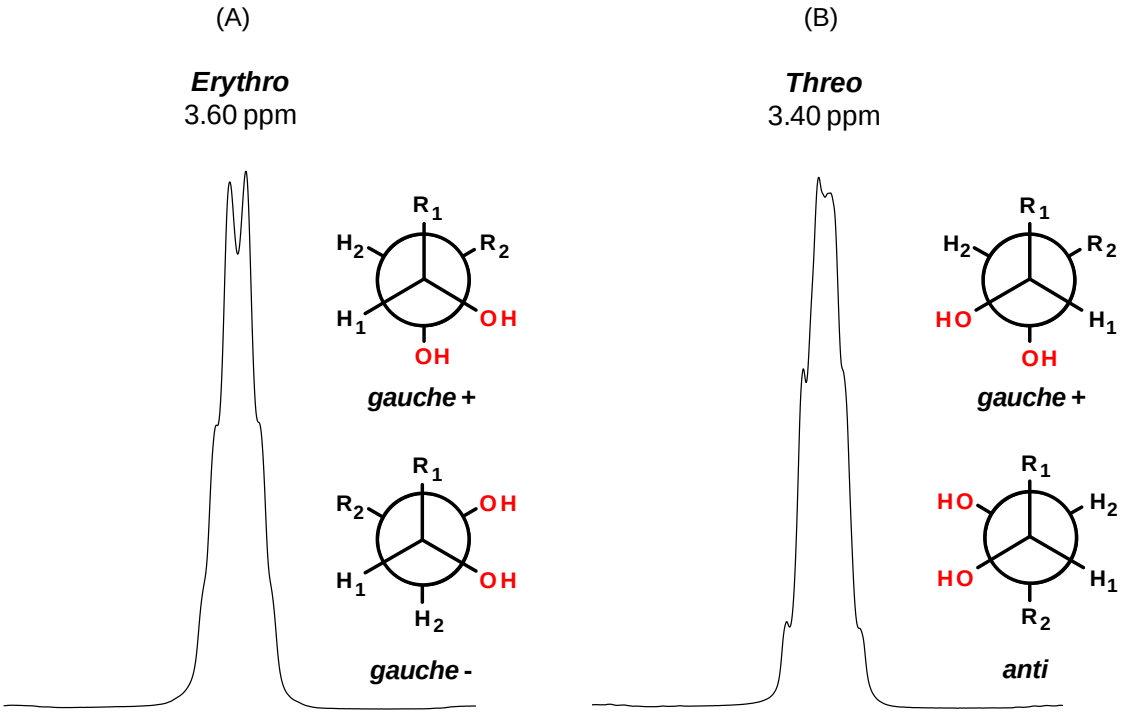

Figure 3. ^{1}H NMR multiplets of the *vic*-diol methine protons (H_1 and H_2) of *erythro* (A) and *threo* (B) model compounds (5,6-dodecanodiol) with the Newman projection conformations that allow hydrogen bonding between the hydroxyl groups (only *R,S-erythro* and *R,R-threo* shown)

Table 3. Chemical shifts differences (Δppm) in ^{1}H and ^{13}C of *vic*-diol methines (from suberin acids and model compounds) with the *vic*-diol group in the free form and as benzylidene acetal (BzAc) derivative

^{1}H	$\Delta\delta^{Ef\text{-}Tf}$	$\Delta\delta^{EBzAc\text{-}TBzAc}$	$\Delta\delta^{TBzAc\text{-}Tf}$	$\Delta\delta^{EBzAc\text{-}Ef}$
Hyd18Diol_Me (cork suberin)			+0.34	
Di18Diol_Me (cork suberin)			+0.35	
5,6-dodecanediol	+0.19	+0.36	+0.35	+0.52
9,10-dihydroxyoctadecanoic acid_Me	+0.19	+0.36	+0.34	+0.51
^{13}C				
Hyd18Diol_Me (cork suberin)			+7.07 & +8.34	
Di18Diol_Me (cork suberin)			+7.06 & +8.34	
5,6-dodecanediol	+0.17 & +0.17	–3.57 & –2.28	+7.05 & +8.32	+4.58 & +4.60
9,10-dihydroxyoctadecanoic acid_Me	+0.22 & +0.23	–3.59 & –2.79	+7.07 & +8.29	+4.48 & +4.05

Legend:
Ef: *Erythro* with free *vic*-diol group; **T**f: *Threo* with free *vic*-diol group; **E**BzAc: *Erythro* with *vic*-diol group in the form of benzylidene acetal derivative; **T**BzAc: *Threo* with *vic*-diol group in the form of benzylidene acetal derivative.

A study carried out in 2,3-butanediol, a much simpler *vic*-diol but with identical stereochemistry, analyzed the dominant conformers by ^{1}H NMR [26]. In low polarity solvents such as deuterated chloroform both the *erythro* (*meso*-2,3-butanediol) and *threo* (±-2,3-butanediol) isomers preferred the conformations that favored hydrogen bonding between the hydroxyl groups. These same conformational preferences can also be valid for the *vic*-diols in the present study, although they have much longer methylene chains attached to the hydroxyl-substituted chiral carbons. Such possible conformations that approximate the vicinal hydroxyls (but avoid the eclipsed forms that would be sterically unfavorable) are shown in Figure 3, *gauche*+ and *gauche*- in the *erythro* forms, and *gauche*+ and *anti*, in the *threo* forms. If these are the preferred conformations in the alkyl-substituted *vic*-diols as we are dealing here, they can explain the observed chemical shifts differences between *erythro* and *threo* isomers (Figure 3). The methine protons have different neighborhoods in the two cases: in the *erythro* forms, only one of the methine protons is spatially close to the opposite methylene group (H_1 to R_2 or H_2 to R_1, Figure 3A); in the *threo* forms, both methine protons are close to their opposite methylene groups (H_1 to R_2 and H_2 to R_1, Figure 3B). The spatially close opposite methylenes shield the methine protons, an effect thus stronger in the *threo* isomers, explaining the difference of +0.19 ppm observed in the *erythro* methine protons of model *vic*-diol compounds (Table 3).

These same conformations just discussed would also explain the comparative shielding observed in the carbons of the adjacent methylenes in *erythro* isomers, ca -2 ppm as measured in the model compounds, by the same mechanism of the "gamma-effect" described for *cis*-epoxide isomers. Spatial proximity between R groups would be more probable in *erythro* isomers, found in both favored conformations, than in *threo* isomers present in only one of the conformations (Figure 3).

Comparing the chemical shifts of the *vic*-diol methine protons of Hyd18Diol_Me and Di18Diol_Me suberin acids with the ones of the model compounds, they are very close to the *threo* isomers (Table 2). Although this

could be eventually used as proof of the relative configuration of the C_{18} 9,10-diol suberin acids, further evidence was searched through the derivatization of the *vic*-diol groups into cyclic structures. In this way, the eventual doubts about the different atoms positions in the many possible conformations could be avoided.

4.3. NMR analysis of the *vic*-diol benzylidene acetal (BzAc) derivatives

All *vic*-diols, including the suberin acids, Hyd18Diol and Di18Diol, and the two pairs of model compounds *erythro* and *threo* C_{18} 9,10-diol monoacids and *erythro* and *threo* C_{12} 5,6-dodecanediols were derivatized as benzylidene acetals (BzAc), producing a "1,3-dioxolane" five-membered ring (Figure 4). Also, the suberin C_{18} 9,10-epoxyacids, Hyd18Epox and Di18Epox, as well as the C_{18} *cis*-9,10-epoxyacid model compound were hydrolyzed into C_{18} 9,10-diols and BzAc derivatized in the same way. The stereospecificity of the epoxide hydrolysis was used to confirm the *cis* or *trans* relative configuration of the suberin epoxyacids, as discussed below. Moreover, as a control, *erythro* and *threo* C_{18} 9,10-diol monoacids, identical to the above model compounds, were obtained by the *syn*-hydroxylation of *cis*-oleic acid methyl ester and *trans*-elaidic acid methyl ester, respectively, and their BzAc derivatives also prepared. The NMR results of these BzAc derivatives in what respects the proton and carbon chemical shifts of the C-9 and C-10 (or C-5 and C-6) methines of the derivatized diols, as well as the BzAc acetal methine (see Figure 4), are presented in Table 2.

4.3.1. Proton spectra

Differences between the chemical shifts of the methine protons of *erythro* and *threo* BzAc *vic*-diol derivatives were conspicuous in model compounds, as shown in Table 3. As a rule, these methine protons in the *erythro*-BzAc derivatives had a chemical shift of ca 4.12 ppm and in the *threo*-BzAc derivatives of ca 3.75 ppm (Table 2). The difference between the signals of

these methine protons was $\Delta H^{\delta erythroBzAc-\delta threoBzAc} \approx +0.36$ ppm (Table 3). Because this difference is significant and the chemical shift values are constant, this seems to be, by itself, a strong diagnostic feature to assign an *erythro* or *threo* configuration in these *vic*-diol structures.

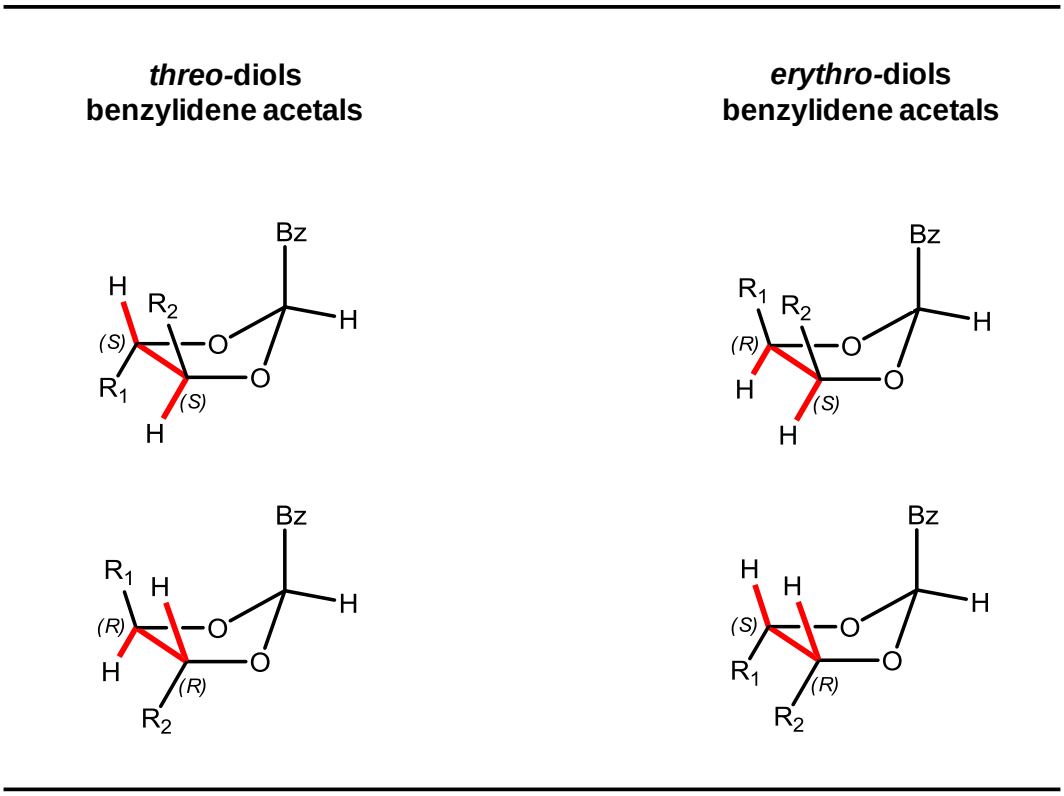

Figure 4. Benzylidene acetal derivatives of *vic*-diols shown in the envelope conformation. R_1 and R_2 as described in Figure 1 (plus a CH_2 for each $(CH_2)_n$ group). [The quirality of the acetal carbon is not represented, depending on the R_1 and R_2 sustituents]

The higher shielding in the *threo* isomers can, as in the case of the epoxide methine protons, again be explained by the "substituent" effect of the opposite methylene group, which is spatially closer to the methine proton under consideration (Figure 4). Due to the restricted conformational mobility of the dioxolane ring, this effect would be here stronger than the one observed in the underivatized *vic*-diols, being in fact almost the double (+0.19 ppm in the underivatized *vic*-diols and +0.36 ppm in the BzAc derivatives, see Table 3). The effect of the phenyl group of the BzAc derivative in the methine

chemical shifts of the derivatized vic-diols is harder to evaluate. Besides some conformational variability of the dioxolane ring, and the free rotation of the phenyl group around the acetal carbon, the BzAc derivates can have actually two different configurations. When the BzAc derivative is formed from the *vic*-diol and the precursor benzaldehyde dimethyl acetal, the acetal carbon of the latter becomes asymmetric, originating two new possible stereoisomers, the (*R*)-BzAc and the (*S*)-BzAc, thus locating the phenyl group in two possible opposite sides (Figure 4). Because in theory both reaction positions are identically probable, both enantiomers should exist in similar proportions, making the interpretation of the phenyl effect in the chemical shifts more complicated.

Another difference between the BzAc derivatives of *erythro* and *threo vic*-diols was observed in the BzAc structure itself, namely in the acetal methine proton. In fact, in the model compounds analyzed, this proton had a chemical shift of 5.77 ppm in the *erythro* isomers and 5.86 ppm in the corresponding *threo* isomers (Table 2). This systematic difference of -0.09 ppm, showing that this proton in the *erythro*-BzAc derivatives is more shielded, and the consistency of the chemical shift values in the model compounds analyzed, suggests that the chemical shift of the acetal proton in the BzAc derivatives of alkyl substituted *vic*-diols, like the ones we are dealing here, can also be a reliable way to assign the *erythro* or *threo* configuration.

4.3.2. ^{13}C carbon spectra

The chemical shifts of the ^{13}C carbons in BzAc derivatives, and their differences between the *erythro* and *threo* isomers, as observed in the model compounds, also showed to be diagnostic of the relative configuration of *vic*-diols (Tables 2 and 3). To compare the ^{13}C chemical shifts we have to consider that in the free *vic*-diol form there are different signals for the C-9 and C-10 carbons (or C-5 and C-6 in case of dodecanediols) (although it was not possible to assign to which specific carbon they corresponded to)

because neither the suberin acids nor the model compounds are completely symmetric in relation to the *vic*-diol group. The exception is the Di18Diol_Me from suberin which, due to its complete symmetry, only shows one signal for both C-9 and C-10 carbons. Comparing the ^{13}C chemical shifts of the *erythro* and *threo* forms of the underivatized model *vic*-diols, $\Delta C^{\delta erythro-\delta threo}$, a small average difference of ca +0.2 ppm was observed (Table 3). This difference is probably too small for a safe assignment of the *vic*-diol configuration. However, much bigger differences were found when this comparison was made in the respective BzAc derivatives, either +2.8 or +3.6 ppm, depending on the carbon chemical shift considered (Table 3). After the BzAc derivatization, each compound presented four signals assignable to the *vic*-diol carbons, with the exception of the Di18Diol BzAc derivative, which only showed two (Table 2). These four carbon signals were, in the ^{13}C NMR spectra, two separated pairs, and within each pair, the difference in the chemical shifts was small and similar to the one observed between the two *vic*-diol carbons in the underivatized form, ca 0.02 ppm. The difference between pairs was markedly bigger, ca 1.28 ppm. Together this made us believe that each pair of carbons corresponded to the (*R*)- or (*S*)-BzAc derivative. For instance, in the Hyd18Diol_Me BzAc, the first pair was 81.52 and 81.54 ppm and the second pair 82.80 and 82.83 ppm (Table 2); within each pair the difference was 0.02 ppm and 0.03 ppm, respectively (identical to the difference between the two carbons 74.46 and 74.48 ppm in the underivatized form), and the difference between pairs was 1.29 ppm (Table 2). As expected, in the case of the Di18Diol_Me, its single signal for C-9 and C-10 in the underivatized form, 74.46 ppm, doubles into two signals, 81.52 and 82.80 ppm, in the BzAc derivative, with a difference of 1.28 ppm (Table 2).

After the BzAc derivatization, the *vic*-diol methine carbons were significantly deshielded compared to its previous free hydroxyl underivatized forms, in an order of magnitude of ca +8 ppm for the *threo* model compounds and ca +4 ppm for the corresponding *erythro* (Table 3). This showed that the deshielding effect of the BzAc group in these carbons was stronger in the *threo* isomers.

Nevertheless, the most diagnostic feature to assign the *erythro* or *threo* configuration for these *vic*-diols using ^{13}C NMR was simply the values of their chemical shifts: in the *erythro vic*-diol BzAcs of model compounds the *vic*-diol carbons were in the window of 78.7 to 79.3 ppm and in the *threo* equivalents, from 81.5 to 82.9 ppm (Table 2). Both ranges are short and unambiguously apart, making the configuration assignment safe. In both C_{18} 9,10-diol suberin acids the chemical shifts of their *vic*-diol methine carbons as BzAc derivatives were in the *threo* range; identically, both C_{18} 9,10-epoxy suberin acids hydrolyzed into the corresponding C_{18} 9,10-diols had values corresponding to a *threo* relative configuration.

4.4. Relative and absolute configuration of the C_{18} 9,10-epoxy and C_{18} 9,10-diol cork suberin acids

The results discussed above showed that the ^{1}H and ^{13}C chemical shifts of the methine protons and carbons of *vic*-diols substituted in alkyl chains derivatized as benzilidene acetals, can unambiguously be used to assign their *erythro* or *threo* configuration. The comparison of these chemical shifts in the model compounds with the ones in the cork suberin acids, Hyd18Diol_Me and Di18Diol_Me (Table 2), proved that both C_{18} 9,10-diol suberin acids exist in only one relative configuration, which is *threo*.

In the same way, comparing the ^{1}H and ^{13}C epoxide methine and methylene NMR chemical shifts of model compounds, with the ones of the C_{18} 9,10-epoxy suberin acids, Hyd18Epox_Me and Di18Epox_Me, the two latter were shown to be concordant with a *cis* configuration. To confirm this assumption, both cork suberin and model epoxyacids were hydrolyzed by a stereospecific *anti*-hydroxylation, where *cis*-epoxides gave rise to *threo-vic*-diols and *trans*-epoxides originated *erythro-vic*-diols. The chemical shifts of the hydrolyzed epoxyacids, either as free *vic*-diols or in the form of BzAc derivatives showed them to be *threo*, definitely proving that the suberin acid epoxides had a *cis* configuration.

In an attempt to elucidate the absolute configuration of the cork suberin acids they were analyzed by polarimetry. The *cis*-Di18Epox is a *meso* compound, since the *S*,*R* and *R*,*S* possible absolute configurations are identical, and therefore exist as only one stereoisomer (Figure 1). All the other can exist in two enantiomeric forms: the *cis*-Hyd18Epox, can be *S*,*R* or *R*,*S*; the *threo*-Di18Diol, *R*,*R* or *S*,*S*, and the *threo*-Hyd18Diol, *R*,*R* or *S*,*S* (Figure 1). In all these three compounds isolated from cork suberin the measured optical activity was practically zero. Although some doubt can remain because we don't know the optical activity of the individual enantiomers in each pair, this result strongly indicates that the C_{18} *cis*-epoxy and *threo-vic*-diol acids exist in cork suberin as racemic mixtures.

4.5. Stereochemistry of the C_{18} suberin acids and the macromolecular structure of suberin

The stereochemistry of the C_{18} 9,10-epoxy and C_{18} 9,10-diol suberin acids in cork is *a priori* conditioned by the stereoselectivity of their biosynthetic pathways and will afterwards condition the macromolecular arrangement of suberin. Biosynthetic studies had shown that *cis*-oleic acid could be the precursor of C_{18} 9,10-epoxy and C_{18} 9,10-diol suberin acids [1]. In this case, the route for the biosynthesis of the latter C_{18} mid-chain substituted suberin acids, would be the stereochemically favored reactions of oxidation of the *cis*-double bond to *cis*-epoxide, and hydroxylation of the *cis*-epoxide to *threo*-diol. This could be behind the configuration that was proved here for the C_{18} cork suberin acids as *cis*-9,10-epoxy and *threo*-9,10-diol.

Although practically nothing is known about how the suberin acids are three-dimensionally organized within the suberin macromolecule, at least a certain ordered arrangement is highly probable. As seen at ultrastructural level, suberized cell walls show a composite lamellar structure, with alternate dark and translucent contrast, with the latter showing a regular thickness of about 3 nm [29]. An ordered packing of the C_{18} suberin acids was proposed to be the

structural basis of these translucent lamellae [2]. As mentioned before, the C_{18} *cis*-9,10-epoxy and C_{18} *threo*-9,10-diol suberin acids surely play a major role in cork suberin structure, since they account for about 50% of all its long-chain monomers [4]. In this discussion, we must also consider the C_{18} 9-unsaturated ω-hydroxyacid and a,ω-diacid suberin acids, which were proven to be of *cis*-configuration [30]. All together, these six C_{18} mid-chain substituted acids amount to about 65% of all suberin acids in cork. In the solid state as it is seen in fats, C_{18} *cis*-9-oleic acid packs its alkyl chains kinked at the double bond in an ordered manner [31], as favored by its *cis* configuration. In the case of the C_{18} *cis*-epoxyacids, a similar bent molecular arrangement of the alkyl chains is also favored by the epoxide ring of *cis* configuration. Finally, if we bend in the same way the *threo-vic*-diol suberin acids, they project the two hydroxyl groups to opposite directions, because of its *threo* configuration, minimizing the steric hindrance between them. If all the C_{18} suberin acids, either mid-chain unsaturated, epoxide and *vic*-diol assume this kinked conformation, they could be conveniently packed in an ordered parallel way (Figure 5). This packing would favor strong intra-molecular bonding, namely hydrogen bonding between epoxides and *vic*-diol groups. Ultimately this molecular arrangement would allow an ordered macromolecular structure for suberin.

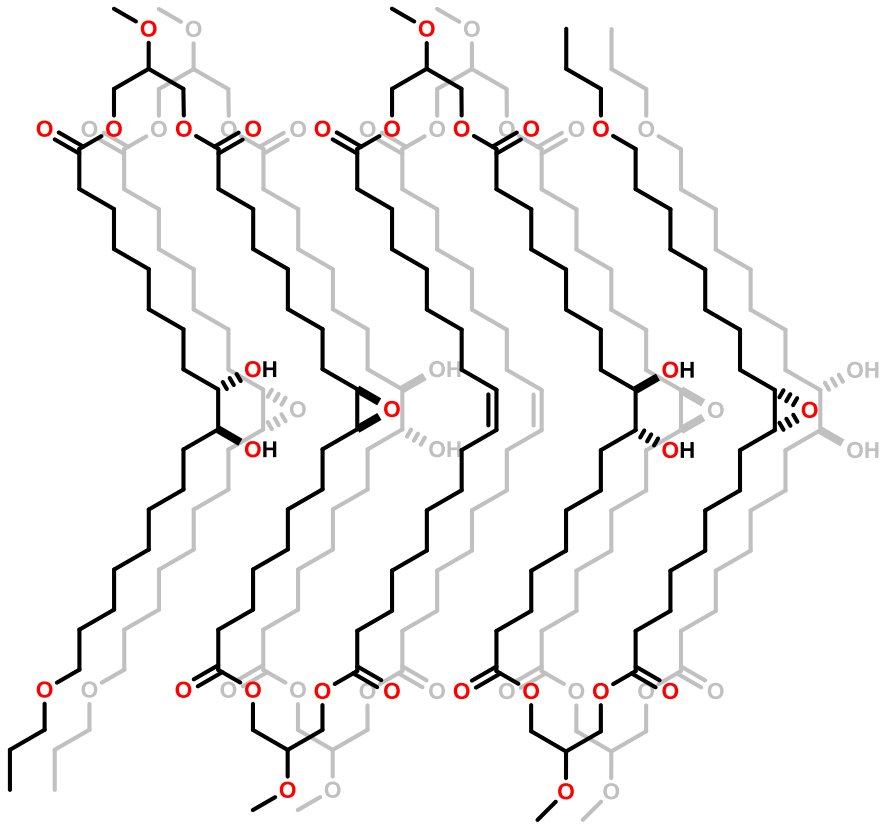

Figure 5. Proposed molecular ordered arrangement of C_{18} monomers in cork suberin

5. References

[1] Kolattukudy, P. 2002. Suberin from plants. In: Doi, Y., Steinbüchel, A., editors. *Biopolymers - Polyesters I*. Wiley-VCH, Weinheim. pp. 41-73.

[2] Graça, J., Santos, S. 2007. Suberin: a biopolyester of plants' skin. *Macromolecular bioscience* **7**(2): 128-135.

[3] Holloway, P. 1983. Some variations in the composition of suberin from the cork layers of higher-plants. *Phytochemistry* **22**(2): 495-502.

[4] Graça, J., Pereira, H. 2000. Methanolysis of bark suberins: analysis of glycerol and acid monomers. *Phytochemical analysis* **11**(1): 45-51.

[5] APCOR. 2012. *Cork statistics*. http://apcor.pt/userfiles/File/Cork%20Statistics.pdf

[6] Seoane, E., Ribas, I. 1951. Sobre la química del corcho. VII. Los ácidos floionico Y floionolico. *Anales de la real sociedad Española de física y química/Ser.B, química* **47***:* 61-66.

[7] Seoane, E., Ribas, I., Fandino, G. 1957. Constitution of phloionolic and isophloionolic acids. *Chemistry & Industry* **16**: 490-491.

[8] Seoane, E., Ribas, I., Fandino, G. 1959. Química del corcho. XIV: constitución y estereoquimica de los ácidos floionólico e isofloionólico. *Anales de la real sociedad Española de física y química/Ser.B, química* **55**: 839-846.

[9] Seoane, E., Arno, M. 1977. Total synthesis and stereochemistry of phloionolic acids. *Anales de química* **73**: 1336-1339.

[10] Dupont, G., Dulou, R., Cohen, J. 1956. Structure stérique de l'acide phloionique. *Bulletin de la société chimique de France* **5**: 819-824.

[11] Conde, E., Garcia-Vallejo, M., Cadahia, E. 1999. Variability of suberin composition of reproduction cork from *Quercus suber* throughout industrial processing. *Holzforschung* **53**(1): 56-62.

[12] Holloway, P., Deas, A. 1973. Epoxyoctadecanoic acids in plant cutins and suberins. *Phytochemistry* **12**(7): 1721-1735.

[13] Seoane, E., Serra, M., Agullo, C. 1977. Two new epoxy-acids from the cork of *Quercus suber*. *Chemistry & Industry* **15**: 662-663.

[14] Eliel, E., Wilen, S. 1994. *Stereochemistry of organic compounds*. John Wiley & Sons, New York.

[15] Seco, J., Quinoa, E., Riguera, R. 2004. The assignment of absolute configuration by NMR. *Chemical reviews* **104**(1): 17-117.

[16] Wenzel, T. 2007. *Discrimination of chiral compounds using NMR spectroscopy*. John Wiley & Sons, New Jersey.

[17] Bhushan, V., Rathore, R., Chandrasekaran, S. 1984. A simple and mild method for the *cis*-hydroxylation of alkenes with cetyltrimethylammonium permanganate. *Synthesis* **5**: 431-433.

[18] McElhanon, J., Wu, M., Escobar, M., Chaudhry, U., Hu, C., McGrath, D. 1997. Asymmetric synthesis of a series of chiral AB(2) monomers for dendrimer construction. *Journal of organic chemistry* **62**(4): 908-915.

[19] Socrates, G. 2001. *Infrared and Raman characteristic group frequencies - Tables and charts 3rd Edition*. John Wiley & Sons, Chichester.

[20] Gunstone, F., Jacobsberg, F. 1972. Fatty-acids. 35: Preparation and properties of complete series of methyl epoxyoctadecanoates. *Chemistry and physics of lipids* **9**(1): 26-34.

[21] Gunstone, F., Schuler, H. 1975. Fatty acids. 46. PMR spectra of several epoxyoctadecenoic, epoxyoctadecynoic, and diepoxyoctadecanoic esters. *Chemistry and physics of lipids* **15**(2): 189-197.

[22] Bascetta, E., Gunstone, F. 1985. C-13 Chemical shifts of long-chain epoxides, alcohols and hydroperoxides. *Chemistry and physics of lipids* **36**(3): 253-261.

[23] Günther, H. 2001. *NMR Spectroscopy*. John Wiley & Sons, New York.

[24] Kleinpeter, E., Seidl, P. 2004. The gamma- and the delta-effects in (13)C NMR spectroscopy in terms of nuclear chemical shielding (NCS) analysis. *Journal of physical organic chemistry* **17**(8): 680-685.

[25] Silverstein, R., Webster, F., Kiemle, D. 2005. *Spectrometric identification of organic compounds*. John Wiley & Sons, New York.

[26] Gallwey, F., Hawkes, J., Haycock, P., Lewis, D. 1990. ^{1}H NMR spectra and conformations of propane-1,2-diol, *meso*- and racemic butane-2,3-diols, and some alditols in non-aqueous media. *Journal of the chemical society-perkin transactions 2* **11**: 1979-1985.

[27] Willy, W., Binsch, G., Eliel, E. 1970. Conformational analysis 23. 1,3-dioxolanes. *Journal of the American chemical society* **92**(18): 5394-5402.

[28] Anteunis, M., Alderweireldt, F. 1964. NMR experiments on ketals IV. PMR spectra and conformations of dioxolanes of 2,3-butanediol and acetophenone. *Bulletin des sociétés chimiques Belges* **73**(11-12): 903-909.

[29] Sitte, P. 1955. Der Feinbau verkorten Zellwände. *Mikroskopie* **10**(5-6): 178-200.

[30] Santos, S., Graça, J. 2013. Stereochemistry of C_{18} monounsaturated cork suberin acids determined by spectroscopic techniques including ^{1}H NMR multiplet analysis of olefinic protons. *Phytochemical analysis*.

[31] Larsson, K., Quinn, P., Sato, K., Tiberg, F. 2006. *Lipids: structure, physical properties and functionality*. The Oily Press, Bridgewater.

6. Supplementary material

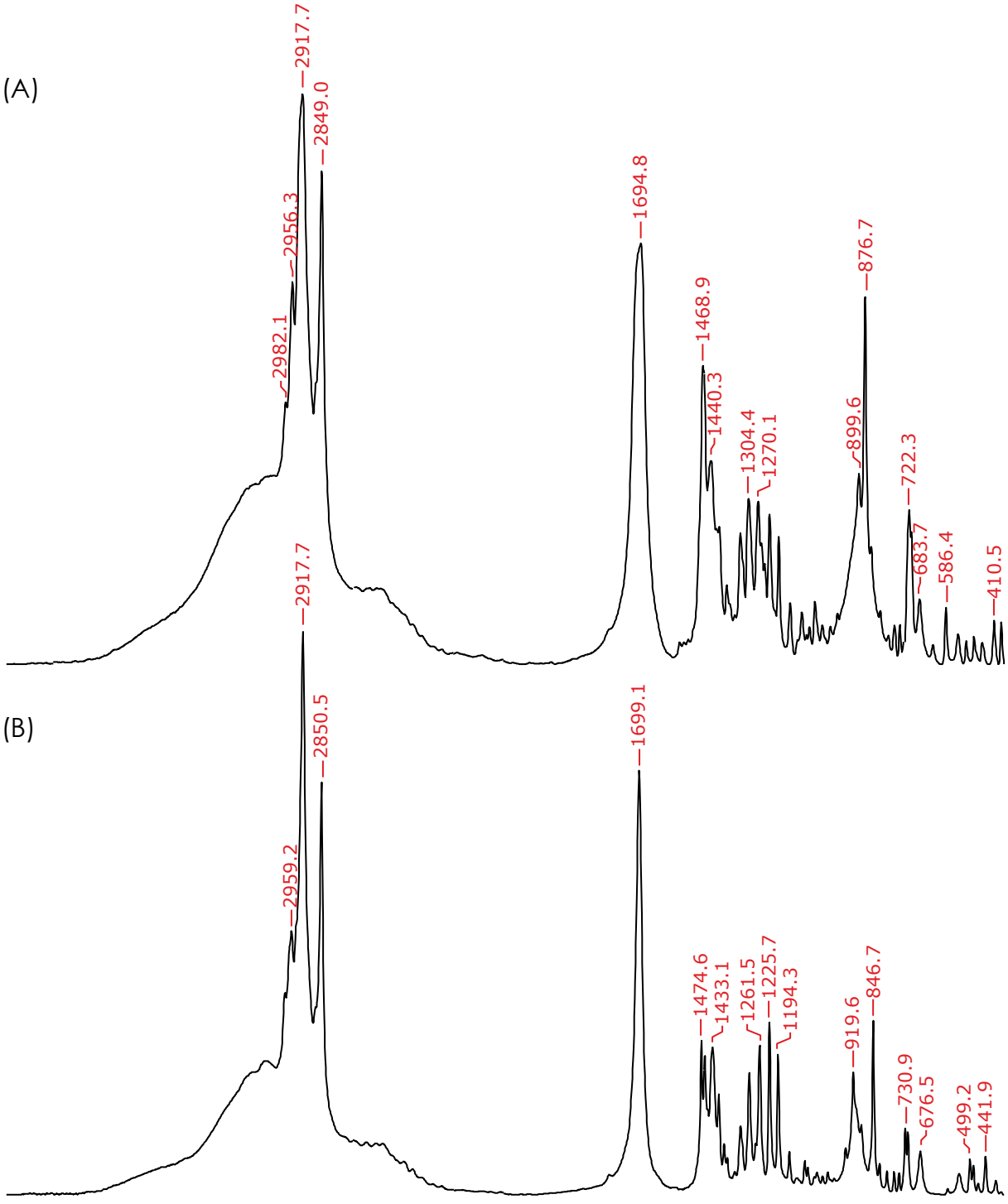

Figure SM1. FTIR (ATR) spectra of model C_{18} 9,10-epoxyacids. (A) *trans*-9,10-epoxyoctadecanoic acid; (B) *cis*-9,10-epoxyoctadecanoic acid

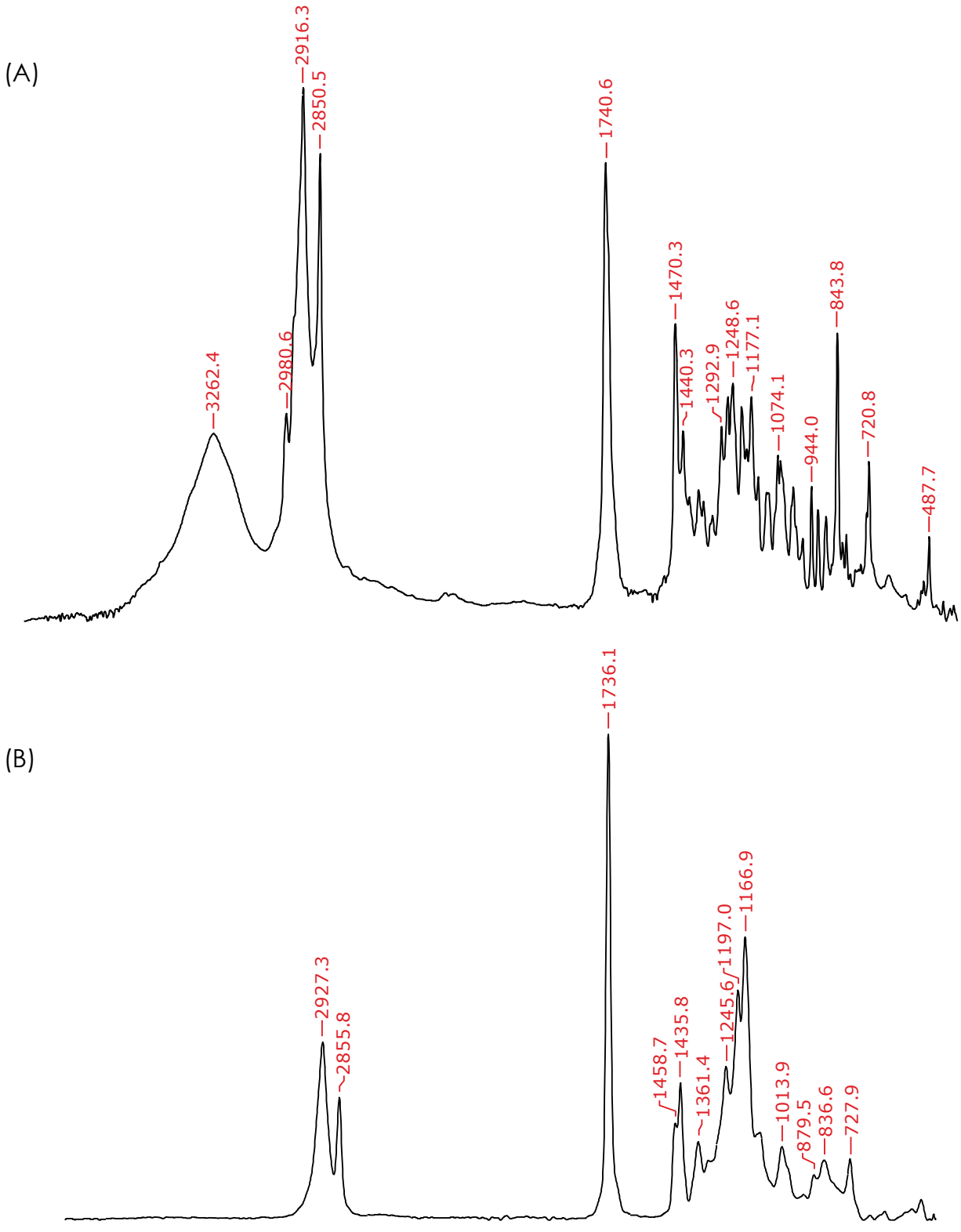

Figure SM2. FTIR (ATR) spectra of C_{18} cork suberin 9,10-epoxyacids. (A) 9,10-epoxy-18-hydroxyoctadecanoic acid methyl ester (C_{18} 9,10-epoxy ω-hydroxyacid [Hyd18Epox_Me]); (B) 9,10-epoxyoctadecanedioic acid dimethyl ester (C_{18} 9,10-epoxy a,ω-diacid [Di18Epox_Me])

Chapter 5: Conclusions and future perspectives

The first set of conclusions from this work is related with the elucidation of the stereochemistry of the cork suberin acid monomers with C_{18} chain-length and mid-chain substituents, namely:

(i) The C_{18} 9-unsaturated a,ω-diacid and C_{18} 9-unsaturated ω-hydroxyacid have a *cis* configuration;

(ii) The relative configuration of the epoxide ring in the C_{18} 9,10-epoxy a,ω-diacid and C_{18} 9,10-epoxy ω-hydroxyacid is *cis*. The C_{18} 9,10-epoxy a,ω-diacid is a *meso* compound, and the C_{18} 9,10-epoxy ω-hydroxyacid is present in cork suberin probably in the form of a racemic mixture (1:1) of its two enantiomers, with the absolute configurations of 9*S*,10*R* and 9*R*,10*S*;

(iii) The relative configuration of the two vicinal hydroxyl groups in the C_{18} 9,10-diol a,ω-diacid and C_{18} 9,10-diol ω-hydroxyacid is *threo*. Both these C_{18} 9,10-diol suberin acids exist in cork suberin probably in the form of racemic mixtures of their two enantiomers, with the absolute configurations of 9*S*,10*S* and 9*R*,10*R*.

These results and conclusions regarding the stereochemistry of the cork suberin acids with C_{18} chain-length and mid-chain substituents are relevant both for the understanding of cork suberin macromolecular structure, as well as for the eventual industrial applications of these compounds.

In what respects its impact in the macromolecular structure of suberin, one has to consider that all together, the C_{18} 9-unsaturated a,ω-diacid and ω-hydroxyacid, the C_{18} 9,10-epoxy a,ω-diacid and ω-hydroxyacid and the C_{18} 9,10-diol a,ω-diacid and ω-hydroxyacid amount for more than 50% of cork suberin composition. Also, as discussed before, these C_{18} suberin acids are typically dominant in the composition of other suberins analyzed so far. This means that they must play a major role in the macromolecular structure of suberin. The stereochemical configuration of their voluminous mid-chain substituents, as the epoxide rings and *vic*-diol groups are, will determine the spatial proximity between the different monomers, their possible conformations, and the location and strength of the inter-monomer covalent and non-

covalent linkages. Ultimately the configuration and conformation of these suberin acids, will determine how they can organize and pack themselves in a three-dimensional level, building up the suberin macromolecule.

The full structural characterization of the main suberin monomers, including their stereochemistry, is by now completed; how monomers are sequentially ester linked is already partly elucidated by the dimeric and trimeric basic oligomer structures that have been solubilized by the partial depolymerization of suberin (reviewed and discussed in Chapter 1). To increase the knowledge about the macromolecular structure of suberin some relevant information is still expected to be gained from degradation studies, like chemical or enzymatic partial or total depolymerization of suberin; the latter will be useful in particular if complemented with the marking of specific linkages or monomers, for instance with heavy isotopes or deuterated reagents. Also the effects of the targeted or marked degradation procedures could be followed by transmission electron microscopy (TEM) to observe the eventual alterations in the ultrastructure of suberin rich cell walls. Although studies based in these principles had already been applied to suberin, some of them could be redesigned taking into account the latter developments added to suberin chemistry knowledge.

To truly take the understanding of the macromolecular (and supramolecular) structure of suberin to the next level, we have to invest in solid-state techniques that can study the polyester in a non-modified form. These include solid-state NMR and X-ray diffraction and scattering techniques. Although a lot of work has already been done using solid-state NMR, namely in cork suberin and potato skin suberin, the conclusions drawn from those results have been somehow impaired by the relatively low resolution of the spectra and the overlapping of signals originated from other cell wall components. So, better techniques to isolate suberin (or fragments of suberin), which keep its *in situ* structure are also needed. Eventually, advantage can also be taken from more recent developments in the NMR hardware (and software) that improve the resolution of solid-state spectra. X-ray scattering techniques will be

needed to elucidate eventual ordered structural arrangements at macromolecular (or supramolecular) level that might exist in suberin, as some circumstantial evidence seems to point to.

Another approach to get new insights on the structure of suberin can be through genetic manipulation. The silencing or over-expression of genes presumably involved in suberin monomers' biosynthesis, and afterwards observing the phenotypic effects on suberin structure and composition, can also give clues on how the suberin polyester is built up. Of course, these latter results can also be eventually used to produce suberized tissues with higher suberin contents and/or suberin enriched in specific monomers. To obtain better or more resilient agricultural species can be the purpose. For instance, there is an international project (in which we participate) intended to genetically modify the potato skin suberin in order to get tubers more resistant to water loss and pathogenic attack. Finally, in the perspective of extracting suberin acids from suberin for industrial use, a modified suberin composition enriched in the more interesting compounds can also be the objective of the genetic manipulation.

The knowledge of the macromolecular structure of suberin will ultimately be decisive for the understanding of: the unique set of properties of cork as a material; the "membrane" role of plants' frontier tissues, including the mechanisms for insulation and protection towards environmental aggressions; and finally to eventually serve as model for the development of "bio-inspired" materials, with properties that could mimic the original roles of suberin.

The second set of conclusions from this work is related with the development of techniques to isolate and purify some of the main suberin acid monomers from cork: in spite of the very complex initial mixture of suberin monomers obtained after suberin depolymerization, the more important suberin acids can be isolated in preparative (at laboratory scale) quantities (10's to 100's mg) following a relatively straightforward procedure, attaining very high purities, reaching in some cases "100%". To accomplish these goals, the isolation and purification procedure developed was based in applying

successively contrasting media or conditions to the suberin acids to be separated: solubility in non-polar/polar solvents, solubility at low/high temperature, and affinity to normal phase/reverse phase chromatographic stationary phases. Although the procedure developed has a relatively high number of steps, only well established and fairly simple technical approaches are used, as well as some of the most common solvents and chromatographic media.

The methods developed to isolate and purify the main suberin acid monomers from cork are expected to serve as the basis for the scaling-up of their industrial production. The relatively "simple" processes of extraction, depolymerization and purification are also expected to help in the industrial scale-up; they can be applied to cork or eventually to other suberized tissues from other plant sources. As discussed briefly in the Introduction, the particular structure of the α,ω-bifunctional fatty acids, like the suberin acids, and their corresponding unique reactivity and properties, are expected to be useful for a number of industrial uses in different areas. The main bottleneck that has hindered the eventual development of these potentially valuable applications is the fact that these compounds are not commercially available. Their extraction from cork suberin and purification to high purity is expected to allow the development of some of these more technological demanding uses, and of course, potentially of higher economic value.